Introduction to Solar Resource Assessments

Carsten Hoyer-Klick

German Aerospace Center

Institute of Technical Thermodynamics

DLR Deutsches Zentrum für Luft- und Raumfahrt e.V. in der Helmholtz-Gemeinschaft

Outline

- Solar radiation basics
- Solar geometry
- Atmospheric transfer and components of solar radiation
- Ground measurements
- Satellite based assessments
- Solar radiation to tilted planes
- Characteristics of solar resources
- Data sources
- Application samples
- Access to data
- Selecting the right data source
- GIS analysis

Getting Renewable Energy to Work

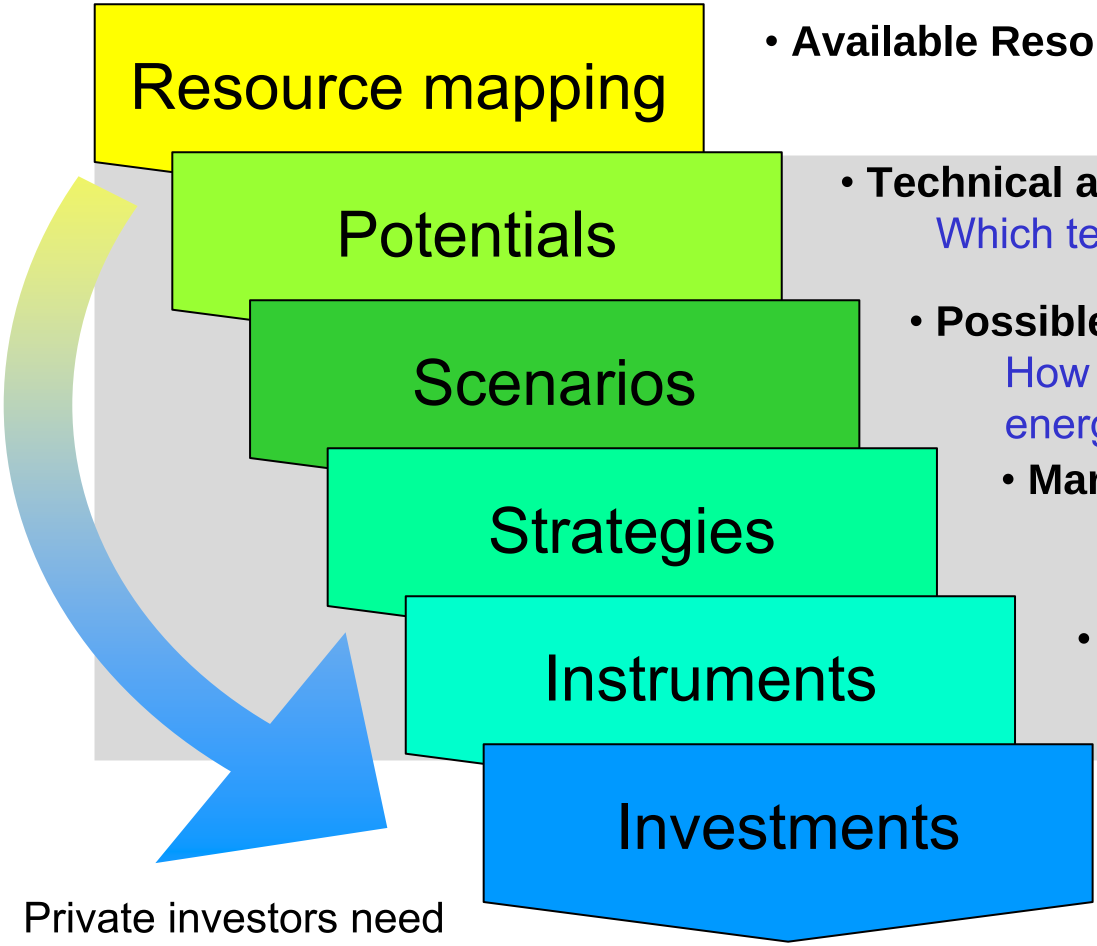

- **Available Resources**
- **Technical and economic potentials**
  Which technologies are feasible?
- **Possible capacity development**
  How can they contribute to the national energy system?
- **Market introduction**
  How to get them into the market?
  Where to start?
- **Political and financial instruments**
  Legislation, incentives
- **Private investments**

Political + Economic Framework

Private investors need resource data for investments

Project Development for Renewable Energy Systems

Resources (Atlas)

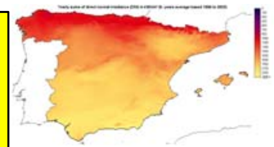

Project development

Resources (time series)

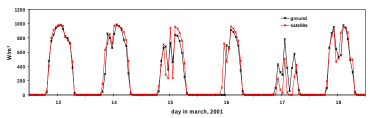

Engineering

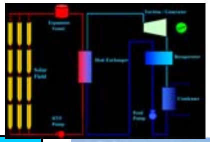

Construction

Commissioning

Operation

- Finding suitable sites with high resolution maps and economic evaluations
- Detailed engineering with site specific data with high temporal resolution as input to simulation software

Solar Radiation Basics

Kirchoff’s law

- **At thermal equilibrium, the emissivity of a body (or surface) equals its absorptivity.**
- *“A good absorber is a good emitter” or “a good reflector is a bad absorber” or vice versa.*
- $\alpha(\lambda) = \varepsilon(\lambda)$

- Practical application:
  Selective coatings: Good absorption/emission in the visible, bad absorption/emission in the infra read

- A body showing perfect absorption and maximum emission ($\alpha_\lambda = 1$, $E_{\lambda} = E_{max}$) is called a **black body**.

Planck's Law

Spectral radiance per wavelength interval

$$L(\lambda,T)d\lambda = \frac{2hc^2}{\lambda^5}\left(\exp\left(\frac{hc}{\lambda kT}\right)-1\right)^{-1} d\lambda$$

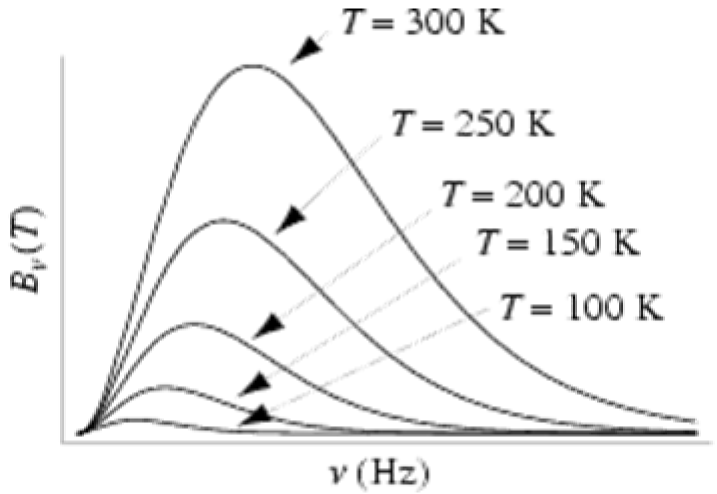

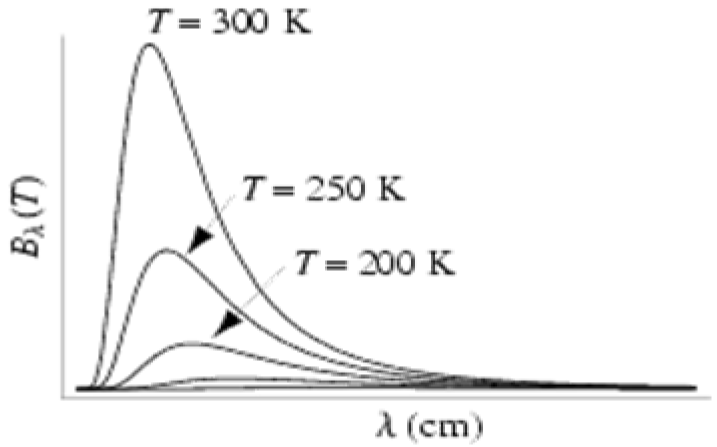

Integration and differentiation of Planck's law:

$$M(T) = \sigma T^4$$

Stefan-Boltzmann law

Emittance solely depends on temperature for a black body

$$T\lambda_{\max} = const$$

Wien's law

Color is an indication of the temperature of a black body

Blackbody Radiation

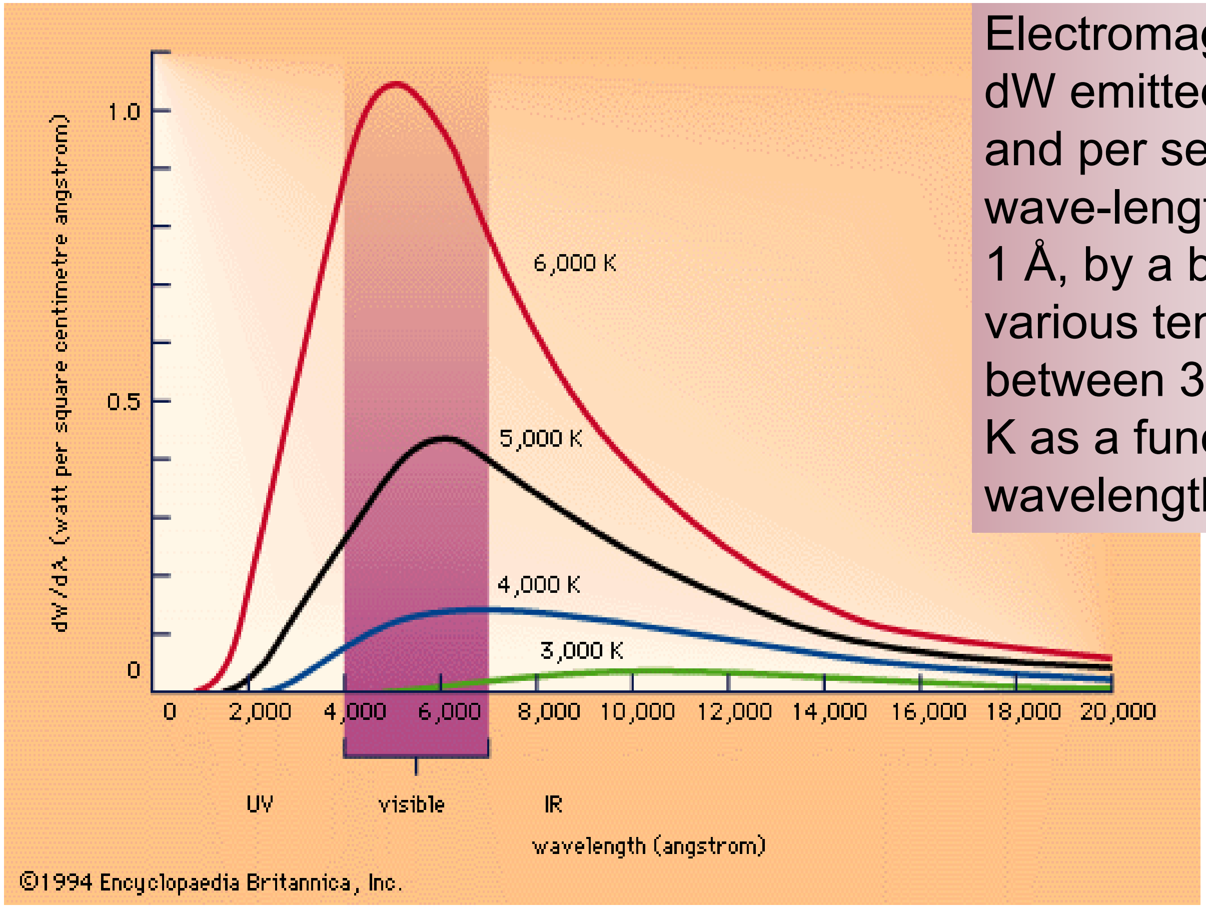

Electromagnetic energy dW emitted per unit area and per second into a wave-length interval, dλ = 1 Å, by a blackbody at various temperatures between 3000 and 6000 K as a function of wavelength

Solar and terrestrial spectrum

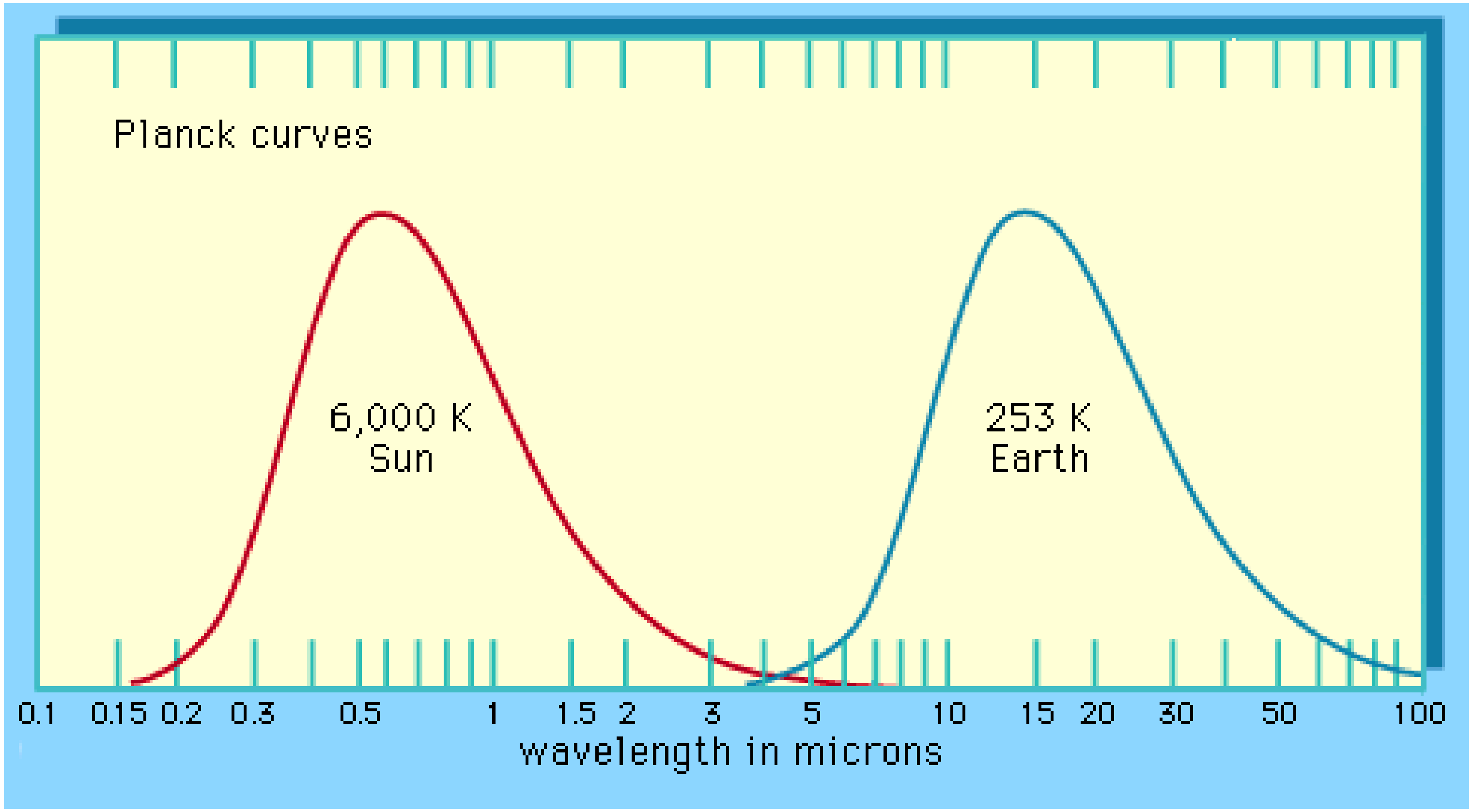

Definition Radiant flux density

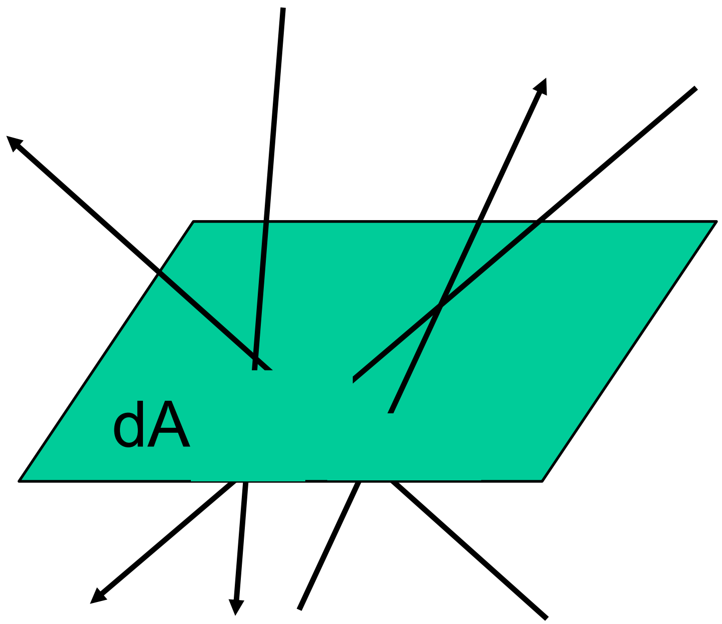

Energy flux density F

defines the radiant energy dQ passing through an area dA in the time interval t, t +dt :

$$d^2Q = F\ dA\ dt$$

Units of F are Whm-2.

Definition: Radiance

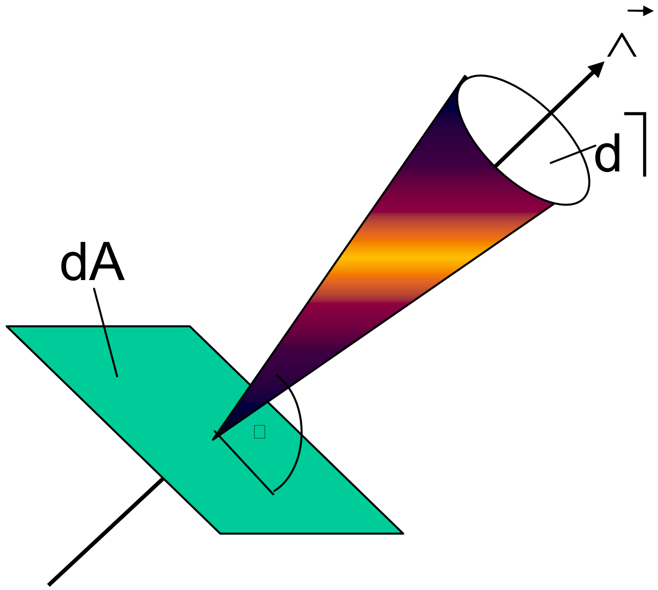

Radiance L

defines the radiant energy flux dΦ = dQ /dt passing through an area dA perpendicular to the direction Ω into the solid angle dω:

$$d^3Q = L\ dA\ dt\ d\omega$$

Units of L are $Whm^{-2}sr^{-1}$.

Solar Constant

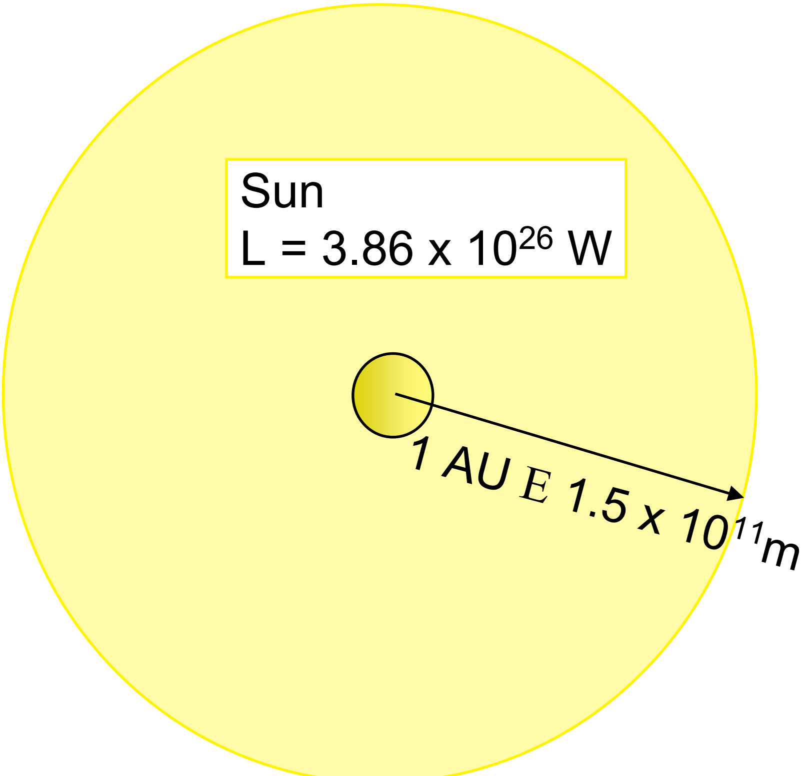

Area of a sphere = $4\pi r^2$

Conservation of energy requires that the total energy flux coming out of the sun must also pass through a sphere at 1 AU.

The energy flux density at 1 AU is

$$\frac{L}{4\pi r^2} = 1367 \frac{W}{m^2}$$

This is the **Solar Constant**.

Variation of the Extraterrestrial Radiation

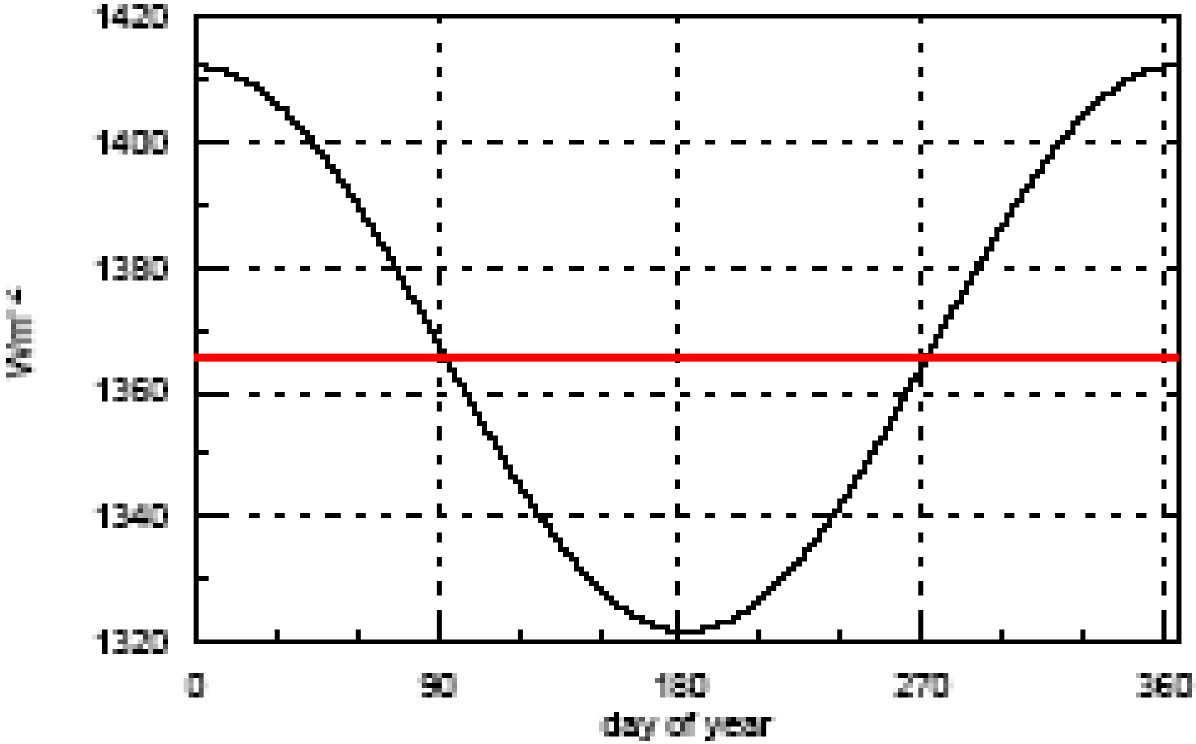

Solar constant = 1367 Wm^{-2}

Extraterrestrial Solar Spectrum

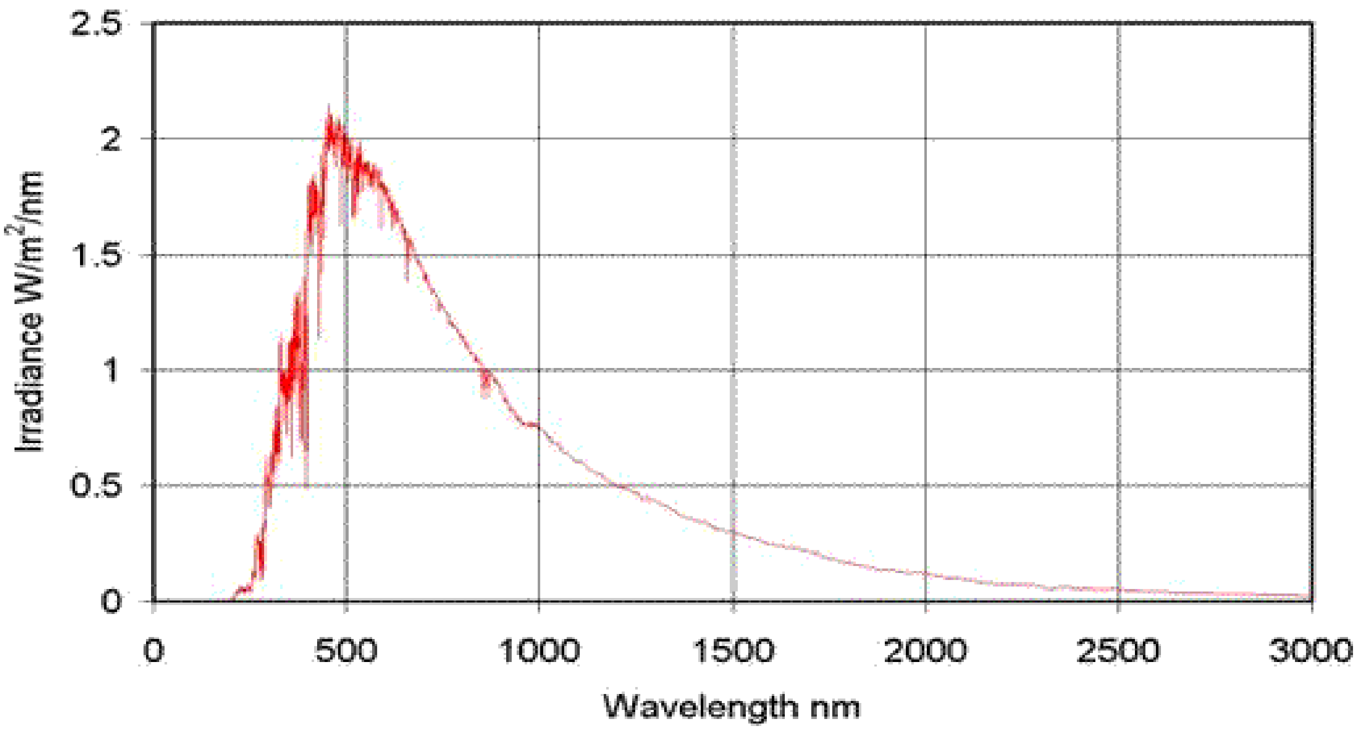

Solar Geometry

Sun – Earth Geometry

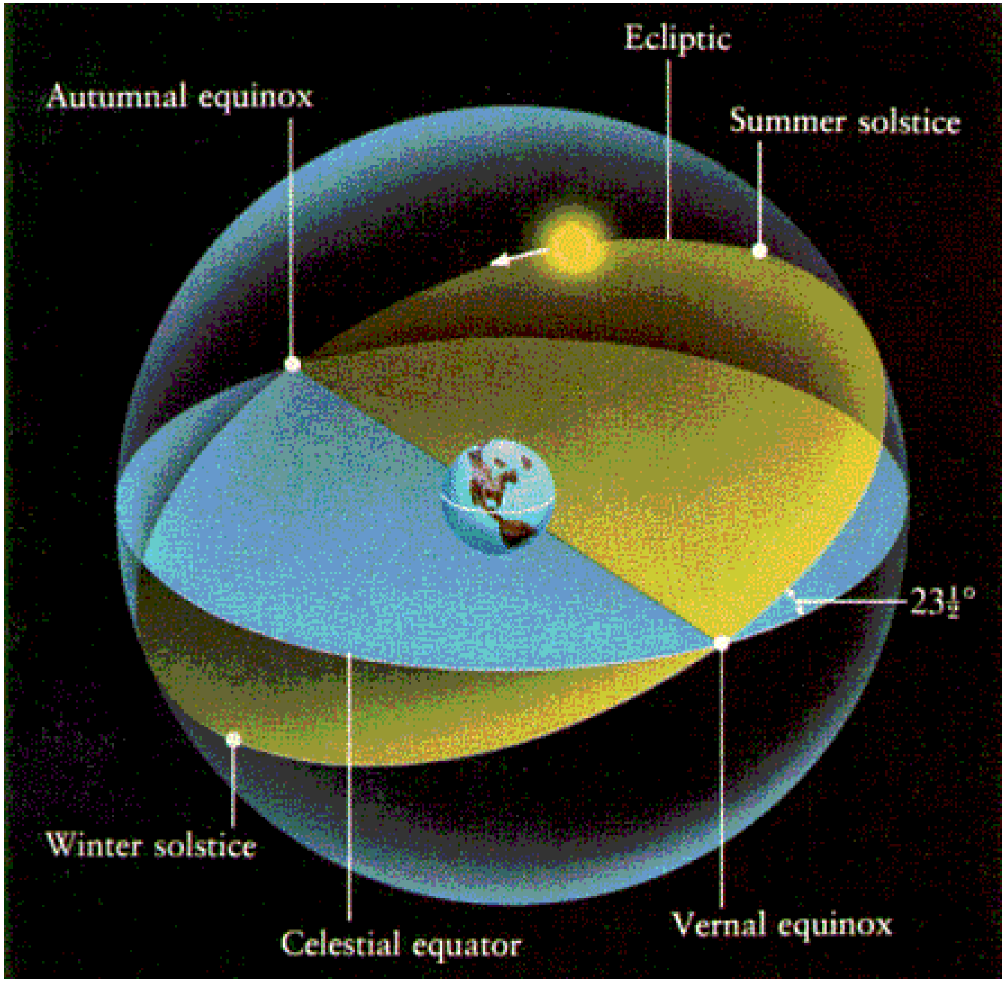

Ecliptic

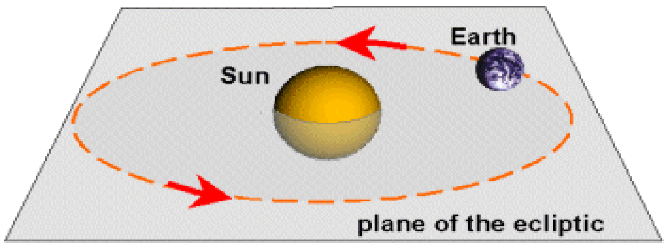

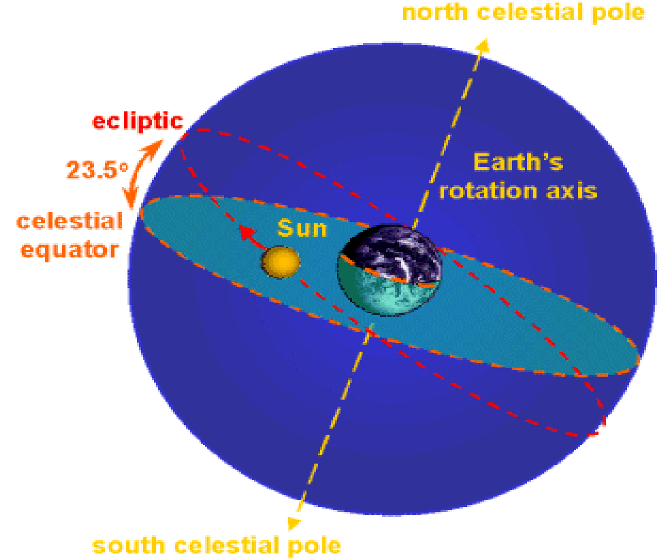

- The ecliptic is the region of sky (of the celestial sphere) through which the Sun appears to move over the course of a year. This apparent motion is caused by the Earth's orbit around the Sun, so the ecliptic corresponds to the projection of the Earth's orbital plane on the celestial sphere. For this reason, the Earth's orbital plane is sometimes called the plane of the ecliptic.
- Due to the tilt of the Earth's rotation axis with respect to its orbital plane, there is an angle of 23.5o between the ecliptic and the celestial equator.

Solar Declination

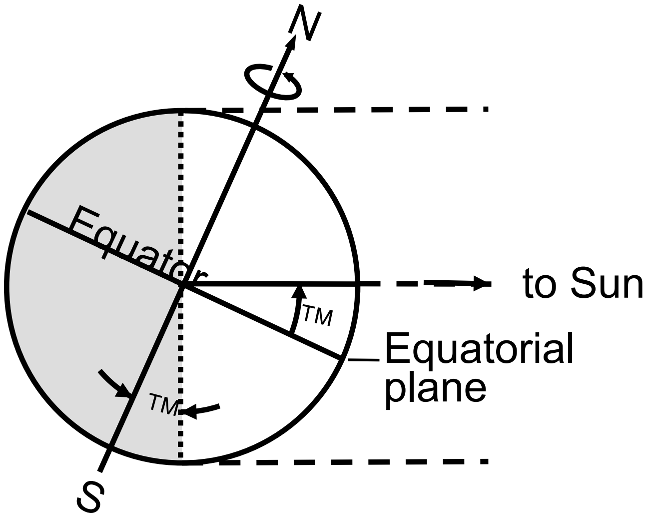

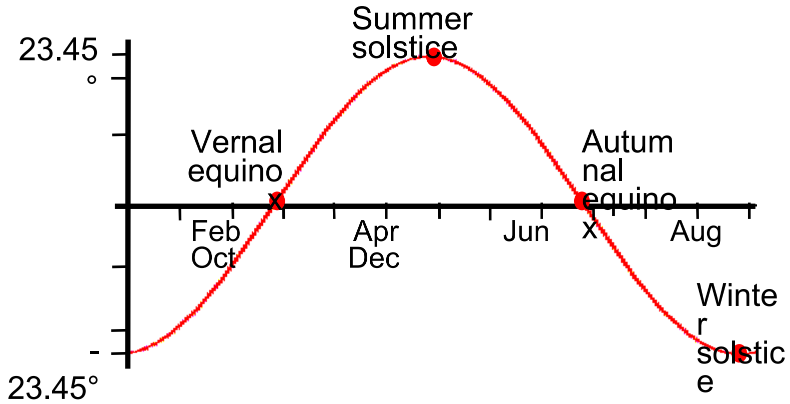

Declination angle δ = 23.45°

Variation of the declination angle:

$\delta = 23.45 * \sin [360 / 365 * (284 + n)]$

with n = day of the year

(Approximation)

Solar Time

- Daily variations of solar radiation are usually described on the basis of **solar time.**

- Definitions:

Solar day: Time interval between two subsequent crossings of the Sun‘s path with the local meridian.

  - length changes from day to day (< 30 sec)
  - mean value: 24h

Solar noon: Time of the crossing of the Sun‘s path with the local meridian

Solar Time

The variation of the solar day length is caused by:

- The elliptical path of the Earth around the Sun
  (Kepler‘s law: Earth sweeps equal areas in equal times)

- The tilt of the Earth‘s axis with respect to the ecliptic plane

Difference between solar time and local mean time
is expressed by Equation of Time

Equation of time

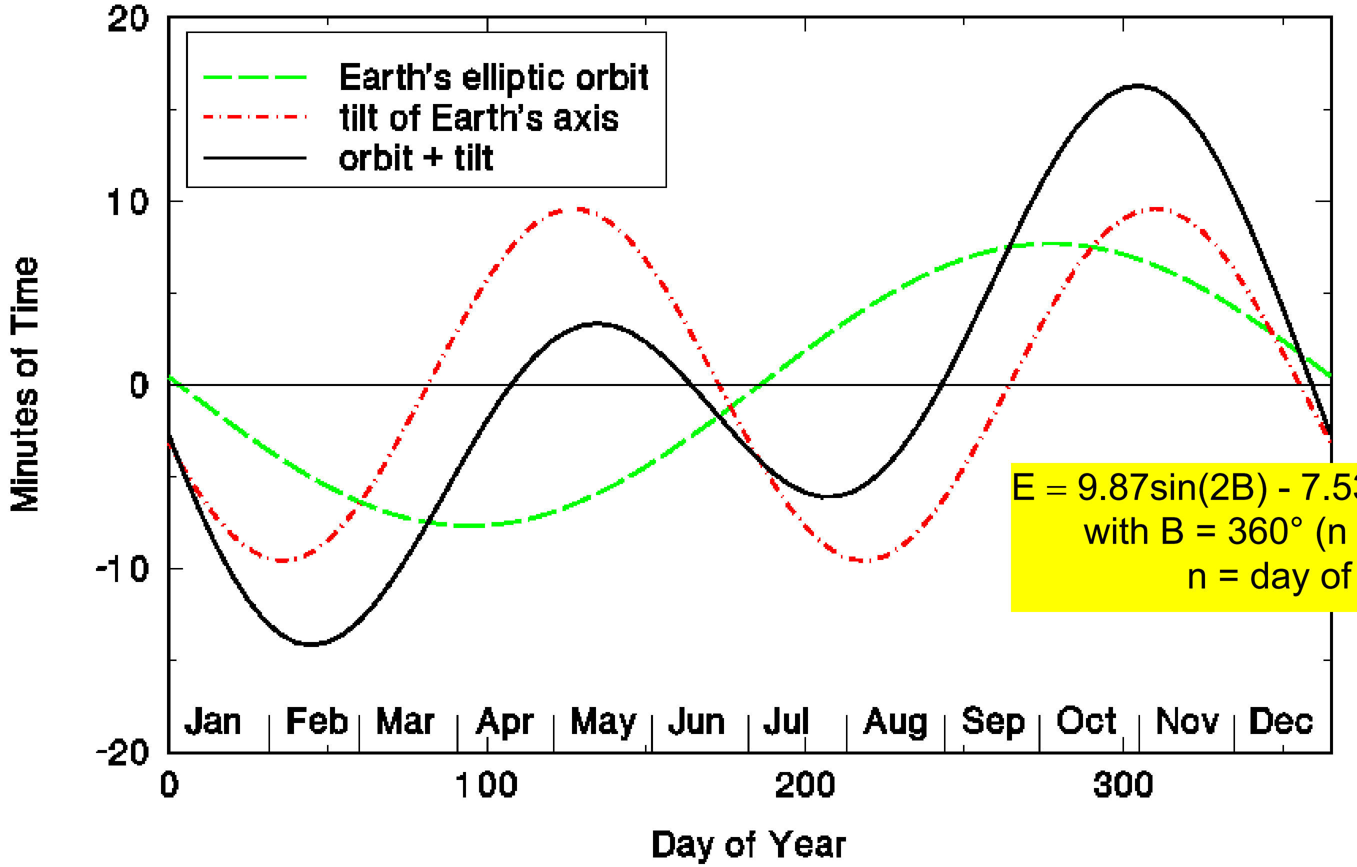

$$E = 9.87\sin(2B) - 7.53\cos(B) - 1.5\sin(B)$$
with $B = 360° (n - 81) / 364$ and
n = day of the year

Hour angle

- The **hour angle** ω describes the solar time in trigonometric terms, i.e as an angle.
- ω equals the angular displacement of the Sun from the local meridian due to the rotation of the Earth
- One hour corresponds to an angle of 360°/24h = 15°
- By convention, morning hours are calculated negative, afternoon hours positive. At solar noon, ω=0°.

Angle of Incidence

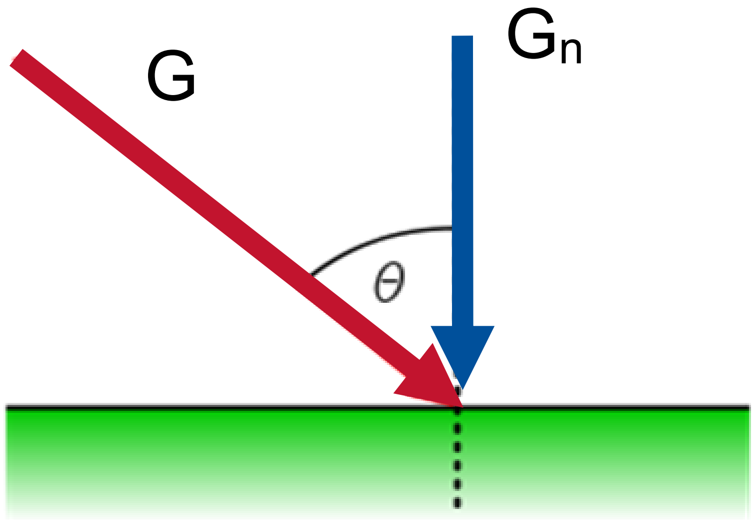

For surfaces not oriented perpendicular to the Sun, the irradiance is given by

$$G = G_n \cos \theta$$

Angle of incidence

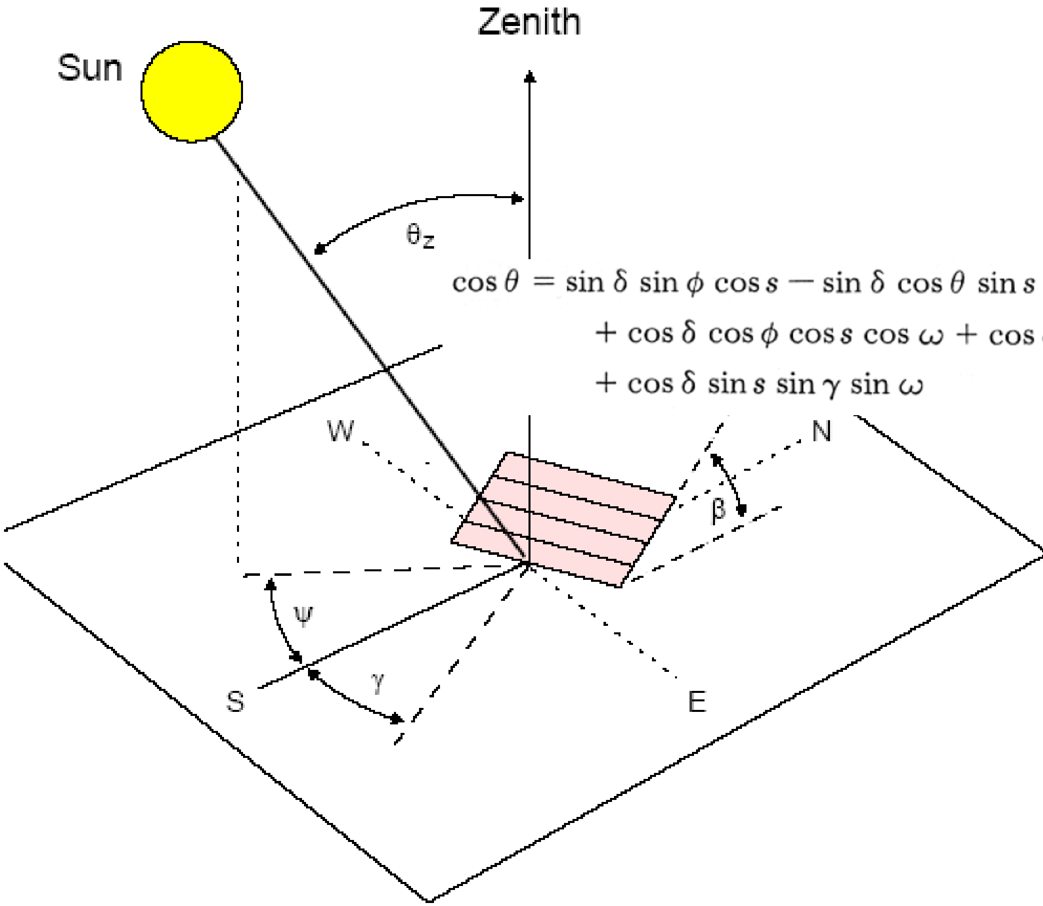

$$\cos\theta = \sin\delta\,\sin\phi\,\cos s - \sin\delta\,\cos\theta\,\sin s\,\cos\gamma$$
$$+ \cos\delta\,\cos\phi\,\cos s\,\cos\omega + \cos\delta\,\sin\phi\,\sin s\,\cos\gamma\,\cos\omega$$
$$+ \cos\delta\,\sin s\,\sin\gamma\,\sin\omega$$

with:

latitude Φ

solar declination δ

hour angle ω

slope β

surface azimuth γ

Atmospheric Transfer and Components of solar radiation

Solar Spectrum and Atmospheric influence

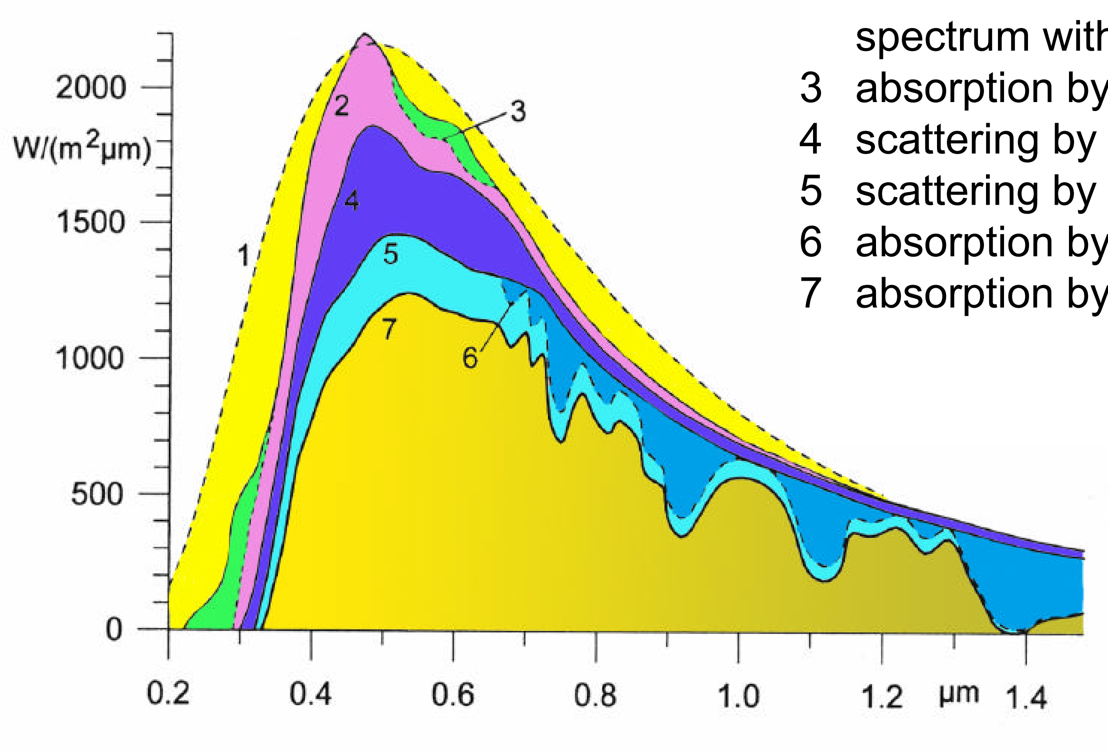

1 Planck curve T=5780 K at mean sun-earth distance
2 extraterrestrial solar spectrum with additional
3 absorption by 0_3
4 scattering by 0_2 und N
5 scattering by aerosols
6 absorption by H_2O vapor
7 absorption by aerosols

Atmospheric Extinction Processes

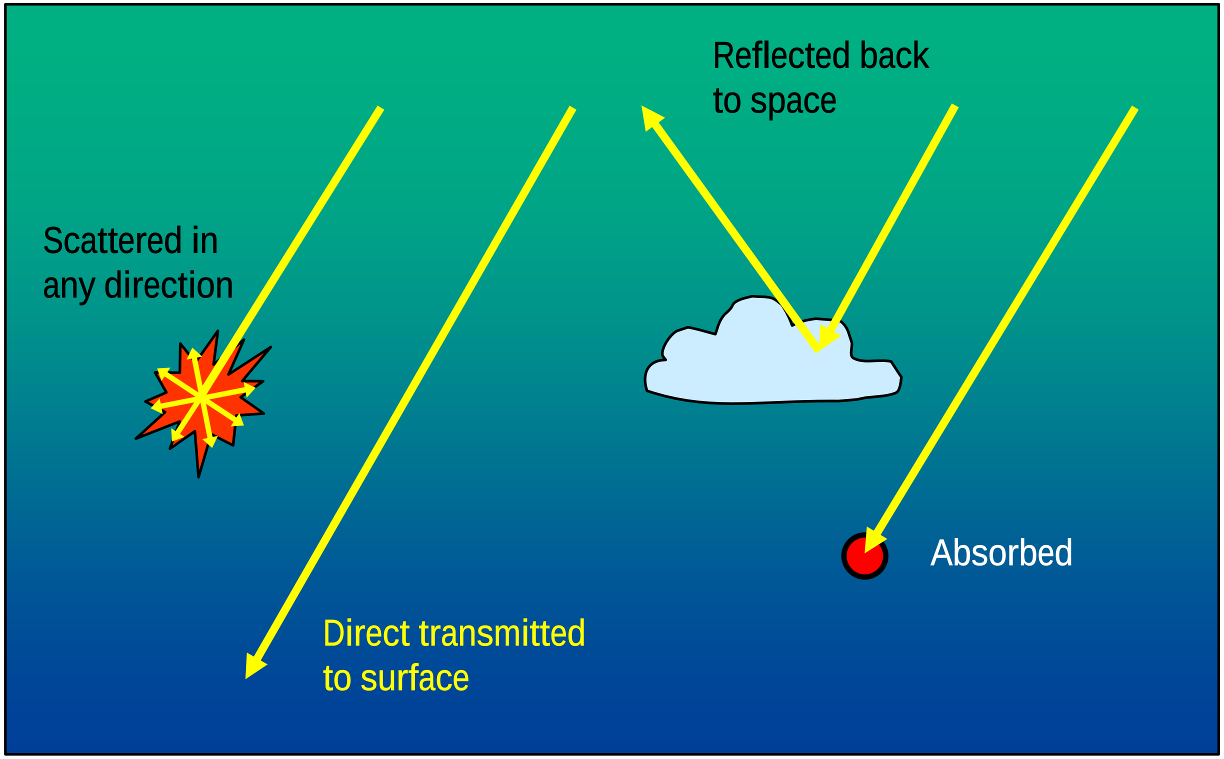

Rayleigh and Mie Scattering

Rayleigh scattering	Mie scattering
particle size << wavelength	particle size ≥ wavelength
~ λ-4	~ λ-1.3
directionality: $(1 + \cos^2 \alpha)$	directionality: very strong foreward scattering
	Large variability by non-uniform particles

Scattering Regimes

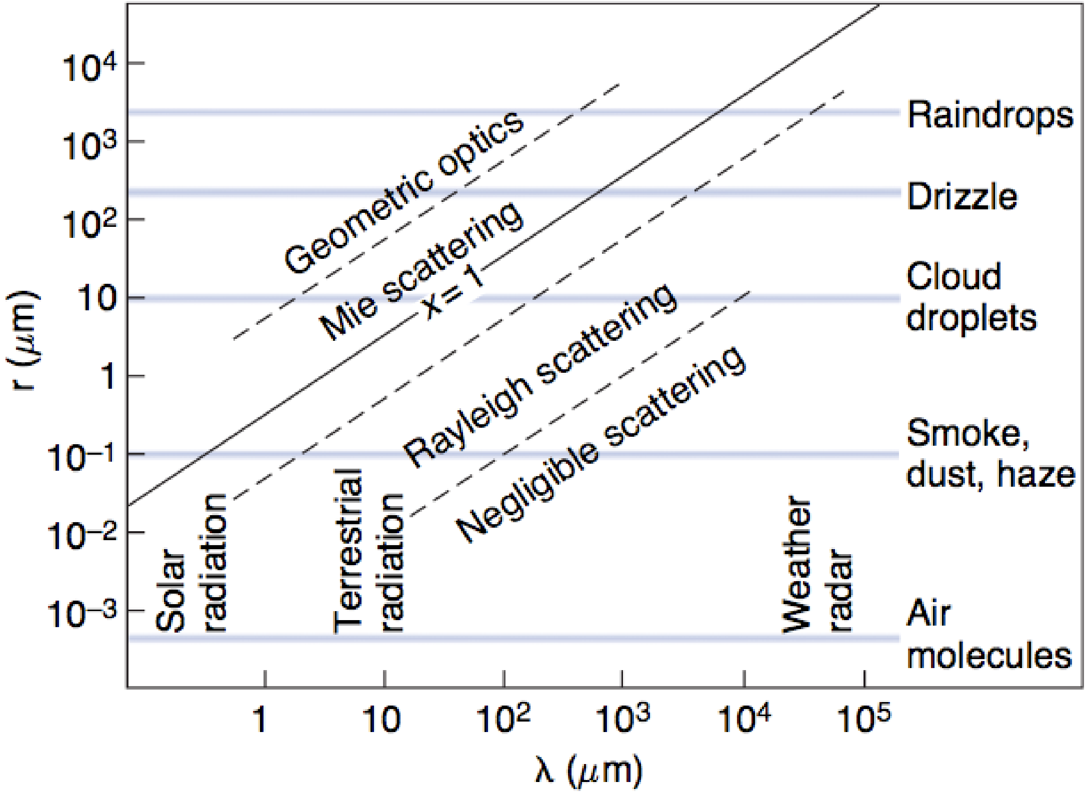

Dimensionless size parameter X=2πr/λ as a function of wavelength (λ) of the incident radiation and particle radius r.

Rayleigh and Mie Scattering

Rayleigh scattering

Mie scttering

Mie Scattering, larger particles

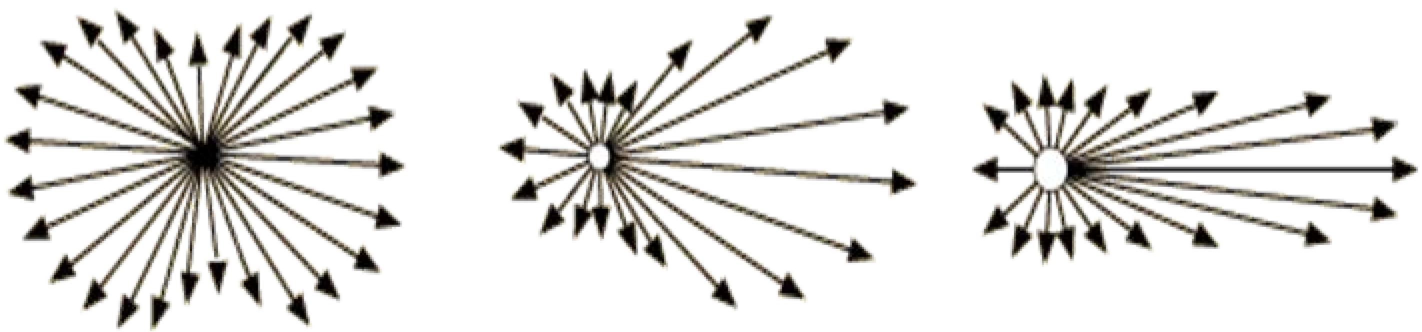

Direction of incident light

Air Mass

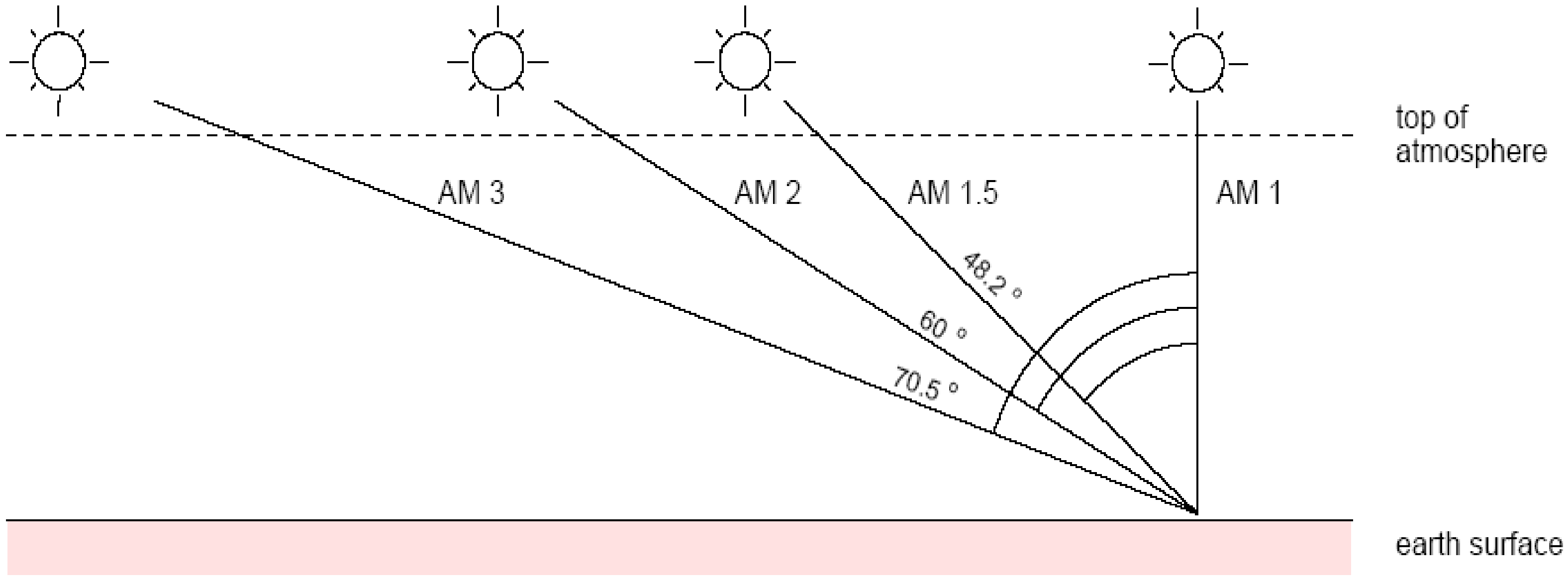

Properties of Solar Radiation

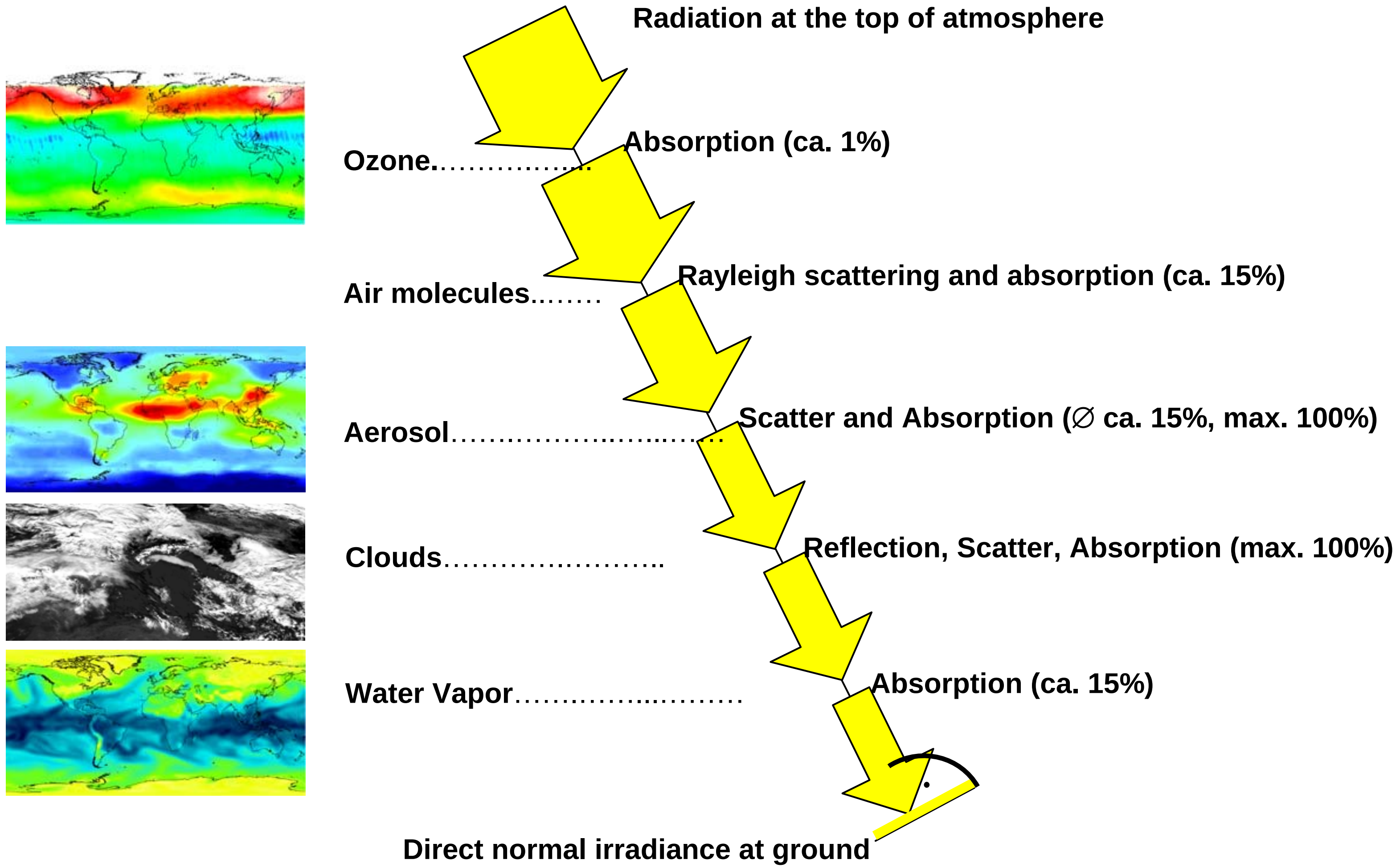

Radiative Transfer in the Atmosphere

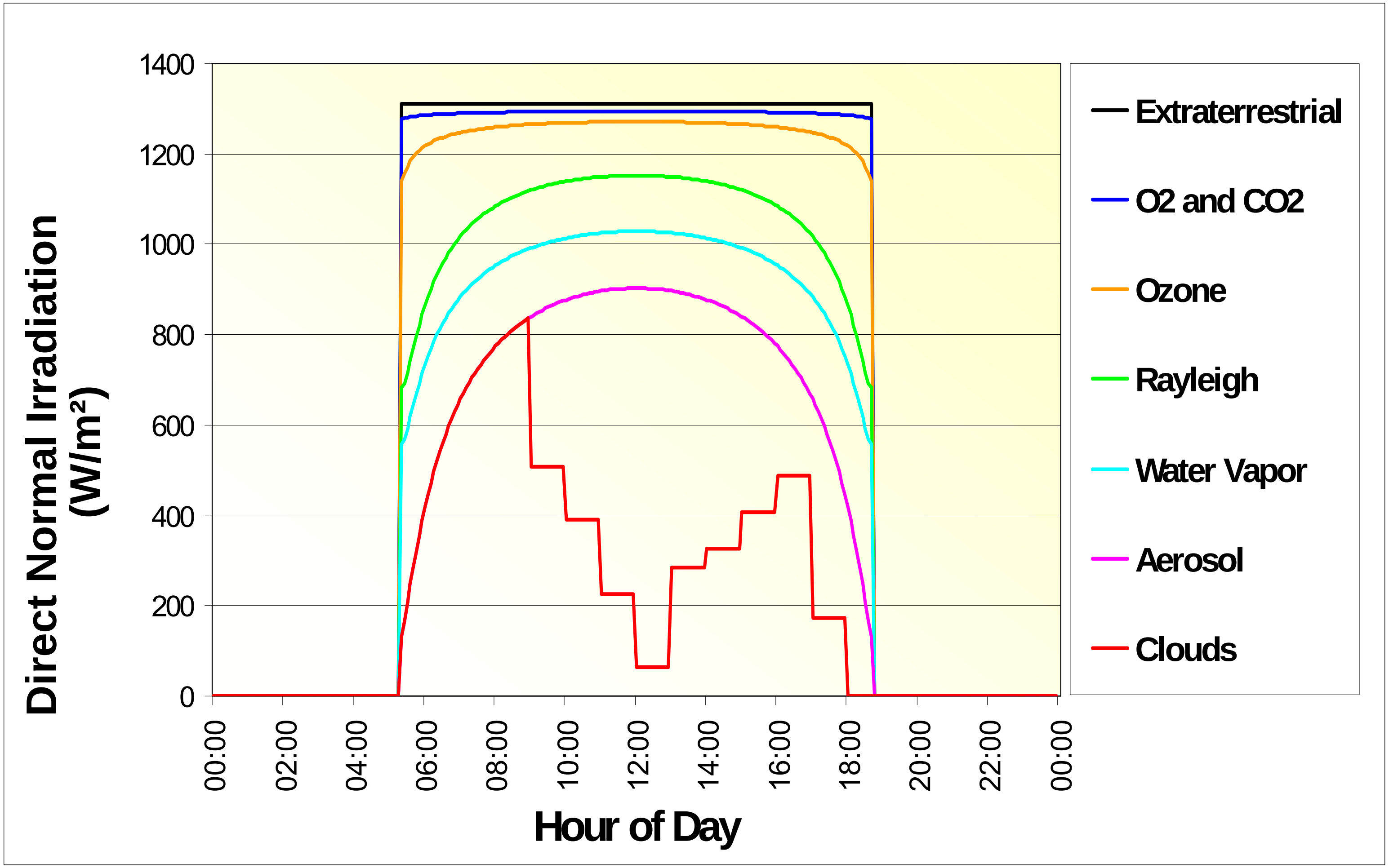

Direct Normal Irradiation (DNI)

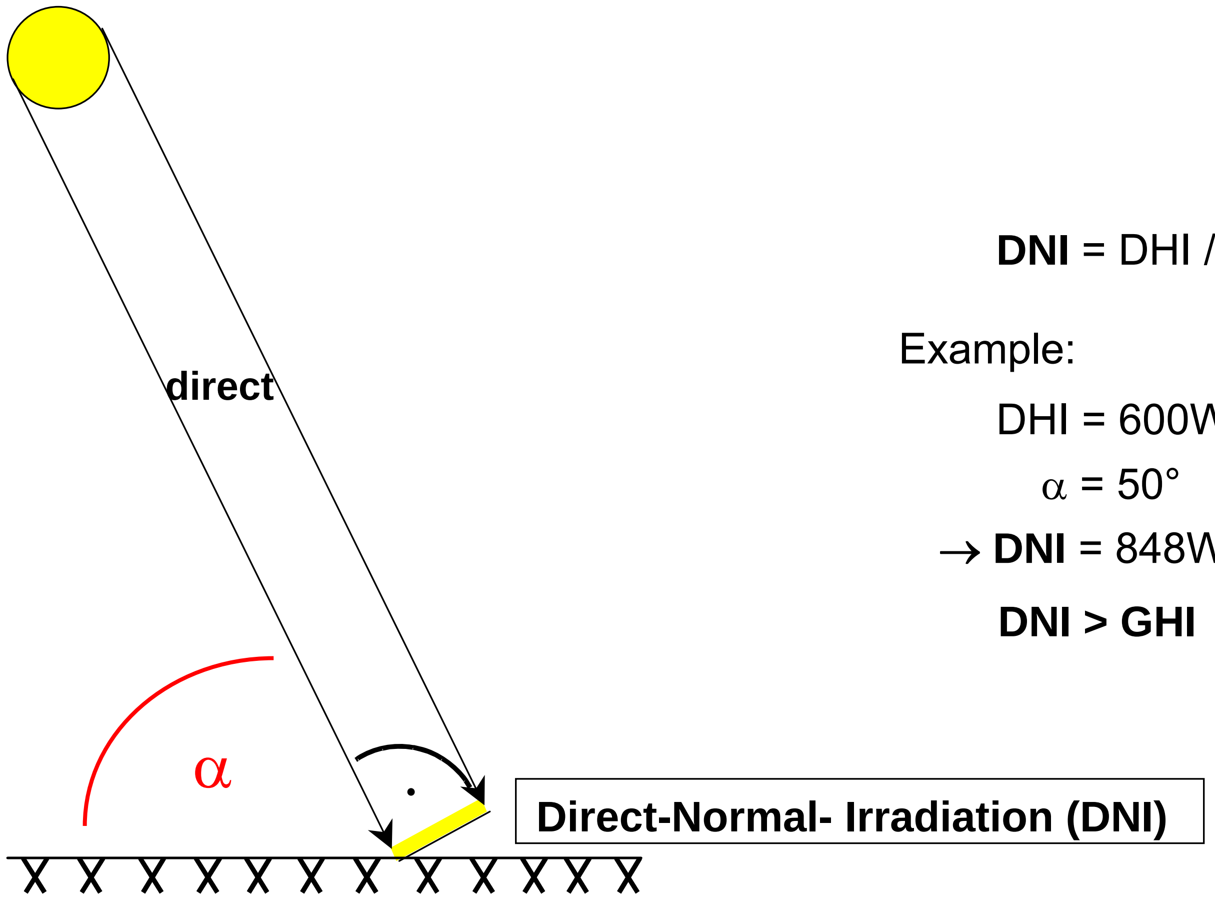

DNI = DHI / sin α

Example:

DHI = 600W/m²

α = 50°

→ **DNI** = 848W/m²

DNI > GHI

Global Horizontal Irradiation (GHI)

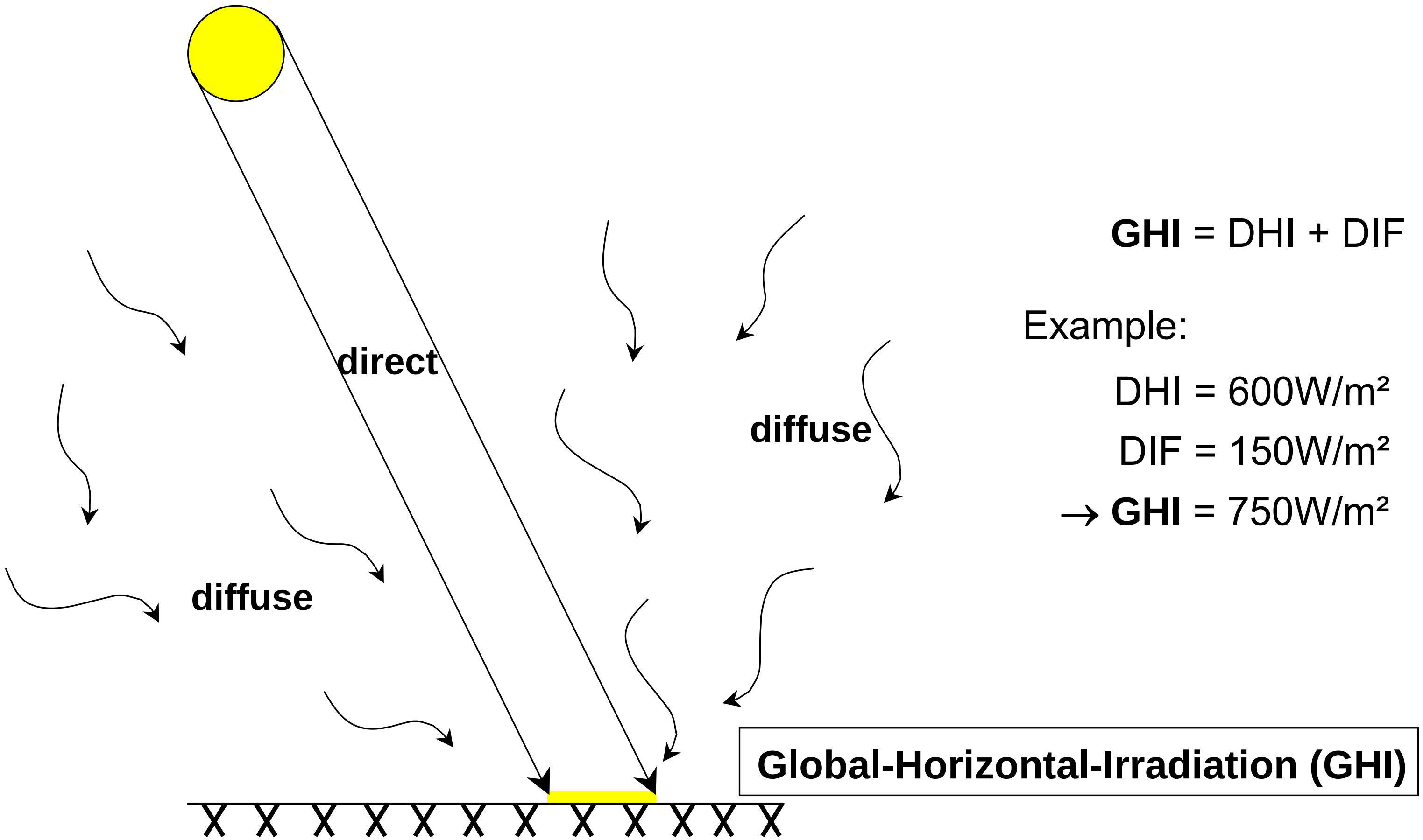

GHI = DHI + DIF

Example:

DHI = 600W/m²

DIF = 150W/m²

→ **GHI** = 750W/m²

Clear sky

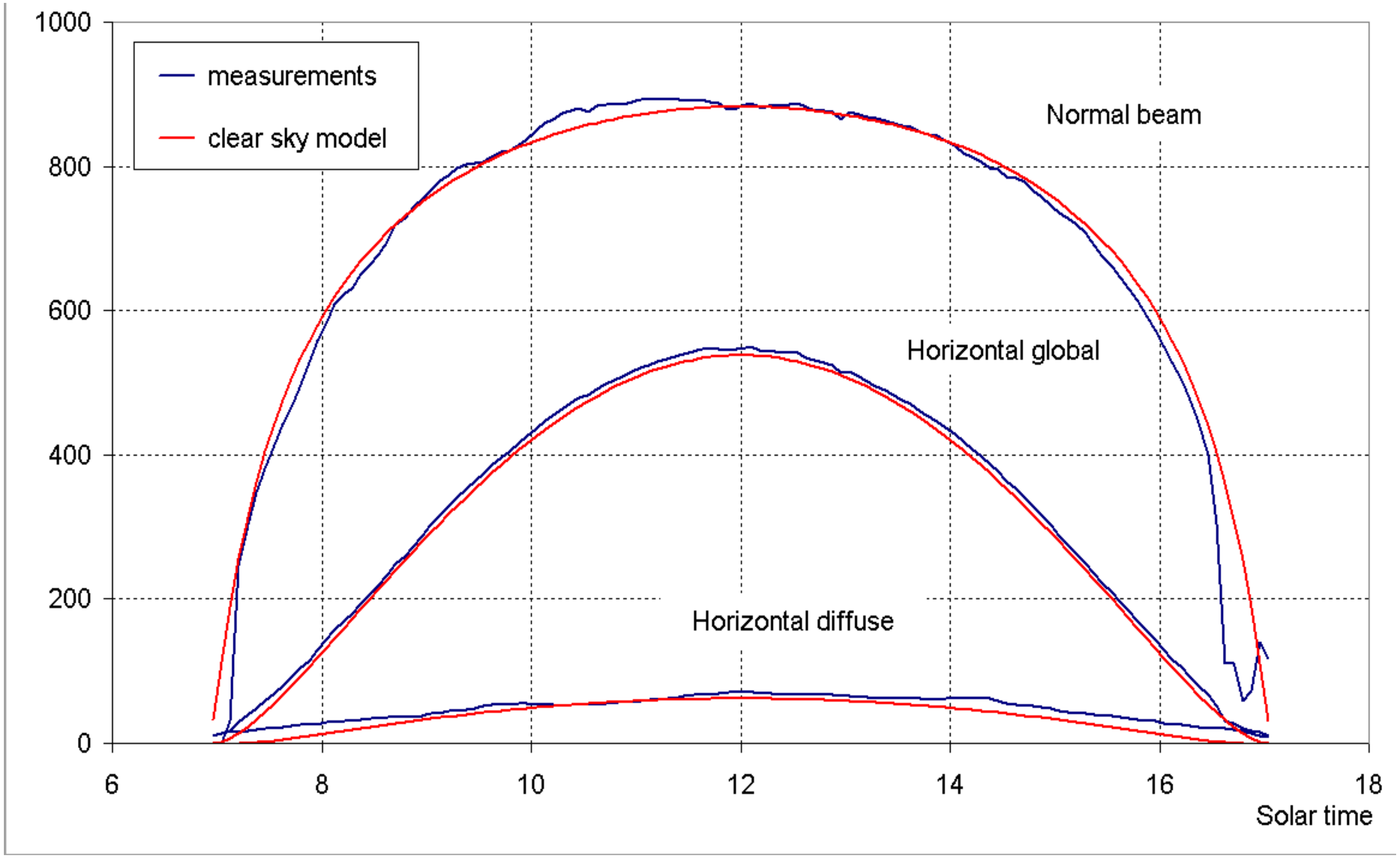
1000
800
600
400
200
0
6
8
10
12
14
16
18
Solar time
measurements
clear sky model
Normal beam
Horizontal global
Horizontal diffuse

Clearness Index

The clearness index k_T is a more general measure of the radiation that is transmitted through the atmosphere (transmittance).

It relates the radiation incident on the earth's surface to the extraterrestrial radiation:

$$k_T = G / G_o$$

As such, the clearness index is independent on solar geometry. Note, that there is still a significant influence of the air mass through increased extinction with increased path length even for constant atmospheric situations.

The monthly average clearness index generally varies from about 0.3 to about 0.8.

Optical Depth

Optical Depth (or Optical Thickness) τ: Dimensionless line integral of the extinction coefficient along any path in a medium.

For the volume extinction coefficient τ has the dimension of length^{-1} (area per volume).

Physical interpretation:

length of a path in units of the mean free path (in an uniform medium)

Aerosol optical Depth (AOD)

- quantitative measure of the extinction of solar radiation by aerosol scattering and absorption between the point of observation and the top of the atmosphere
- not directly measurable; retrieval from ground-based observations of atmospheric spectral transmission by sunphotometers
- The solar irradiance I at a given wavelength can be expressed as

  $$I = I_0 \exp(-m\delta)$$

  with I_0 the extraterrestrial solar irradiance, m the air mass and δ the total optical depth.
- The total optical depth δ at a given wavelength is composed of several components such as scattering by gas molecules, δR (Rayleigh scattering), extinction by aerosol particles, δA, absorption of trace gases, δG, like ozone, and possible cloud contamination. Thus, the AOD can be obtained from the total optical depth by subtracting modeled estimates of the other components:
- AOD = δA = δ - δR - δG

Atmospheric Turbidity

- **Linke turbidity factor T_L**: Measure of optical depth of the atmosphere due to aerosol particles and water vapour relative to a dry and clean atmosphere: $T_L = \tau(m_r) / \tau_{Rayl}(m_r)$
- Interpretation: Number of clean and dry atmospheres necessary to get the same extinction effect as that produced by the actual atmosphere
- T_L depends on the optical depth of the clean and dry atmosphere which is very sensitive to the air mass AM (or m_r). Therefore, T_L depends on AM, and consequently, on solar elevation.
- T_L generally lies between 2.0 (for a clean and dry atmosphere) and 6.0 (for a humid and polluted atmosphere). A complete clean and dry atmosphere (‘Rayleigh atmosphere‘) gives the value TL=1.

Clear sky modeling

Simple broadband clear sky model for direct and diffuse irradiance (Bird)

Basic equations:

$$I_{dir} = I_o (\cos\theta)\ (0.9662)\ \tau_{Rayl}\ \tau_{O3}\ \tau_{MolAbs}\ \tau_{H2O}\ \tau_{Aer}$$

$$I_{atm\_sc} = I_o (\cos\theta)\ (0.79)\ \tau_{O3}\ \tau_{Rayl}\ \tau_{MolAbs}\ \tau_{H2O}\ \tau_{AerAbs}\ [0.5 (1- \tau_{Rayl}) + B_a (1- \tau_{AerSc})] / 1 - m + (m)^{1.02}$$

$$Ig = (I_{dir} + I_{atm\_sc}) / (1-r_g r_s)$$

with I_o: extraterrestrial irradiance

τ : atmospheric transmittances

Clear Sky Index

- The clear sky index k_T* is a more general measure of the radiation that is transmitted through the atmosphere (transmittance).
- It relates the radiation incident on the earth's surface to the radiation in the clear sky case
- $k_T^* = G / G_{clear}$
- As such, the clear sky index is independent on solar geometry and should be free of influence of the atmospheric path length. As clear sky models are not perfect, there is some influence left.
- The clear sky index varies from almost 0 to about 1.1. Values above one are possible, if the sky is clearer than then model expects or in broken cloud situations where reflections from cloud add to the radiation at the ground.

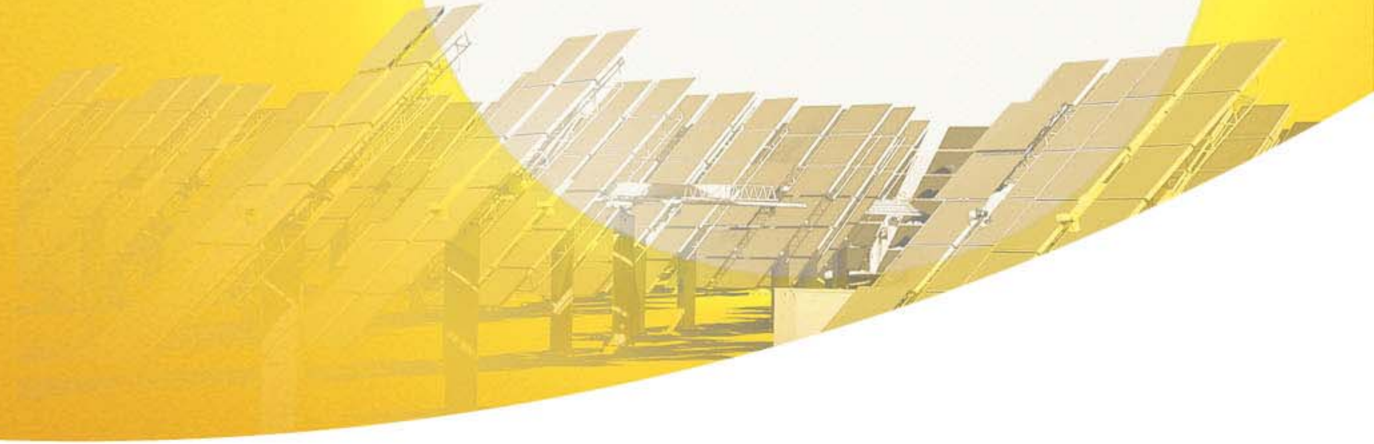

Ground Measurements

Instruments

- **Absolute Cavity Pyrheliometer**
  A self-calibrating, electrical-substitution, view- limited thermopile radiometer the aperture of which is maintained normal to the sun's beam radiation.

- **Pyrheliometer**
  Same as an absolute cavity except that it is not self-calibrating; i.e., a view-limited radiometer the aperture of which is maintained normal to the sun's beam component.

- **Pyranometer**
  A radiometer used to measure all radiation incident on its flat receiver from a 2-pi steradians hemisphere.

Solar radiation instruments

direct irradiance

- absolute cavity radiometer (current world reference of calibration, used to transfer calibration from the Word Radiation Reference in Davos to working phyherliometers)
- field pyrheliometer
- Field of view usually 5°
- combined measurement uncertainty: 1%*
- rotating shadowband pyranometer uncertainty: 2%

*target accuracy of Baseline Surface Radiation Network (BSRN)

Solar radiation instruments

- Most pyranometers use a thermopile as means of converting solar irradiance into an electrical signal.
- Conversion of temperature difference between hot and cold junctions of the thermopile to electrical voltage (~40 µV C^{-1} jct^{-1}).
- Advantage: Thermopile is spectrally neutral across the entire solar spectrum (domes may have spectral dependencies)
- Disadvantage: Output is temperature dependent and the instruments must ‘create’ a cold junction.
- Three primary types of instruments:
  - Black and White
  - Non-temperature compensated (Single and double domed)
  - Temperature compensated (Single and double domed)
- uncertainty: 2%* – 5% (*target accuracy of Baseline Surface Radiation Network (BSRN))

Pyranometer Types

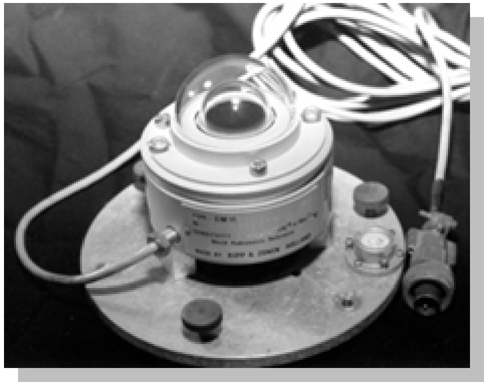

K & Z CM11
(double dome, temperature compensated)

EKO Black & White (single dome)

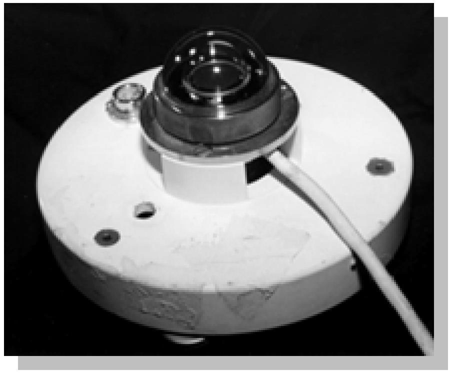

K & Z CM5
(single dome, non-temperature compensated)

Photoelectric Pyranometers

- Spectral response is non-linear and does not match solar spectrum.
- General calibrations are through comparison with pyranometers, therefore there are spectral mismatch problems.
  must be used in the same lighting conditions as those under which it was calibrated.
- Pyranometer sensors are calibrated against an Eppley Precision Spectral Pyranometer (PSP) under natural daylight conditions. Typical error under these conditions is ±5%.
- Similar problems arise when using sensors calibrated in one climate regime and used in a different regime.

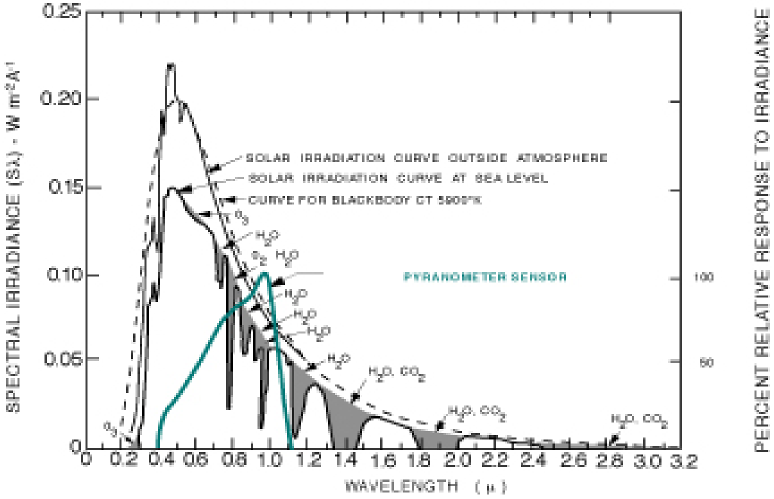

Solar radiation instruments

diffuse irradiance

- shaded pyranometers
  - pyranometer with shading ring
  - pyranometer with shading disc and sun tracking device
- uncertainty: 4%*- 8%

*target accuracy of Baseline Surface Radiation Network (BSRN)

Precise sensors *(also for calibration of RSP)*:

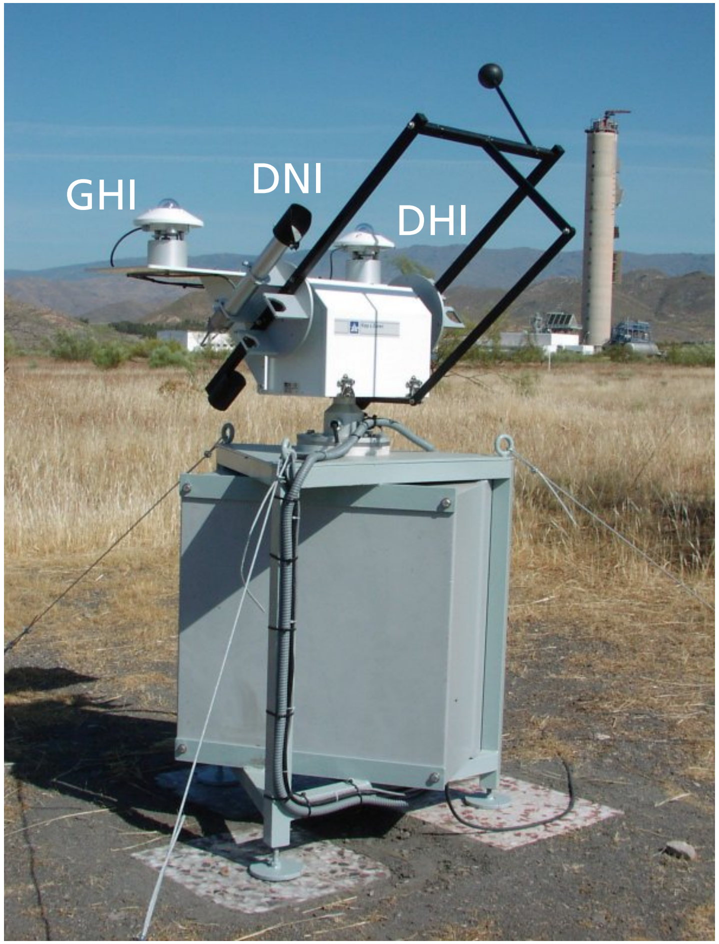

Thermal sensors:
pyranometer and pyrheliometer,
precise 2-axis tracking

Advantage:

+ high accuracy
+ separate GHI, DNI and DHI sensors
  (cross-check through redundant measurements)

Disadvantages:

- high acquisition and O&M costs
- high susceptibility for soiling
- high power supply

Instrumentation for unattended abroad sites:

Rotating Shadowband Pyranometer (RSP)

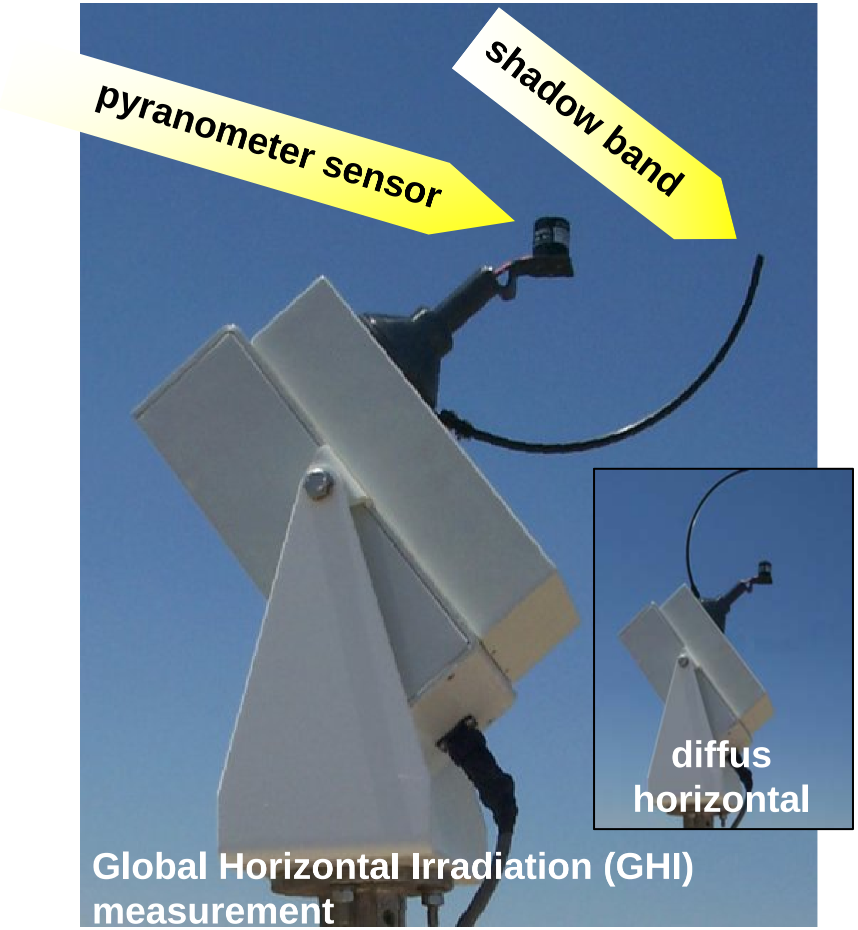

Sensor: Si photodiode

Advantages:

+ fairly acquisition costs
+ small maintenance costs
+ low susceptibility for soiling
+ low power supply

Disadvantage:

- special correction for good accuracy necessary *(established by DLR)*

Soiling – Why pyrheliometers don´t meet the need

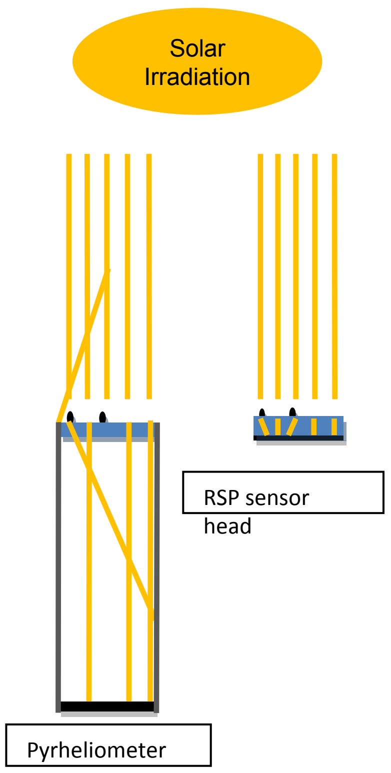

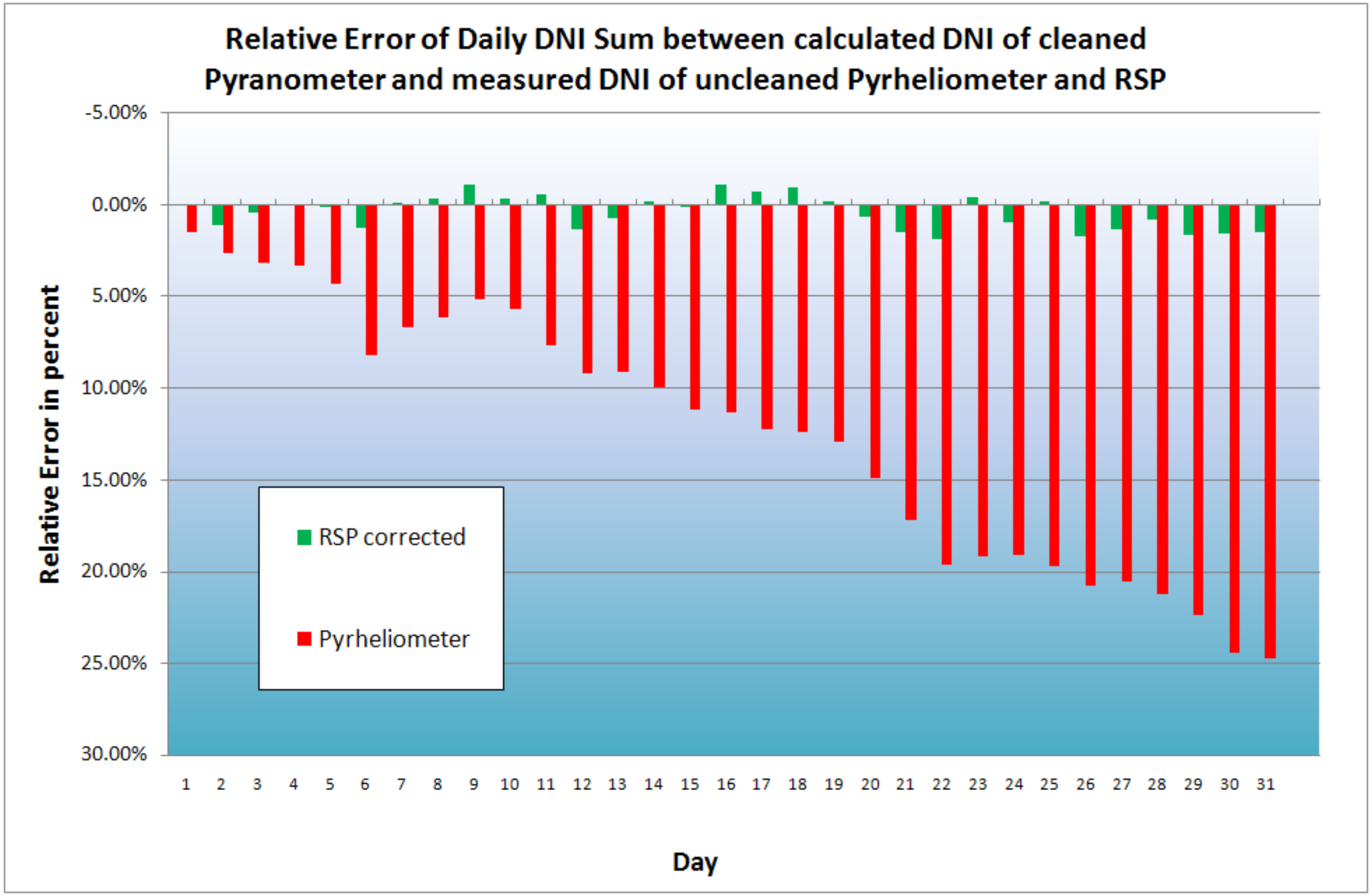

RSP – Principle of Measurement

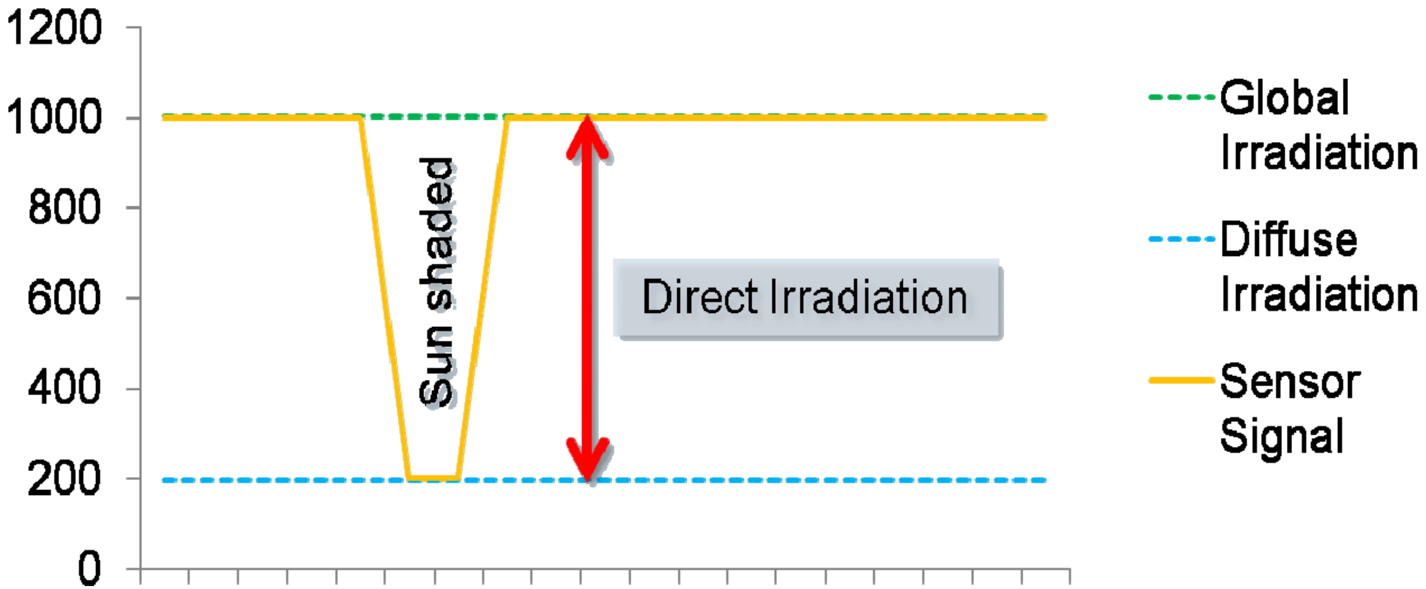

Simplified sensor signal during shadow band rotation, which takes place once per minute and lasts about 1.5 seconds per rotation.

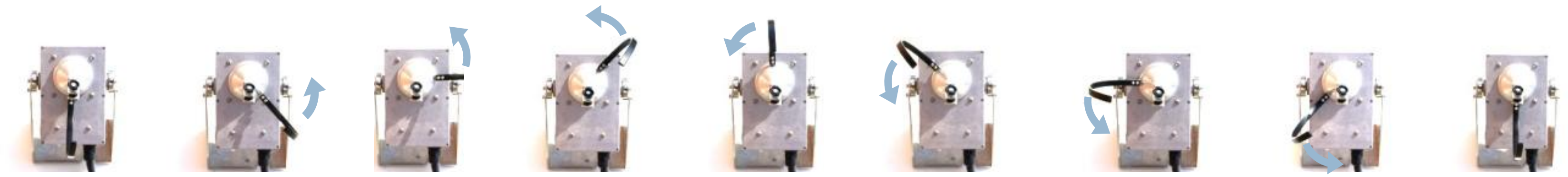

Solar Millennium Meteostations

Measurements

- → All relevant meteorological data for CSP in 1-10 min intervals
  - → Direct Normal Irradiation (DNI)
  - → Global Horizontal Irradiation (GHI)
  - → Diffuse Horizontal Irradiation (DHI)
  - → Temperature
  - → Relative Humidity
  - → Wind speed
  - → Wind direction
  - → Atmospheric pressure or others on request

Solar Millennium Meteostations

Main Features

- Fully automated measurement and data acquisition at arbitrary remote sites
- Automated daily data transfer via mobile communication network
- Autarkic power supply by solar panel and battery
- Minimal maintenance effort
- Rugged station for tough climatic conditions
- Certified Quality:
  - One by one radiation sensor calibration by German Aerospace Center (DLR)
  - Standard deviation in radiation ~4% (individually determined by DLR)
  - Sophisticated correction formulas developed in cooperation with DLR

Radiometer Characteristics

- **Calibration Stability**
  can it maintain a calibration over a long period of time?
- **Cosine response**
  are the optics of a quality that the signal output is independent of solar elevation?
- **Temperature stability**
  will a given input provide the same output voltage independent of temperature?
- **Spectral Quality**
  is the instrument spectrally flat across the solar spectrum so that it responds linearly to changes in the solar spectrum?
- **Tilt**
  does the instrument behave the same when tilted?

Calibration

International calibration methods

- Pyranometer and pyrheliometer calibration scales are traced to the World Radiometric Reference (WRR) (maintained by the World Radiation centre (WRC) in Davos, Switzerland)
- WRC maintains the World Standard Group (WSG), and thus the World Radiometric reference (WRR), with the highest possible stability and to provide the highest possible world-wide homogeneity for solar irradiance measurements.

Calibration – World Radiometric Reference

- measurement standard representing the SI unit of irradiance
- introduced to ensure world-wide homogeneity of solar radiation measurements
- in use since 1980determined from the weighted mean of the measurements of a group of 15 absolute cavity radiometers which have been fully characterized
- Currently, the WSG is composed of 6 instruments: PMO-2, PMO-5, CROM-2L, PACRAD-3, TMI-67814 and HF-18748.
- estimated accuracy of 0.3%
- mandatory use introduced by WMO in its statutes in 1979

Availability of ground measured data

long term measurements at meteorological stations

- National Meteorological offices
- World radiometric Network (by World Meteorological Organisation)
- Baseline Surface Radiation Network

World radiometric network

- global irradiance & sunshine duration
- ca. 1200 stations
- monthly or daily values

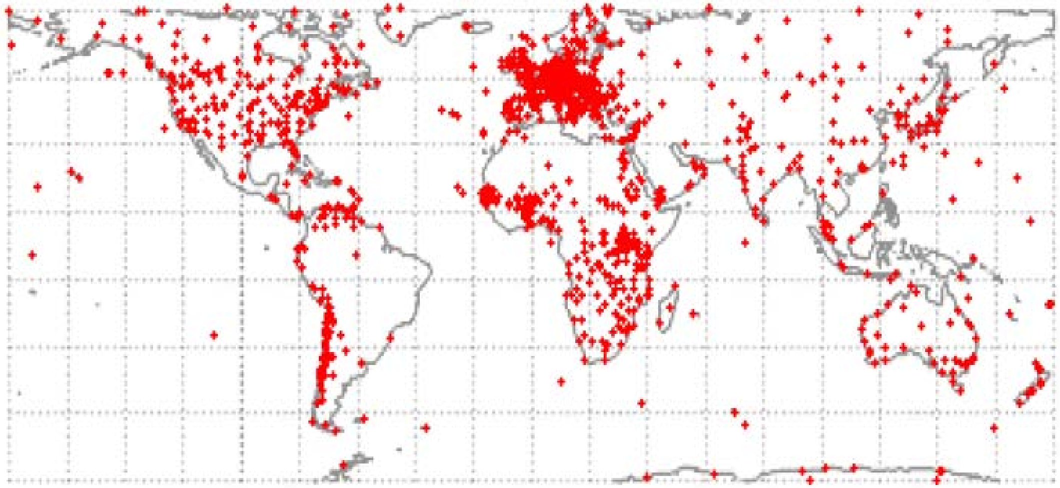

World Radiometric network 1966- 1993
(source: WRDC/WMO, Cros et al. , 2004)

Baseline surface radiation network

- high quality measurements
- global, direct, diffuse
- minute values

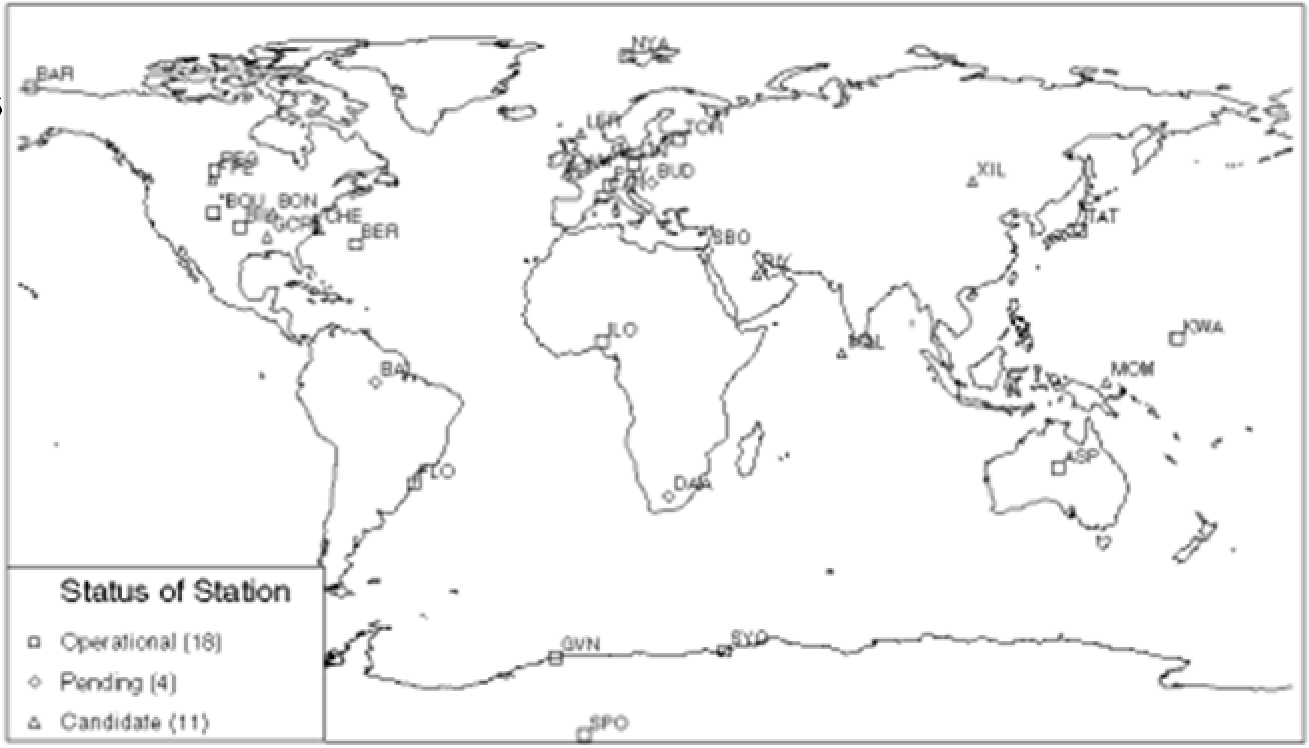

Resource products based on ground measured data

- **spatial interpolation techniques** to derive maps and site specific data
- **stochastic models or average daily profiles**
  to derive values with high temporal resolution
  (daily, hourly or minute values)
- **statistical global to beam models** to derive DNI

Satellite based assessments

How two derive irradiance data from satellites

- The Meteosat satellite is located in a geostationary orbit
- The satellite scans the earth line by line every half hour

Das Meteosat System – Image recording

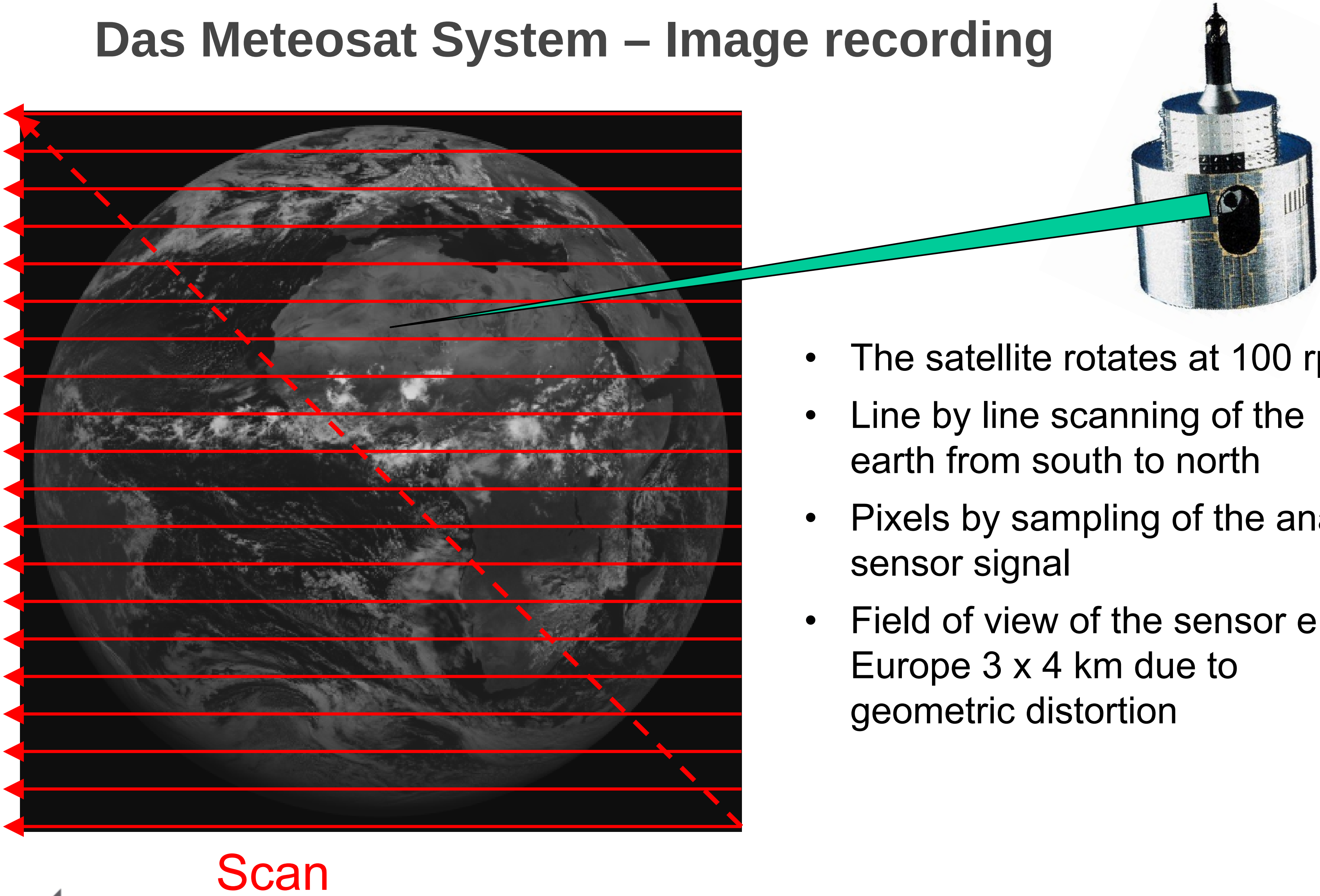

- The satellite rotates at 100 rpm
- Line by line scanning of the earth from south to north
- Pixels by sampling of the analog sensor signal
- Field of view of the sensor e.g. in Europe 3 x 4 km due to geometric distortion

How two derive irradiance data from satellites

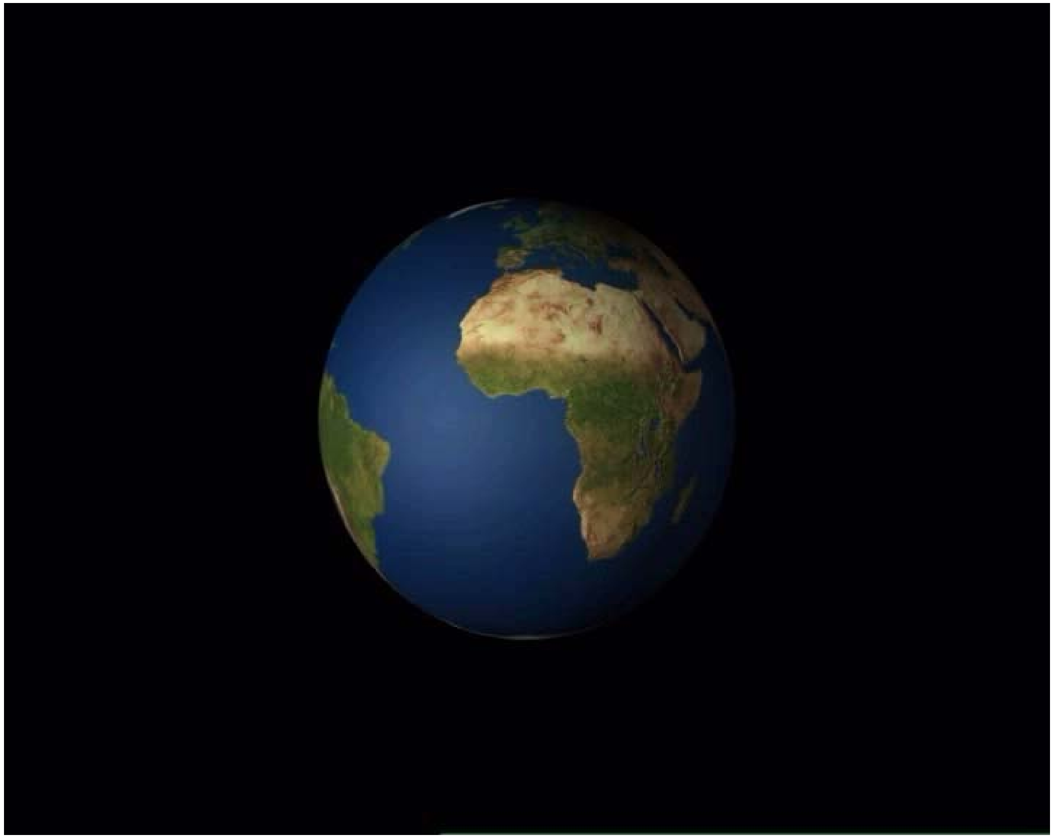

- The Meteosat satellite is located in a geostationary orbit
- The satellite scans the earth line by line every half hour
- The earth is scanned in the visible …

How two derive irradiance data from satellites

- The Meteosat satellite is located in a geostationary orbit
- The satellite scans the earth line by line every half hour
- The earth is scanned in the visible and infra red spectrum

How two derive irradiance data from satellites

- The Meteosat satellite is located in a geostationary orbit
- The satellite scans the earth line by line every half hour
- The earth is scanned in the visible and infra red spectrum
- A cloud index is composed from the two channels

Clear sky Model input data

- Aerosol optical thickness
  GACP Resolution 4°x5°, monthly climatology
  MATCH Resolution 1.9°x1.9°, daily climatology

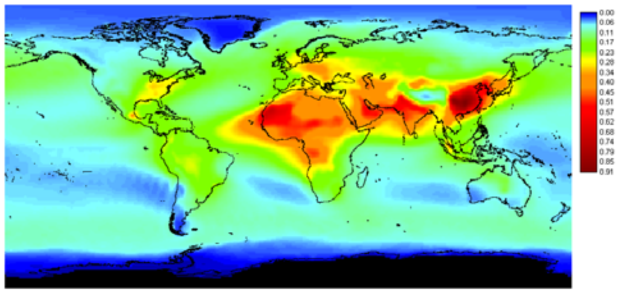

- Water Vapor: NCAR/NCEP Reanalysis
  Resolution 1.125°x1.125°, daily values

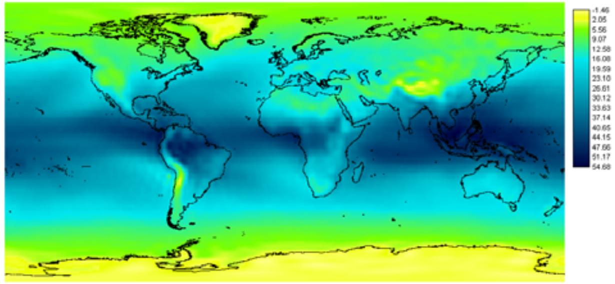

- Ozone: TOMS sensor
  Resolution 1.25°x1.25°, monthly values

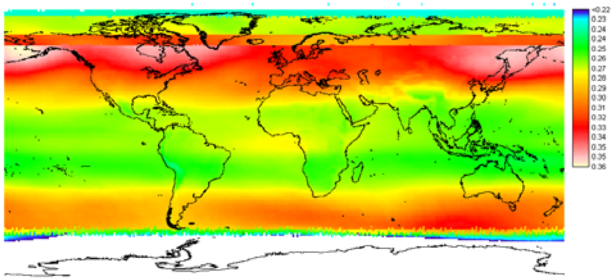

Uncertainty in Aerosols

- All graphs are for July
- Scales are the same! (0 – 1.5)
- Large differences in Aerosol values and distribution

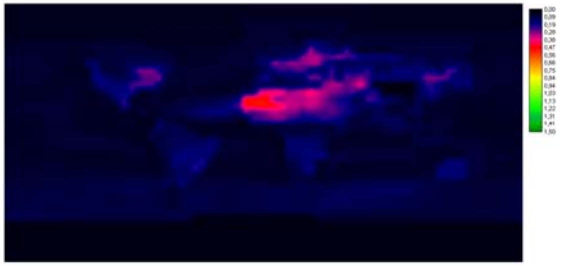

GADS

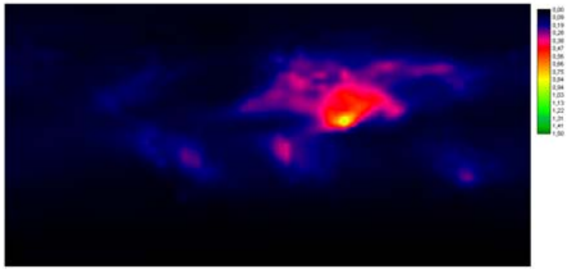

NASA GISS v1 / GACP

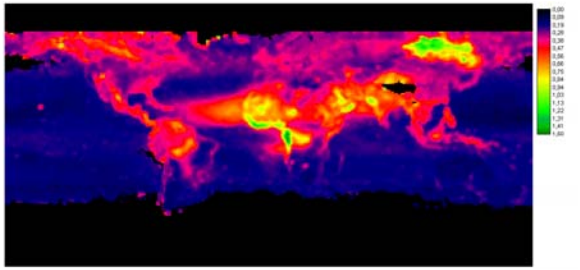

Toms

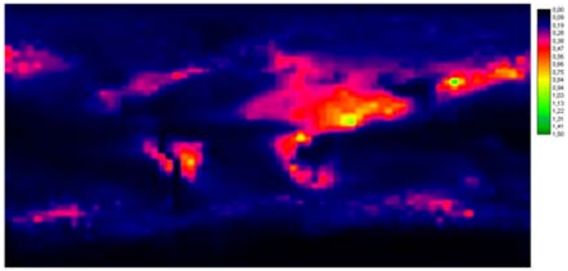

NASA GISS v2 1990

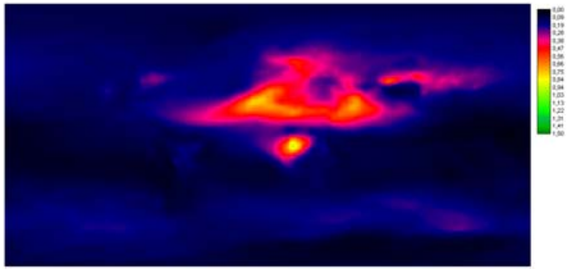

GOCART

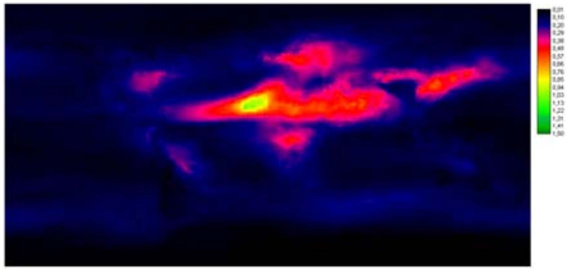

AeroCom

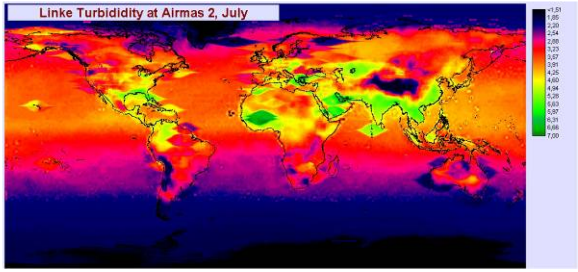

Linke Turbidity

Calculation of solar radiation from remote sensing

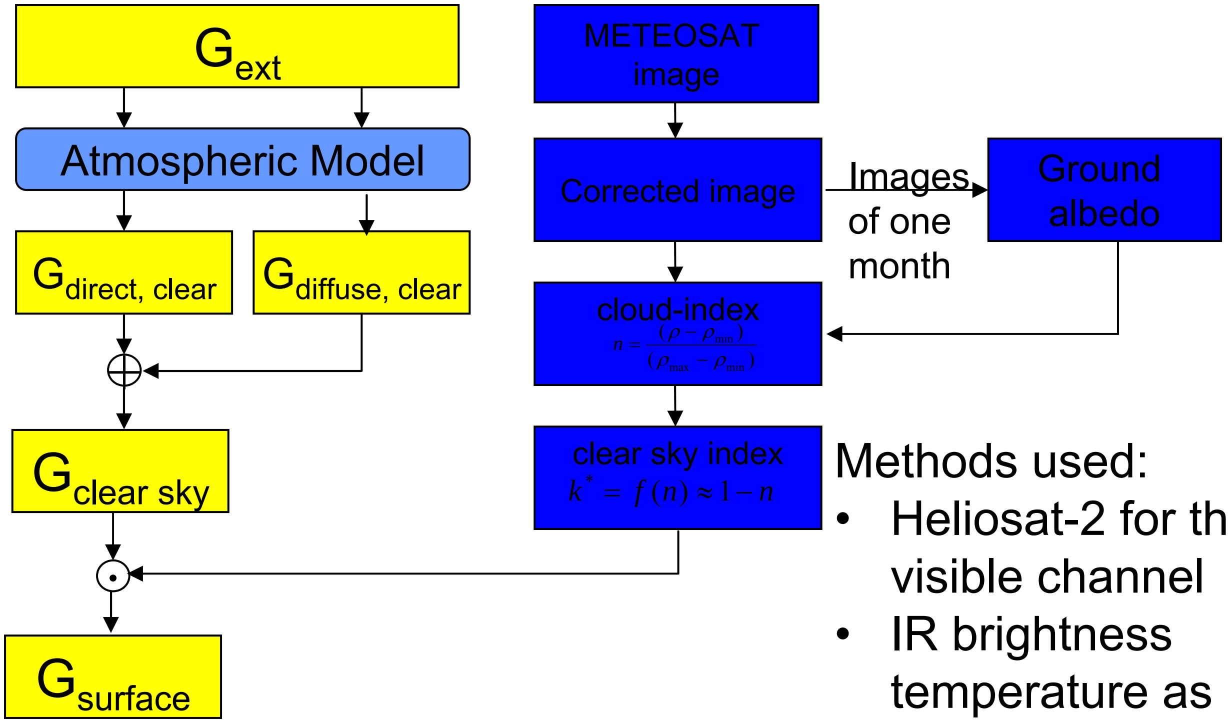

Methods used:

- Heliosat-2 for the visible channel
- IR brightness temperature as indicator for high cirrus clouds (T < -30°C, DNI = 0)

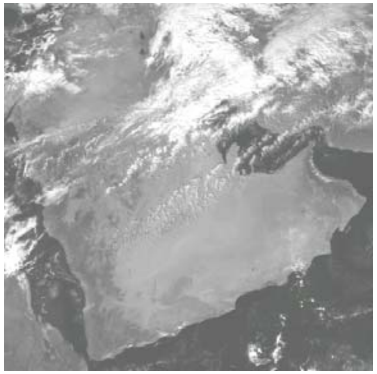

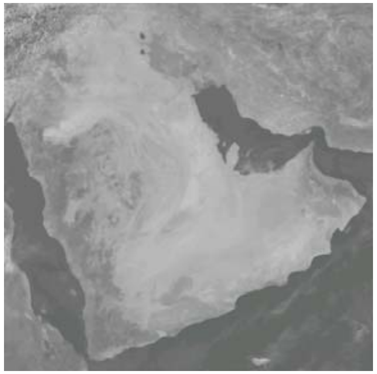

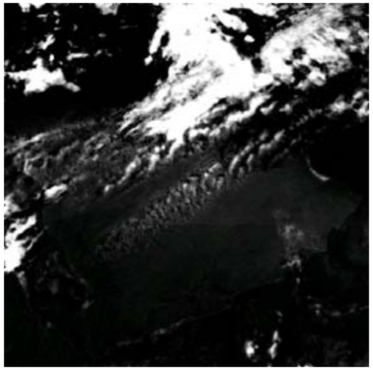

Cloud Transmission for GHI

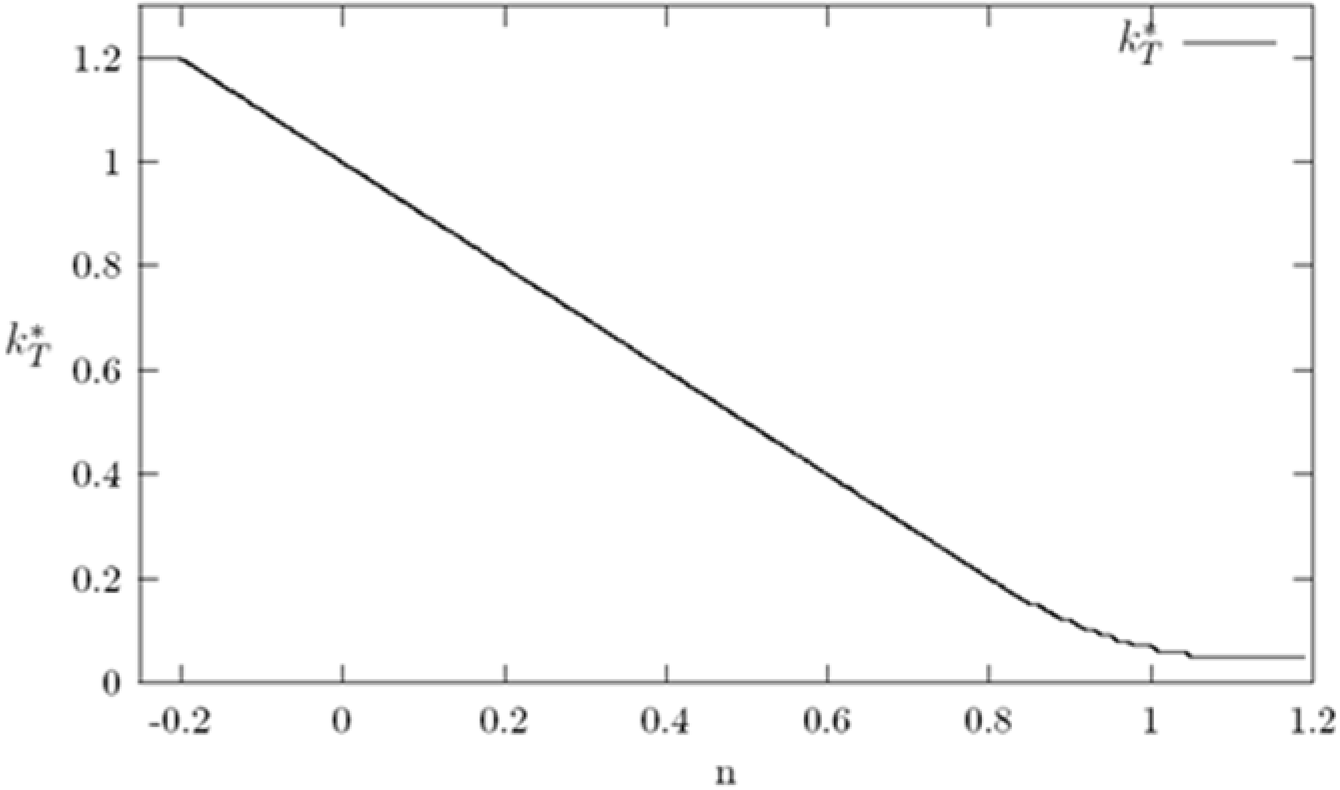

Cloud Transmission for DNI

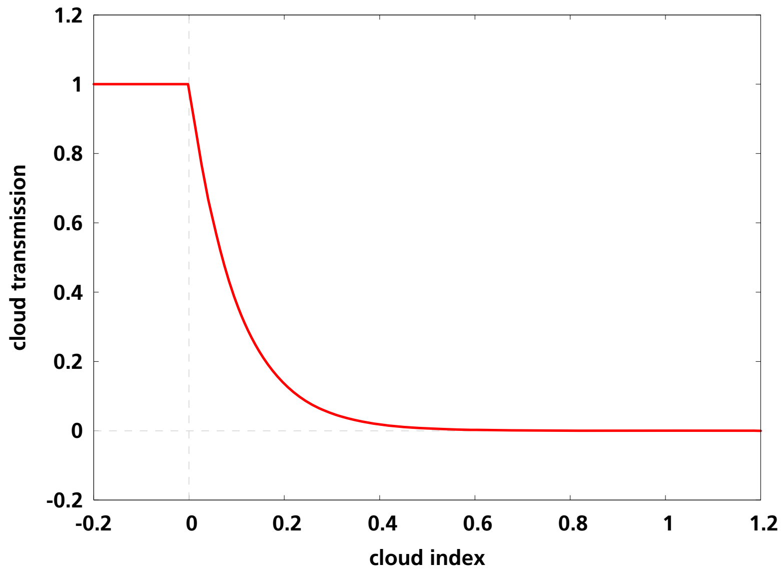

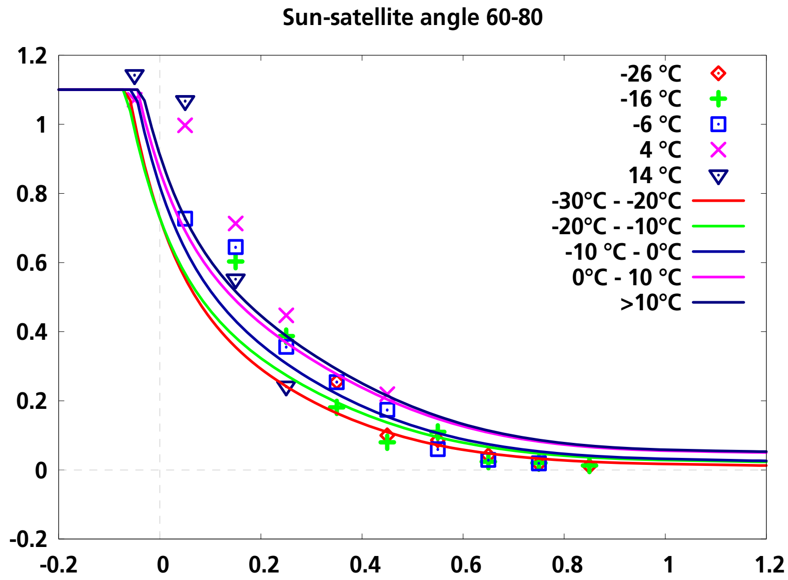

Simple function $\tau = e^{-10*ci}$

Complex functions:
Different exp. function for various viewing angles and brightness temperatures

Comparing ground and satellite data: time scales

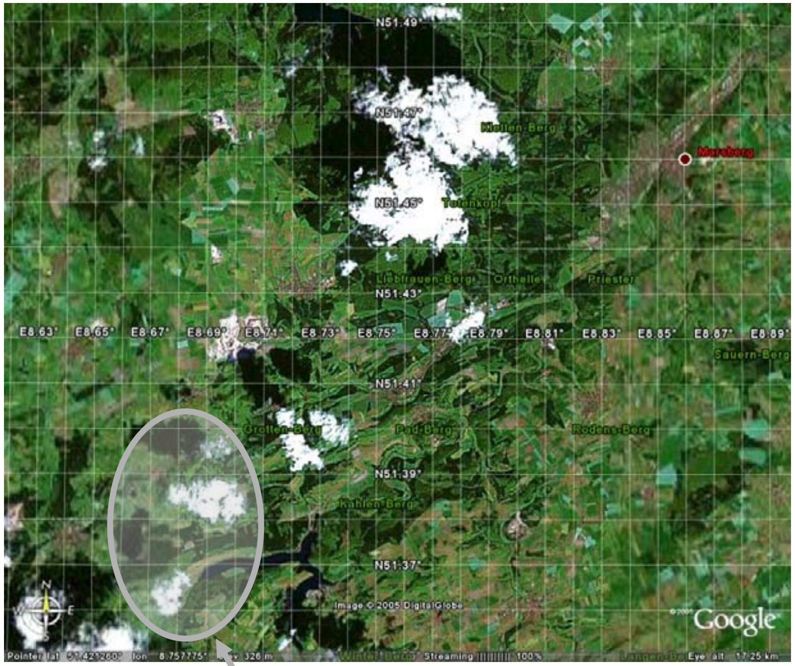

Hi-res satellite pixel in Europe

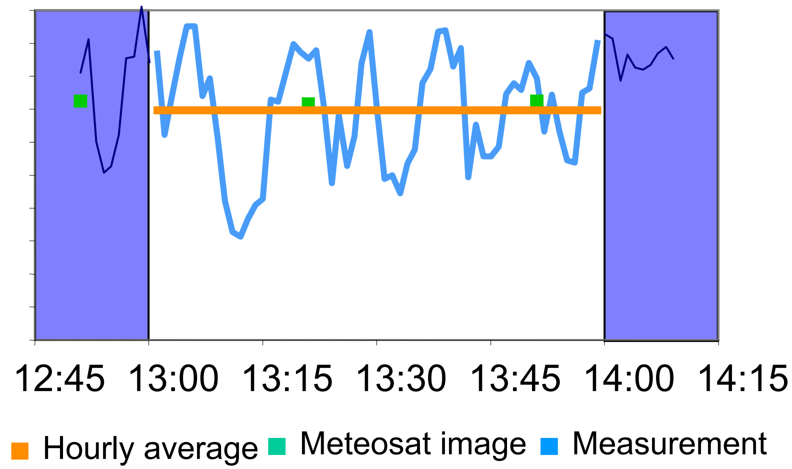

- Ground measurements are typically pin point measurements which are temporally integrated
- Satellite measurements are instantaneous spatial averages
- Hourly values are calculated from temporal and spatial averaging (cloud movement)

Constrution of hourly averages from satellite images

- The hourly irradiance values are calculated by a weighted average

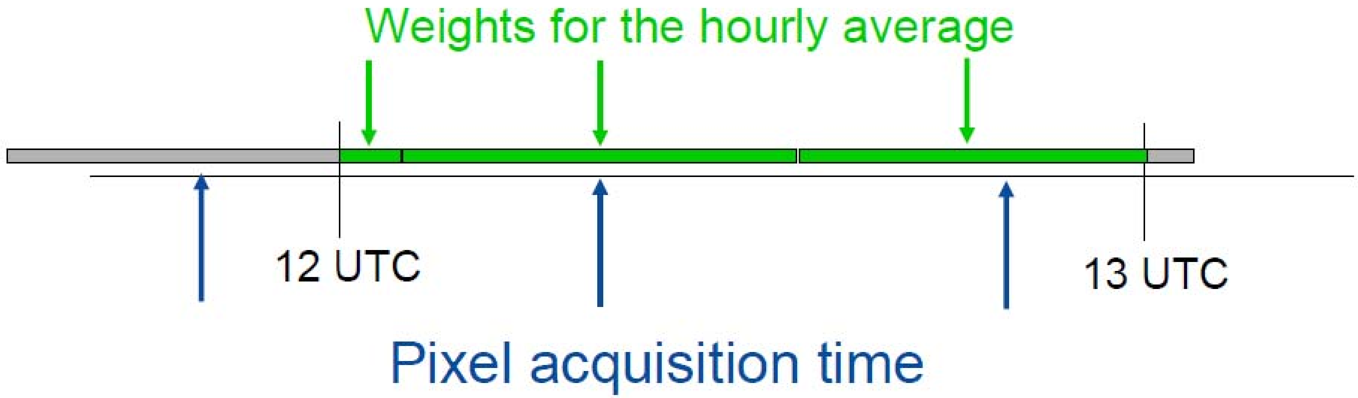

- full scan : 3 images per hour

Comparing ground and satellite data: “sensor size”

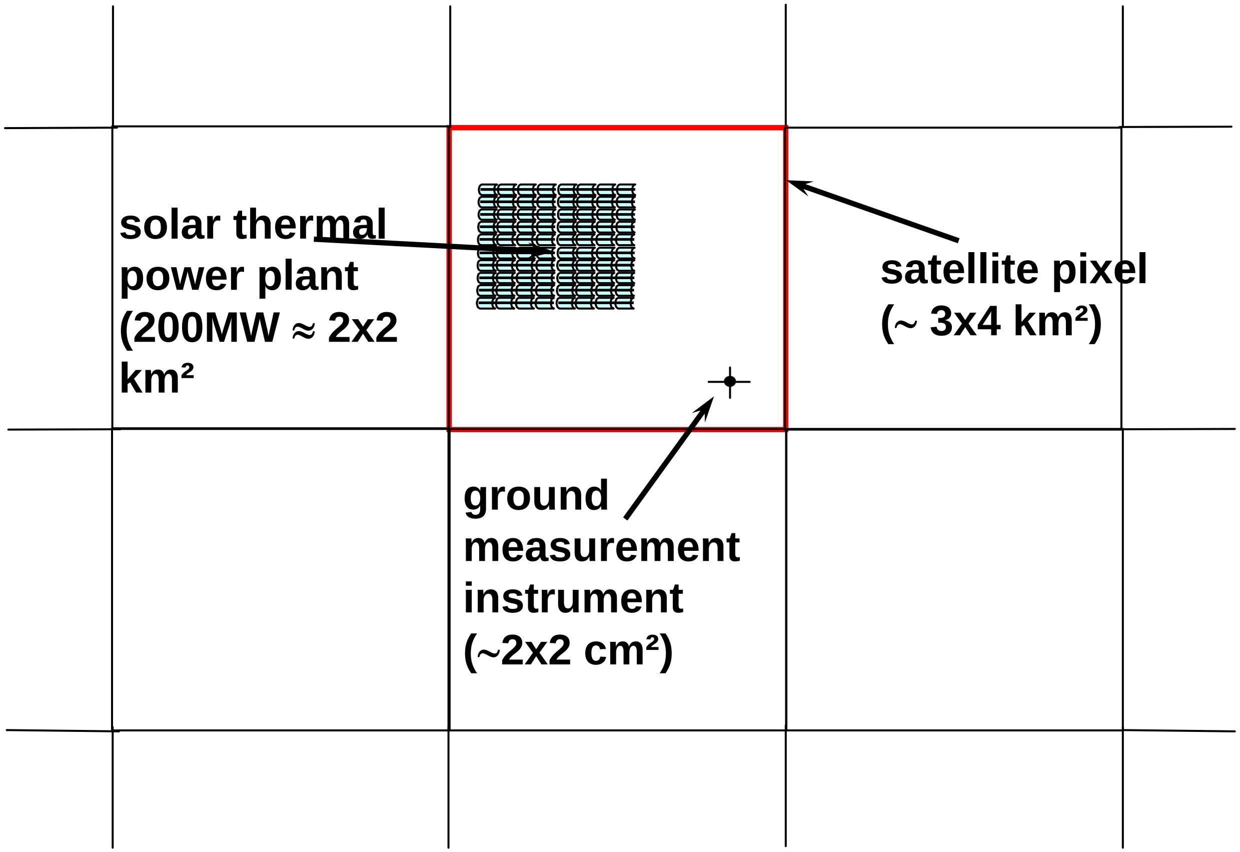

Comparison with ground measurements and accuracy

general difficulties: *point versus area* and
time integrated versus area integrated

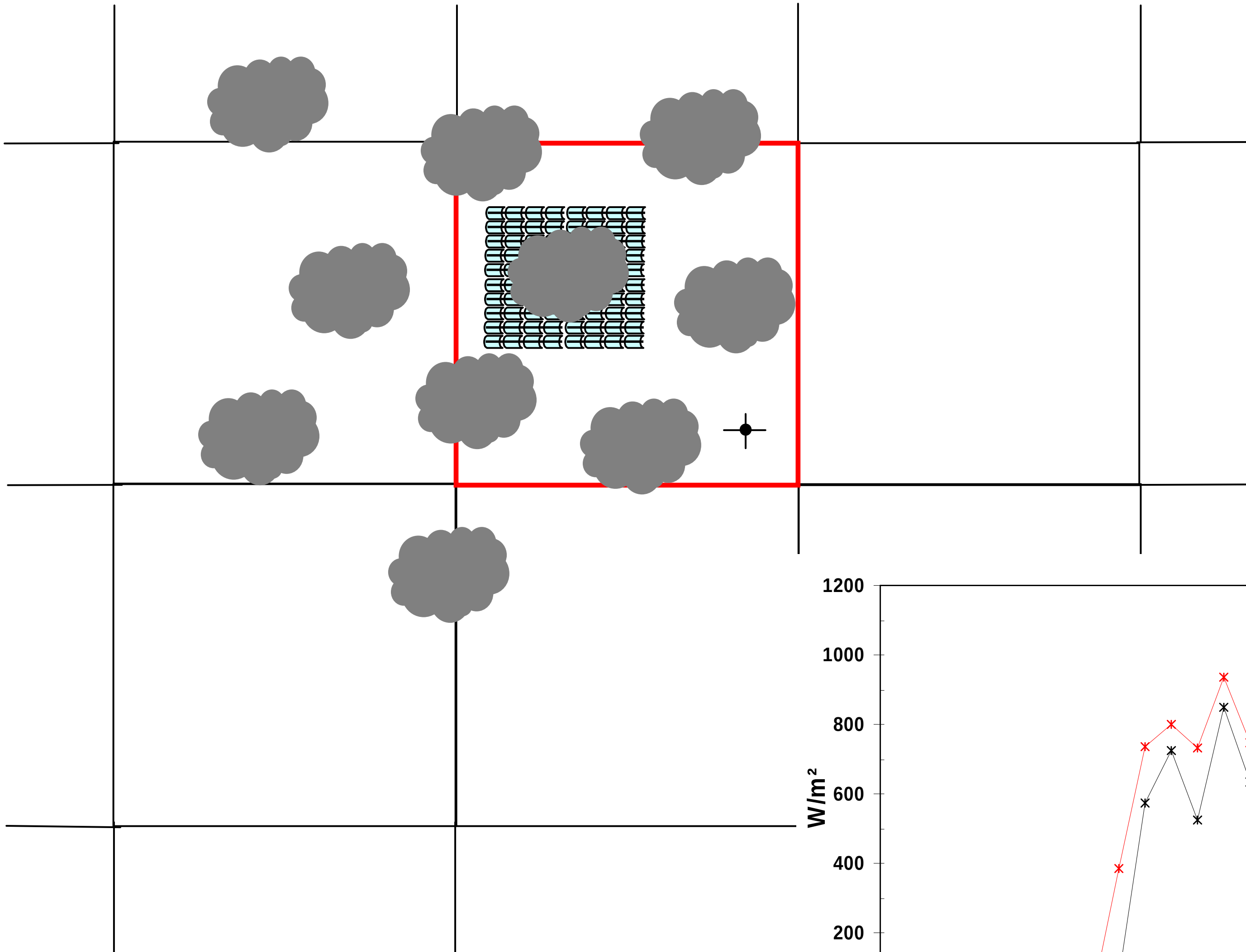

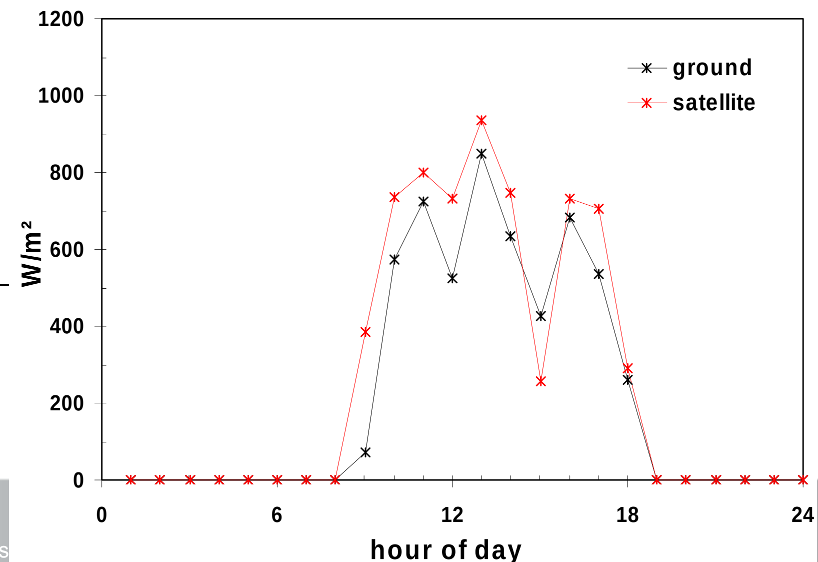

DNI time serie for 1.11.2001, Almería
Partially cloudy conditions, cumulus humilis

Comparison with ground measurements and accuracy

general difficulties: *point versus area* and
time integrated versus area integrated

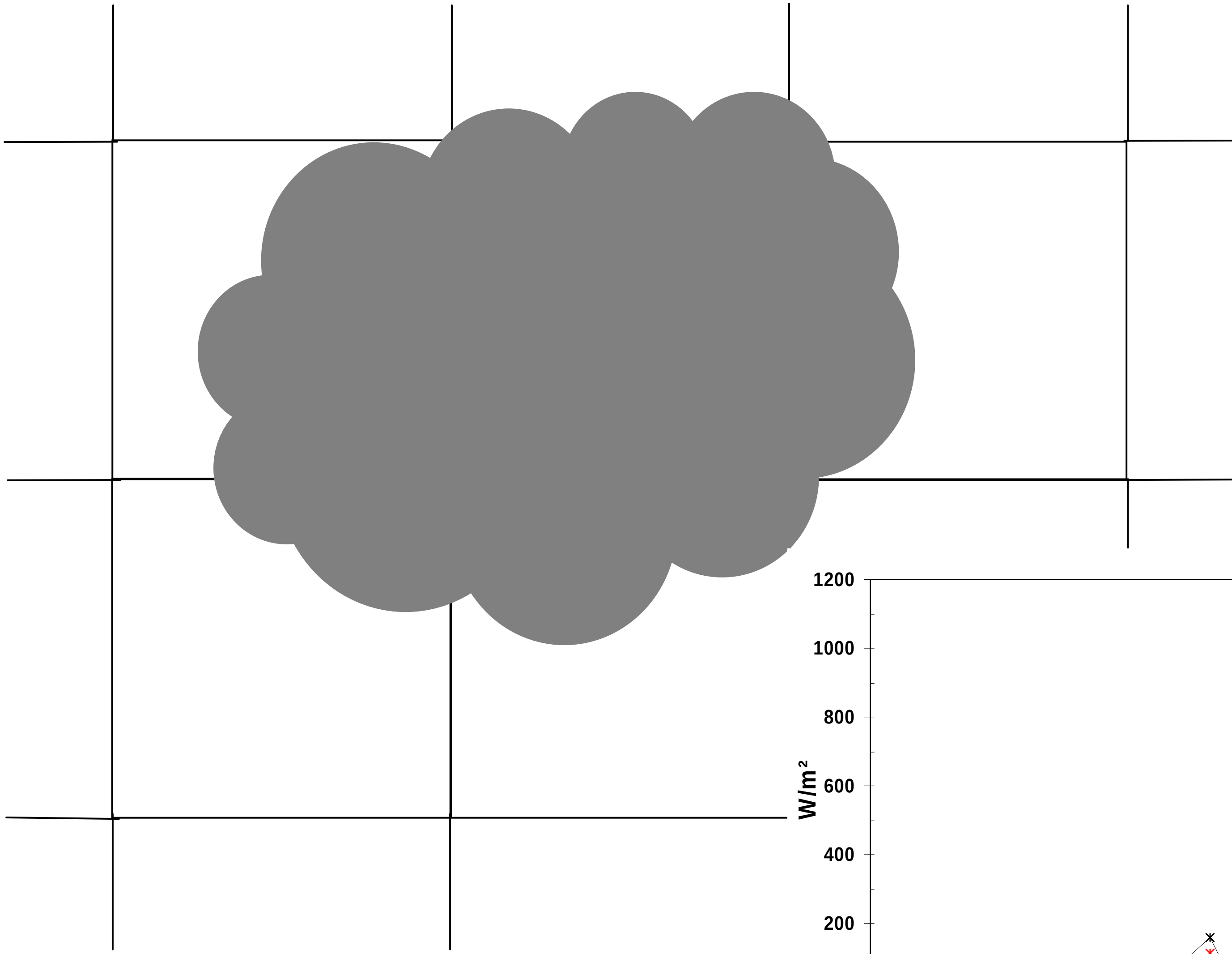

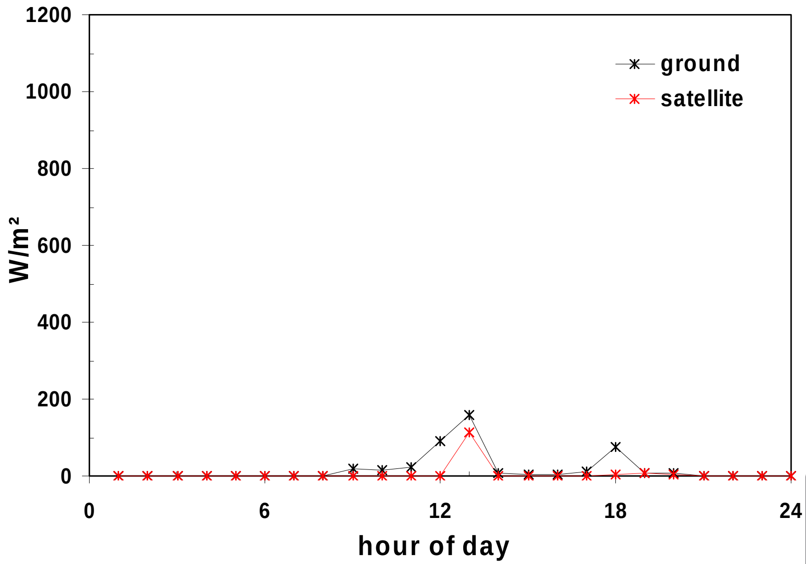

DNI time serie for 30.4.2000, Almería
overcast conditions, strato cumulus

Satellite data and nearest neighbour stations

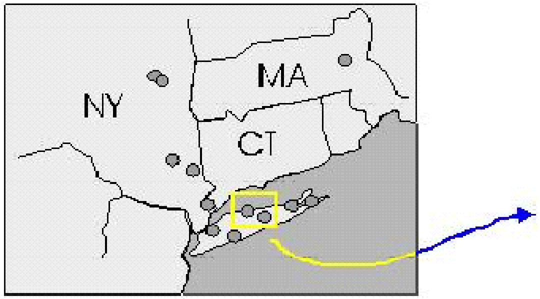

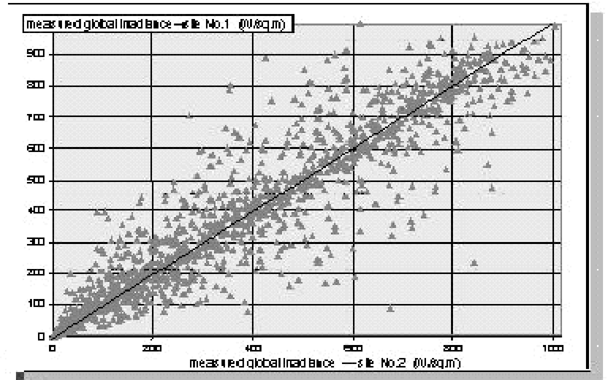

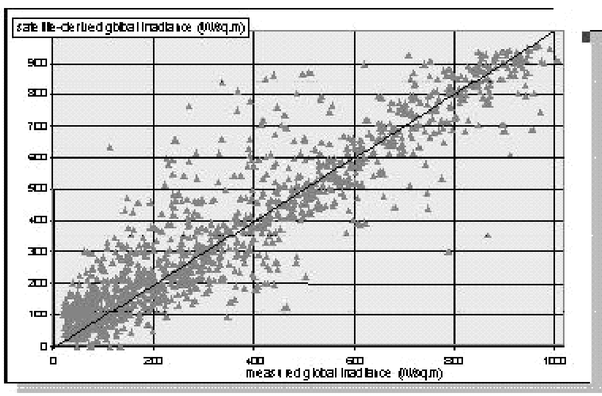

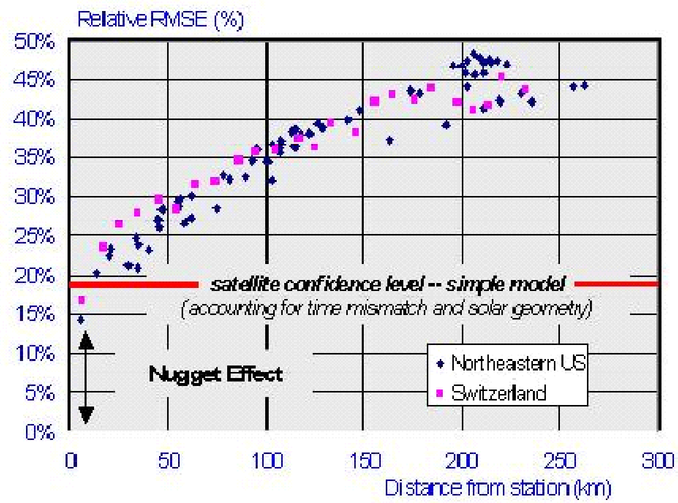

Perez et al., ASRC

- Satellite derived data fit better to a selected site than ground measurements from a site farther than 25 km away.

Meteosat Positions

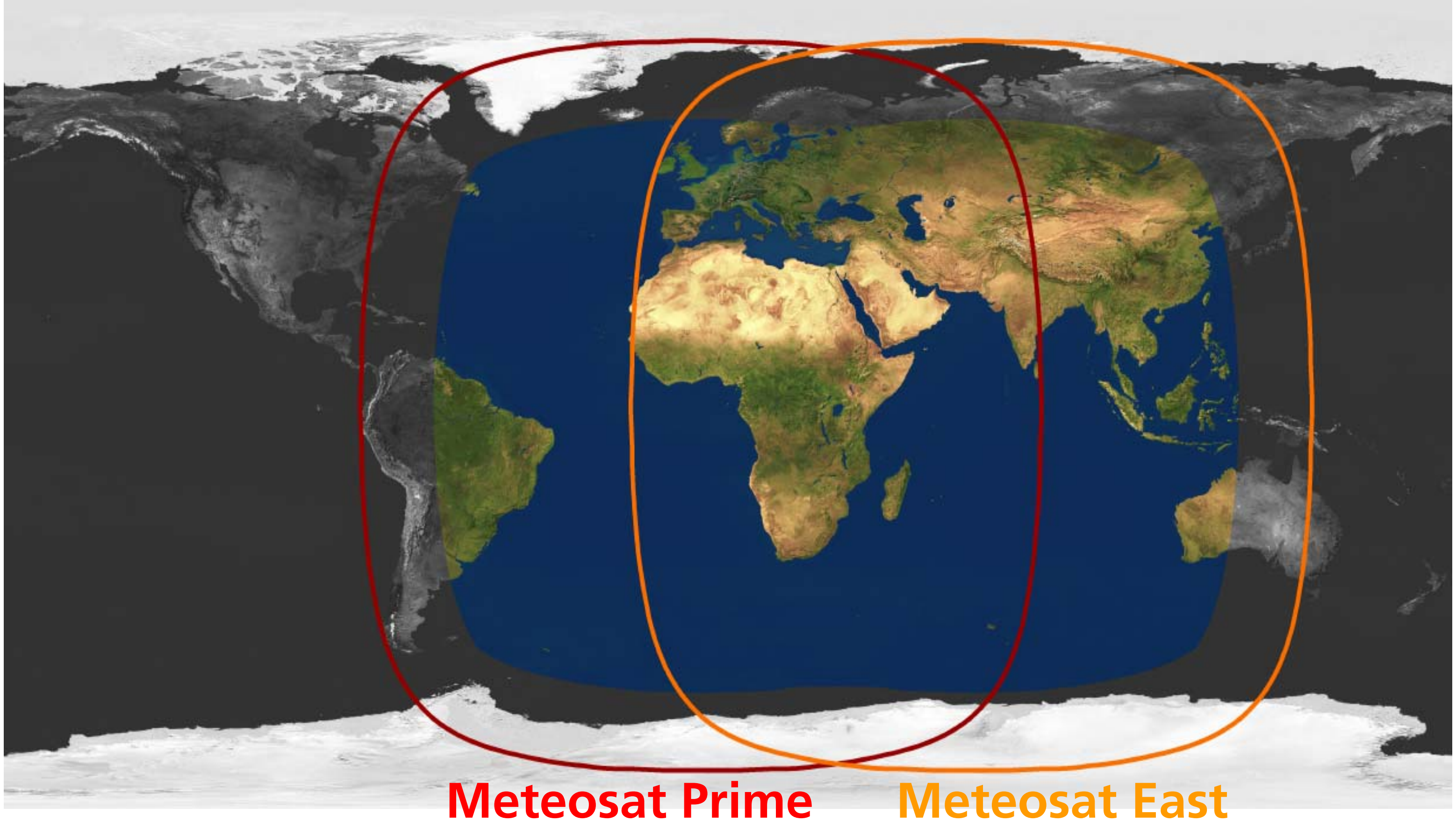

Satellite data

Comparision First und Second Generation

	1st Generation (MOP)	2nd Generation (MSG)
Radiometric	8 bit	10 bit
Spatial (VIS - HRV)	2.5 km	1 km
Spatial (all other)	5 km	3 km
Temporal	30 min	15 min
Spectral	3 channels	12 channels

Necessary changes in MSG Processing

- MSG does not have a full disc broadband vis channel. The HRV channel is due to the split coverage difficult to use.
- Two narrowband channels at 0.6 and 0.8 µm can be use to create a pseudo broadband channel We apply a method by Cros / Albuisson / Wald (2005).

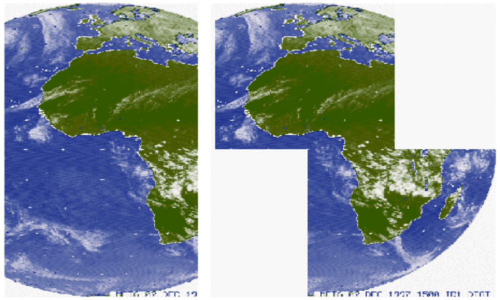

HRV Coverage

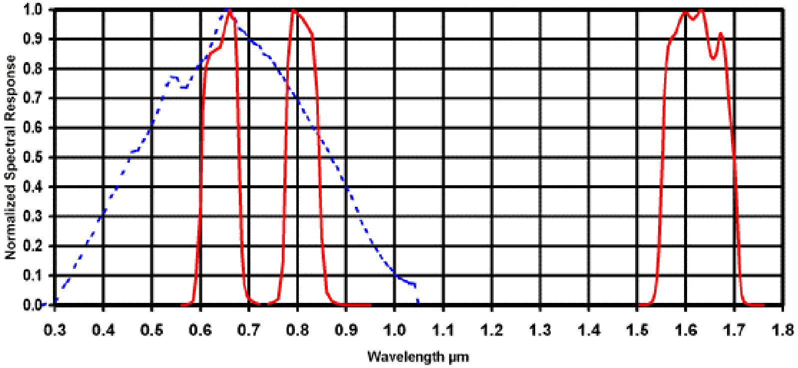

Spectral sensitivity

Solar radiation to tilted planes

Solar radiation on a tilted plane

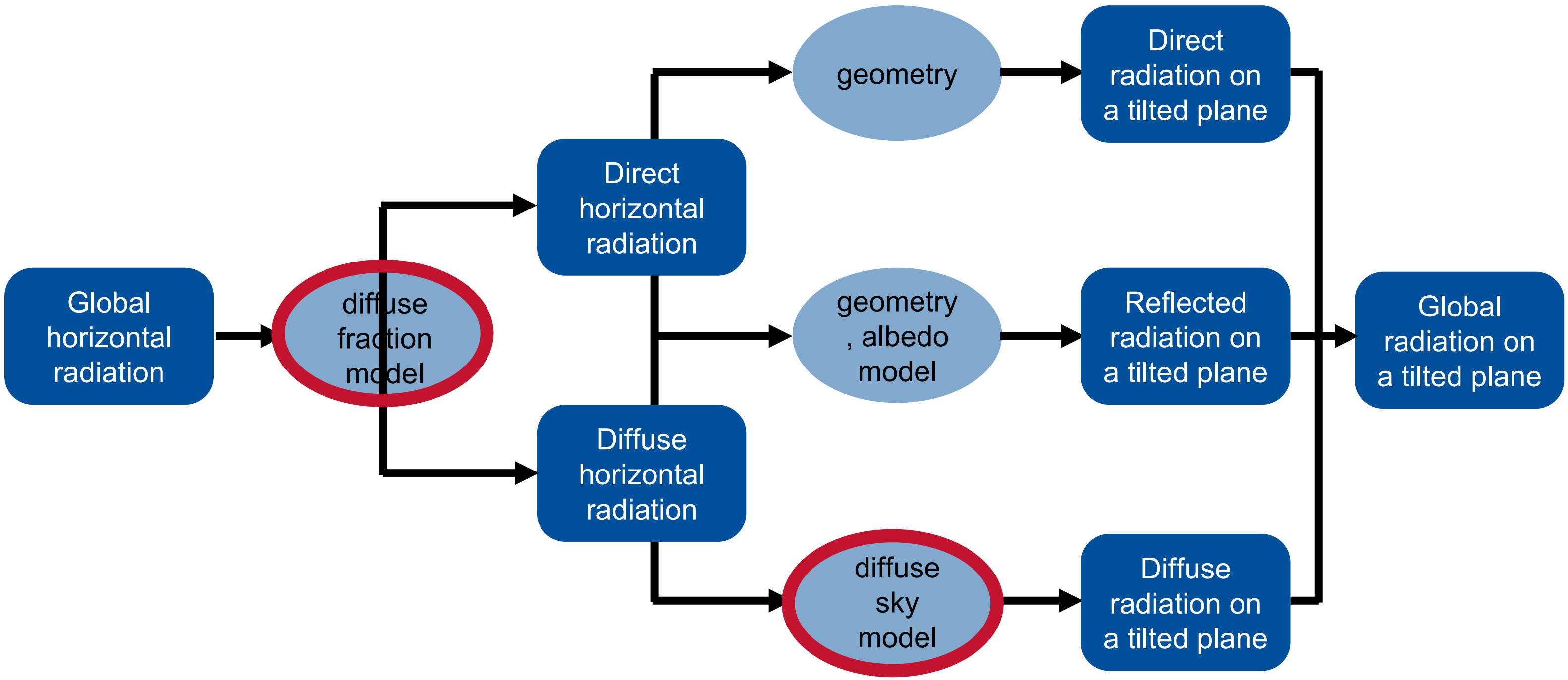

Direct radiation on a tilted plane

$$G_{bt} = G_{bn} \cos\theta$$

$$\text{With}: G_b = G_{bn} \cos\theta_z$$

$$G_{bt} = G_b \frac{\cos\theta}{\cos\theta_z}$$

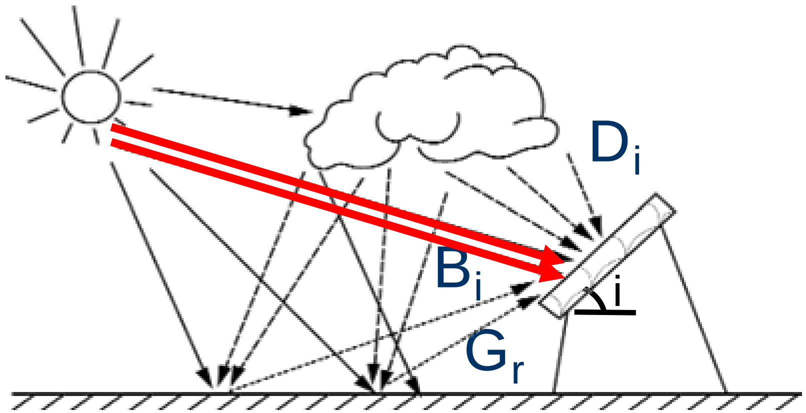

this is often referred as the geometric factor R_b

Radiation reflected from ground

$$G_{rt} = G\rho \frac{1-\cos\beta}{2}$$

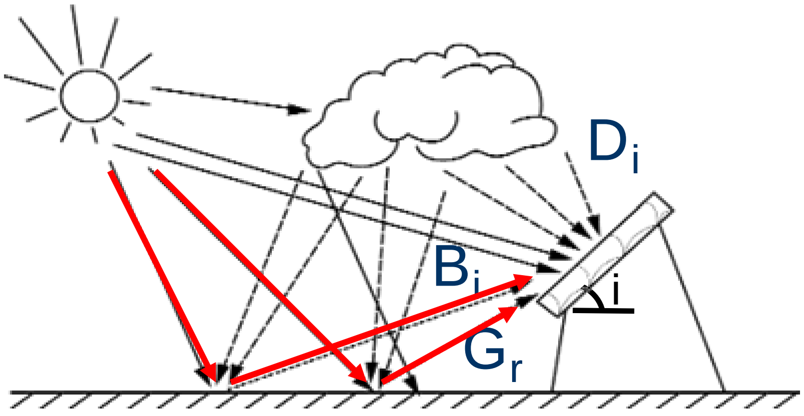

for isotropic ground reflectance ρ

Diffuse radiation to a tilted plane

$$G_{dt} = G_d \frac{(1+\cos\beta)}{2} \quad M_x M_y$$

Liu - Jordon

Temps / Coulson
Klucher

anisotropic effects

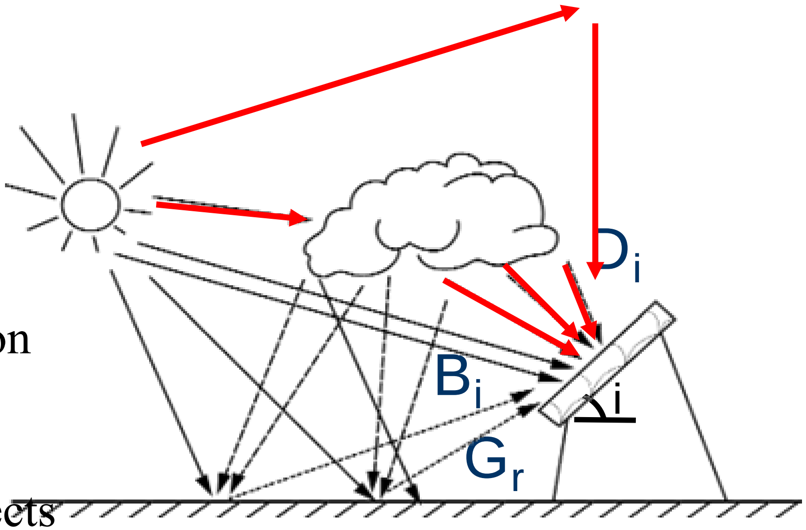

Radiation on a titled plane – more complex – Perez Model

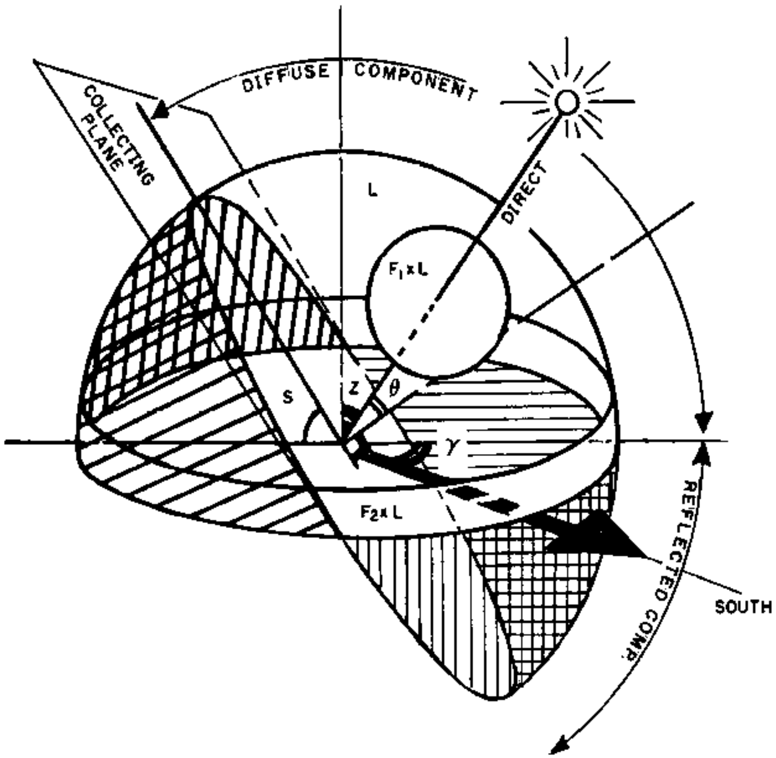

- Representation of the three radiation components seen by a tilted plane (direct, diffuse and reflected) and representation of the sky dome used in the Perez algorithm.
- Sky radiance is respectively equal to L, F_1L, and F_2L for the main, the circumsolar, and the horizon zone.
- Highly empirical approach!

Splitting Global in the components Diffuse + Direct

- Calculation of radiation on tilted planes needs diffuse fraction
- but: depends heavily on empirical tuning
- depending on considered time scale
- nonlinear!
- mainly related with: clearness index (global irradiance), solar elevation, turbidity, hour-to-hour-variability, surface albedo
- important: proper probability distribution of diffuse fraction

Isotropic versus non Isotrotropic diffuse radiation

- Circumsolar
- Horizon Brightening

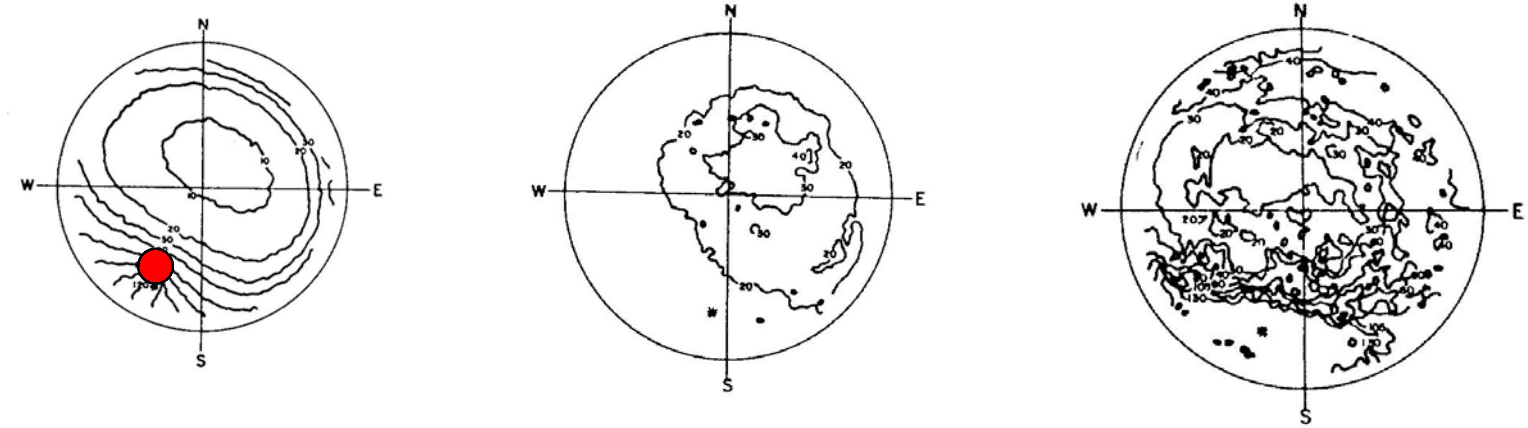

Clear sky

Cloudy sky

Intermediate sky
(broken cloudiness)

Diffuse fraction models

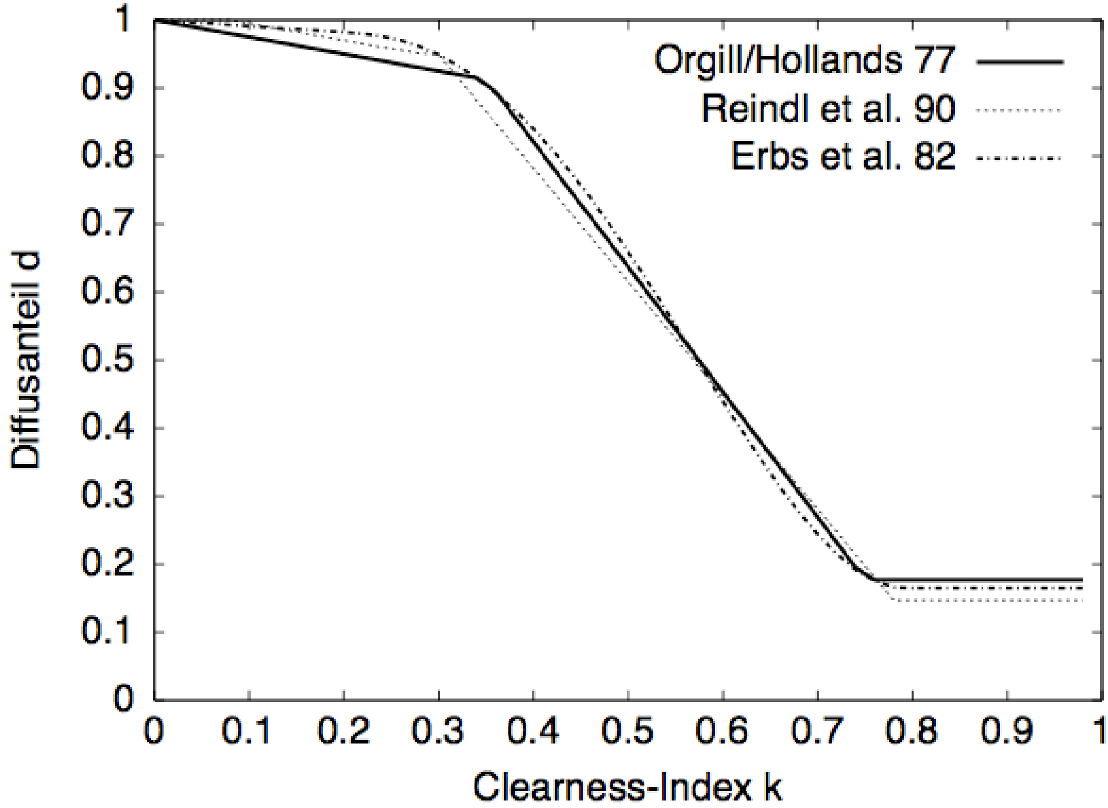

- Simple models based only on clear-sky index kt
- piecewise linear function with threshold values for clear (k_c) and cloudy (k_0) skies

Diffuse fraction – more complex

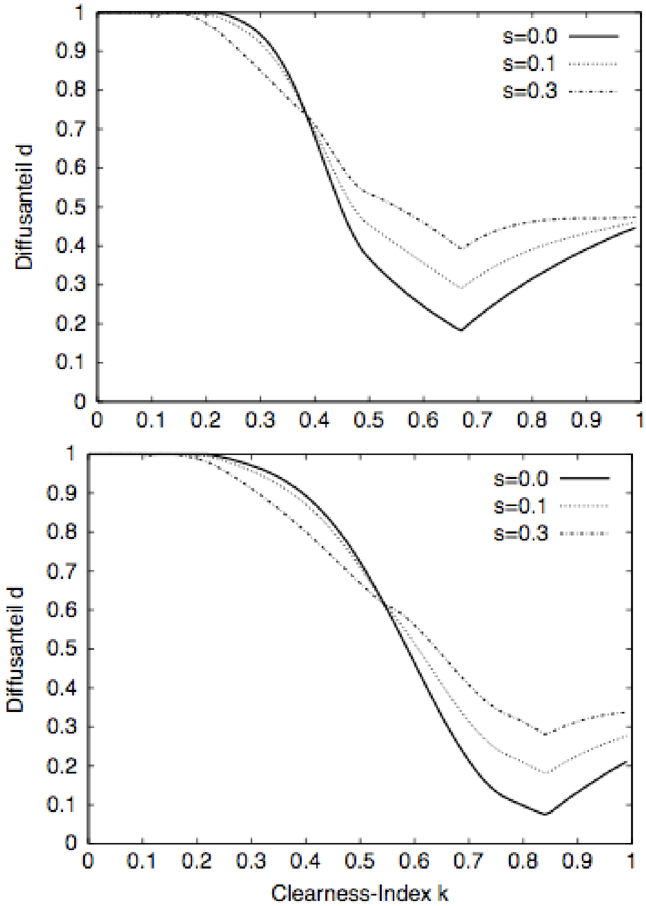

- Skartveit/Olseth model (1997)
- adding effects of increasing diffuse irradiance by reflecting clouds depending on variability index s and solar altitude (i.e., 90° - solar zenith):
- 10° (top),
- 50° (bottom)

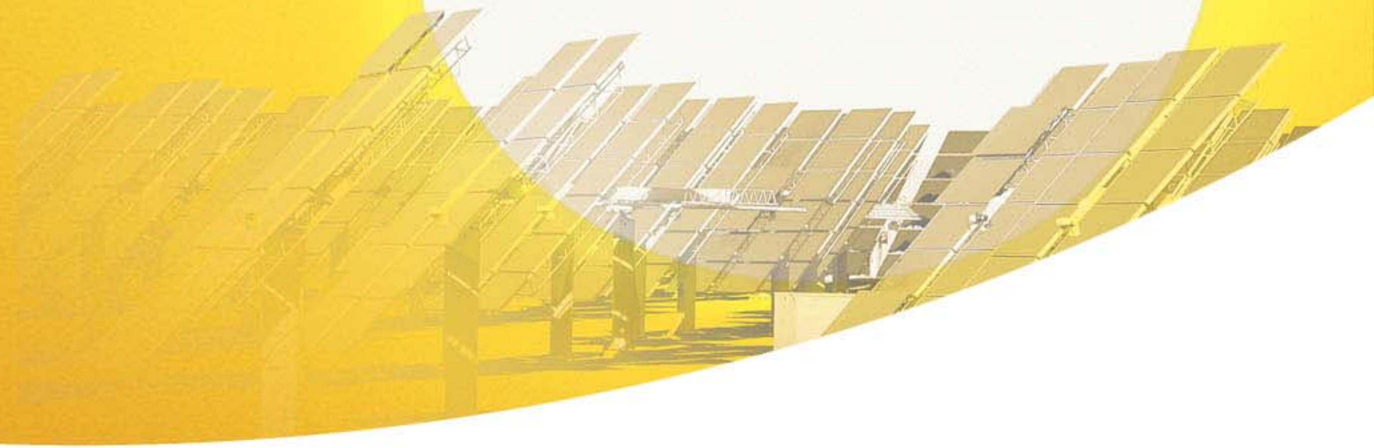

Characteristics of Resource Assessments

Inter annual variability

- Strong inter annual and regional variations

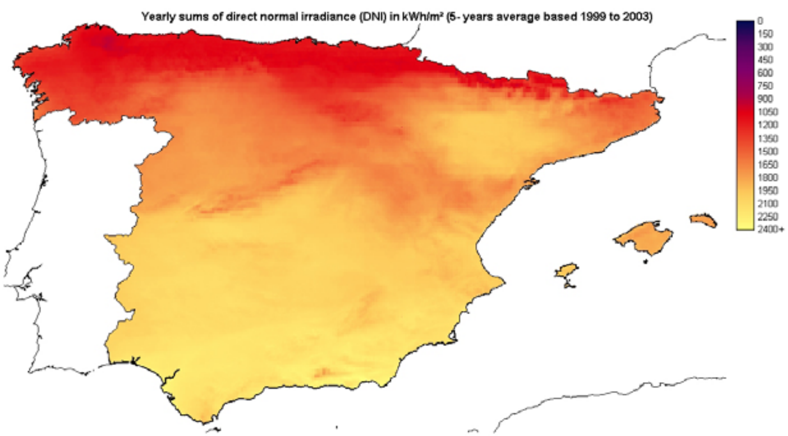

Average of the direct normal irradiance from 1999-2003

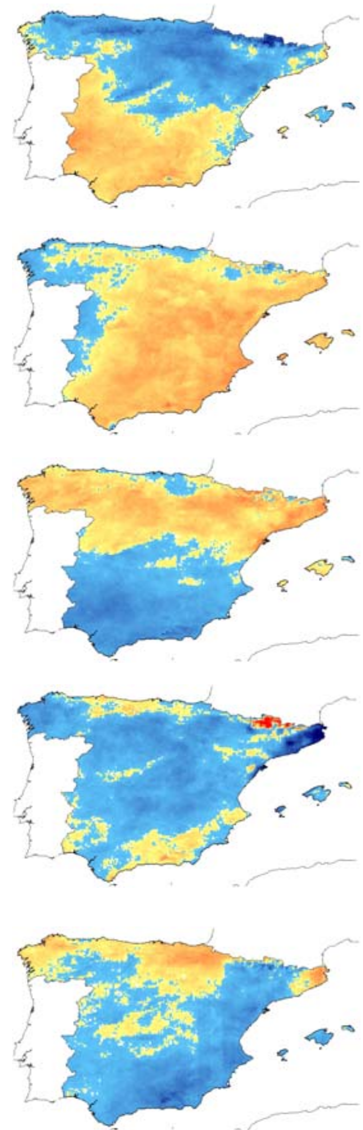

1999

2000

2001

2002

2003

deviation to mean

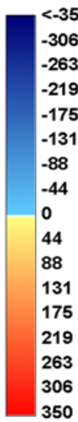

Long-term variability of solar irradiance

- 7 to 10 years of measurement to get long-term mean within 5%

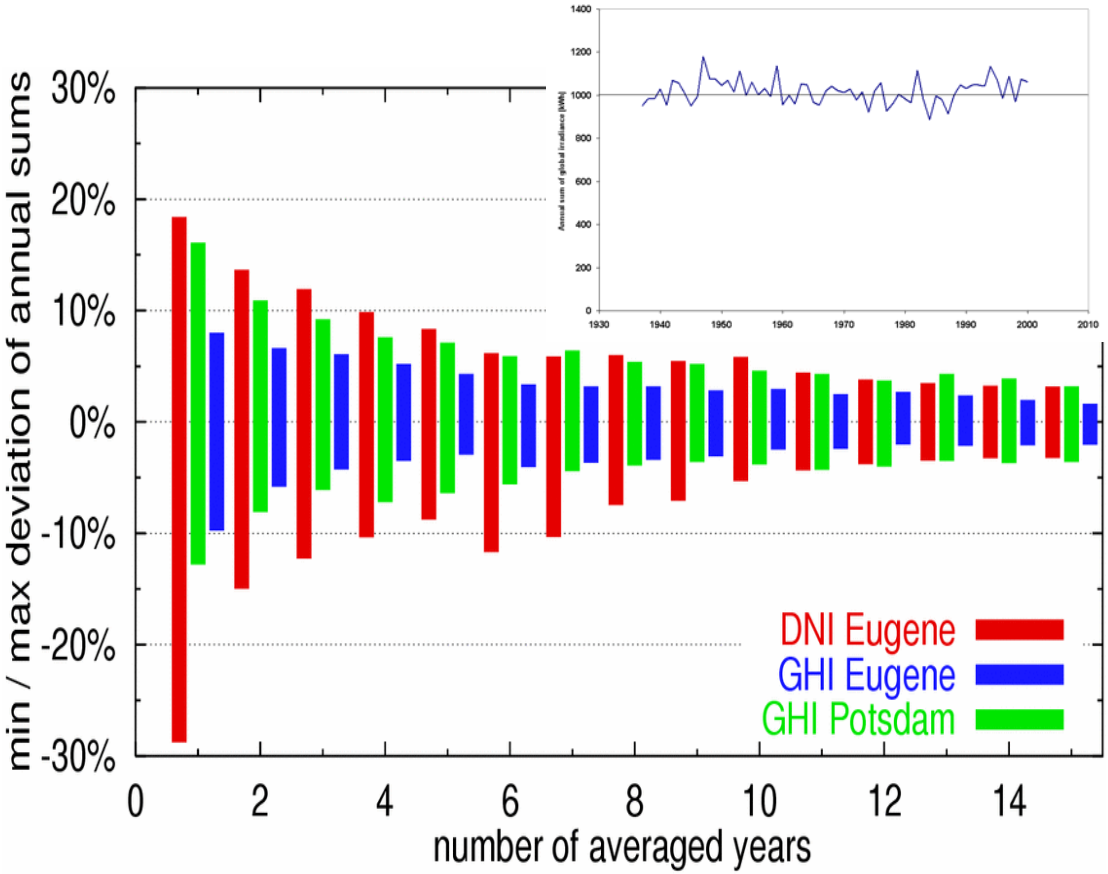

Ground measurements vs. satellite derived data

Ground measurements

Advantages

+ high accuracy *(depending on sensors)*
+ high time resolution

Disadvantages

- high costs for installation and O&M
- soiling of the sensors
- sometimes sensor failure
- no possibility to gain data of the past

Satellite data

Advantages

+ spatial resolution
+ long-term data *(more than 20 years)*
+ effectively no failures
+ no soiling
+ no ground site necessary
+ low costs

Disadvantages

- lower time resolution
- low accuracy at high time resolution

Combining Ground and Satellite Assessments

- Satellite data
  - Long term average
  - Year to year variability
  - Regional assessment

- Ground data
  - Site specific
  - High temporal resolution possible
    (up to 1 min to model transient effects)
  - Good distribution function

Matching Ground and Satellite Data

Why do ground and satellite data not match?

Due to uncertainties in:

- Atmospheric Parameters, most prominent Aerosols

- Cloud transmission:
  - The cloud index is a combination of cloud fraction and transparency. A semi transparent cloud can be distinguished well from a fractional cloud cover.
  - Parameterization may depend on prevailing cloud types in the region.

Procedure for Matching Ground and Satellite Data

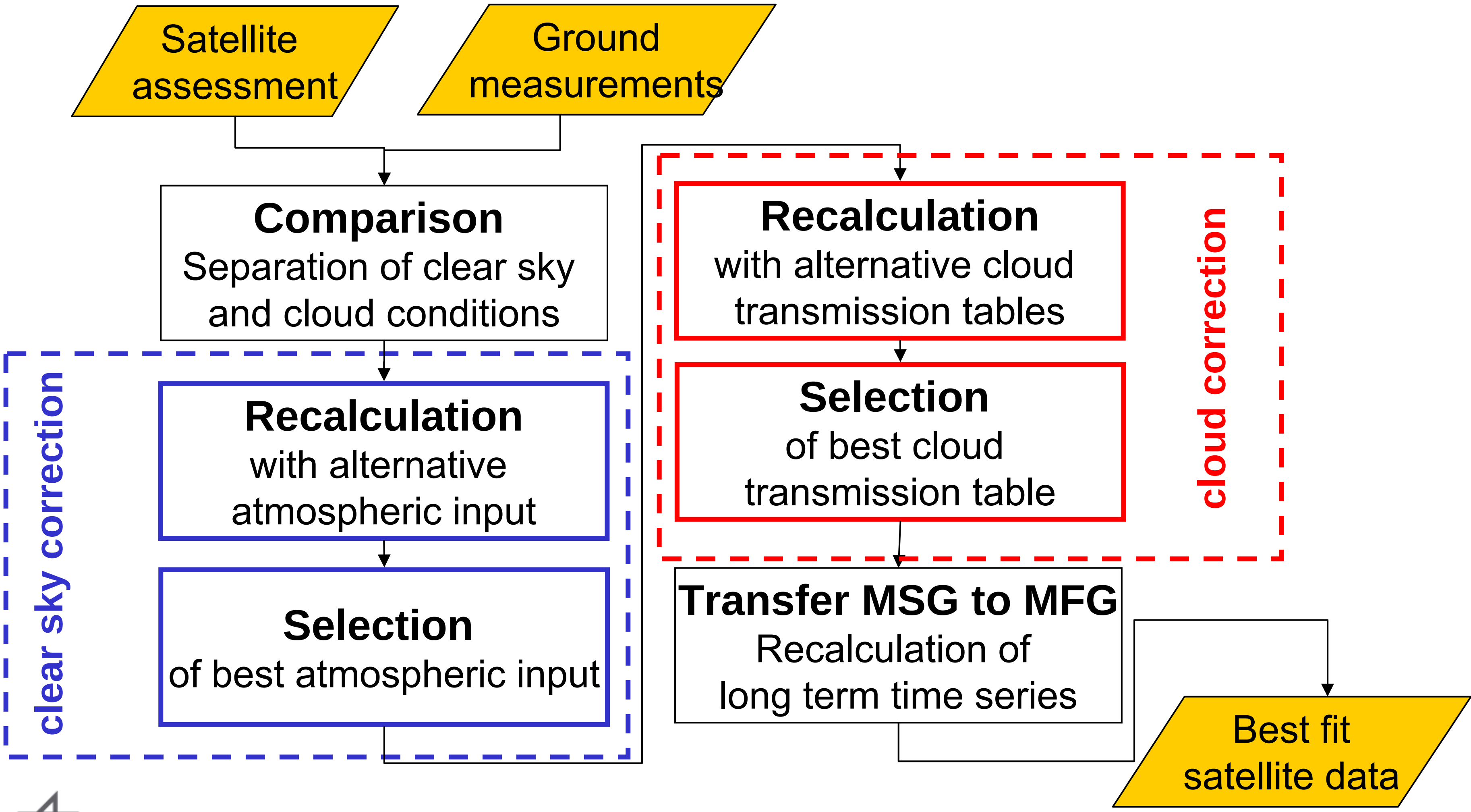

Guidance and Access to Data

- Many sources for solar resource knowledge are available
- Every source has its own access mechanism and data format
- Quality of the sources is often not well known
- Results are difficult to compare

There is quite a number of data sources, but this creates uncertainty of the results, especially if they do not agree

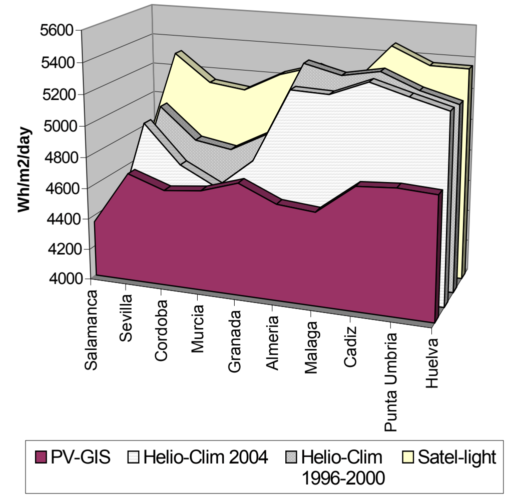

Benchmarking of Time Series Products

- **First order measures:**
  Bias, root mean square error, standard deviation

  Exact match of data pairs in time

  Sometime this match is not necessary (e.g. system layout with historical data)

- **Second order measures:**
  Based on Kolmogrov-Smirnov Test

  Match of distribution functions

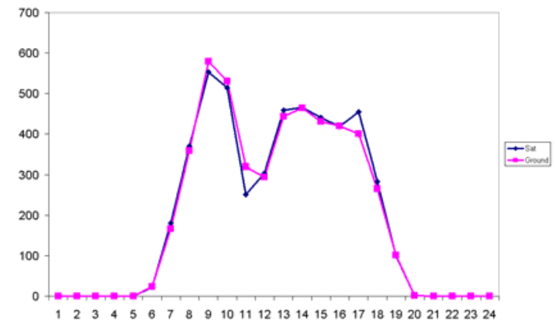

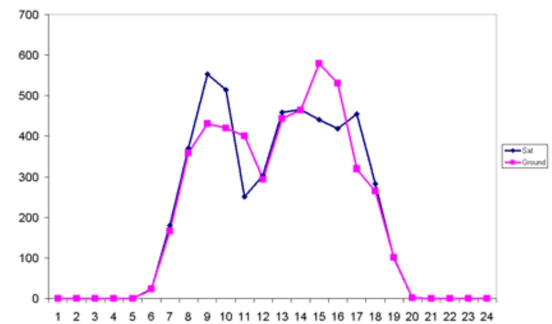

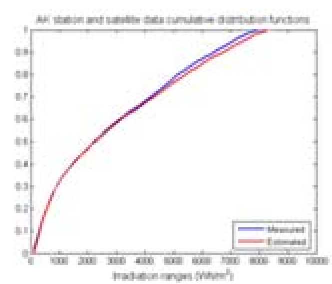

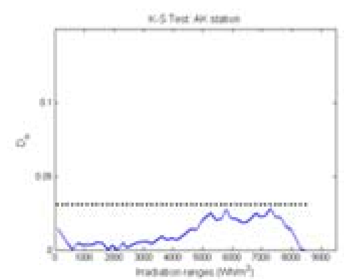

Benchmarking Rules

- The ground data has passed the QC procedure
- Global irradiance/illuminance is greater zero (exclude night values and missing measurements).
- The modelled value is valid.
- Averages are calculated from all valid data pairs.

Quality Control

- Are values phyically possible ?
  Phyical limits of the variables
- Are they reasonable?
  e.g. comparison to a clear sky model
- Are they consistent?
  Comparison of redundant information?
- Visual inspection

BSRN Limit Checking

- Physical Limits

Parameter	Min	Max
Global SW downward	$-4\frac{W}{m^2}$	$G_{SC} \times \epsilon \times 1.5(\cos\theta_z)^{1.2} + 100\frac{W}{m^2}$
Diffuse SW downward	$-4\frac{W}{m^2}$	$G_{SC} \times \epsilon \times 0.95(\cos\theta_z)^{1.2} + 50\frac{W}{m^2}$
Direct Normal SW downward	$-4\frac{W}{m^2}$	$G_{SC} \times \epsilon$

ε Eccentricity correction
Θ_z Solar zenith angle
G_{SC} Solar constant

Limits of a clear sky model

- Comparison with a clear sky model with a dry clear atmosphere (no water vapor, no aerosols) (DNI + GHI)
- Application of the Bird model (sample for DNI)

$$\tau_r = e^{-0.0903 m_a^{0.84} (1.0 + m_a - m_a^{1.01})}$$

- With the Kasten air mass

$$m_a = \frac{e^{-0.001184 \cdot h}}{\cos\theta_z + 0.15(9.3885 - \theta_z)^{-1.253}}$$

$$G_{Direct} = 0.9751 G_{SC} \tau_r$$

Redundancy of Measurements

$$G_{Global} = G_{Diffuse} + G_{Direct} \cdot \cos\theta_z$$

- Suggested Limits

Parameter	condition	Limits
$\frac{G_{\text{Global}}}{G_{\text{Diffuse}} + G_{\text{Direct}} cos\theta_z}$	$\theta_z < 75^\circ, G_{\text{Diffuse}} + G_{\text{Direct}} cos\theta_z > 50 \frac{W}{m^2}$	1.0 ± 8 %
$\frac{G_{\text{Global}}}{G_{\text{Diffuse}} + G_{\text{Direct}} cos\theta_z}$	$93^\circ > \theta_z > 75^\circ, G_{\text{Diffuse}} + G_{\text{Direct}} cos\theta_z > 50 \frac{W}{m^2}$	1.0 ± 15 %
$\frac{G_{\text{Diffuse}}}{G_{\text{Global}}}$	$\theta_z < 75^\circ, G_{\text{Global}} > 50 \frac{W}{m^2}$	< 1.05
$\frac{G_{\text{Diffuse}}}{G_{\text{Global}}}$	$93^\circ > \theta_z > 75^\circ, G_{\text{Global}} > 50 \frac{W}{m^2}$	< 1.10

QC flagging

-1	Missing values
0	Sun is below horizon
1	Data seams to be okay
2	Data did not pass the lower BSRN limit
3	Data did not pass the upper BSRN limit
4	Data is higher than in a clear dry atmosphere
5	Sum of GHI + DHI + coszen DNI dos not match (difference is more than 10% (only applicable GHI > 10 W/m2and DNI and DHI > 0 W/m2)

SET 1

Norrkoping - 1996-1997
Toravere - 2 000
Lindenberg - 1996-2000
Nantes - 1996-2000
Geneva - 1996-2000
Vaulx-en-Velin - 1996-2000
Carpentras - 1997-2000
Thessaloniki - 1996-2000

Benchmarking Radiation Time Series Data Set "Pre 2000"

Station name	Data set	Lat	Lon	Height	years
Carpentras	BSRN	44.04	5.03	100	1997-2000
Lindenberg	BSRN	52.22	14.12	124	1996-2000
Payerne	BSRN	46.82	6.95	491	1996-2000
Toravere	BSRN	58.27	26.47	70	2000
Norrkoping	IDMP	58.58	16.15	43	1996-1997
Vaulx-en-Velin	IDMP	45.78	4.93	170	1996-2000
Nantes	IDMP	47.25	-1.55	30	1996-2000
Geneva	IDMP	46.12	6.02	420	1996-2000
Davos	GAW	46.82	9.83	1610	1996-2000
Thessaloniki	GAW	40.63	22.97	60	1996-2000

Exercise I – GHI Bias

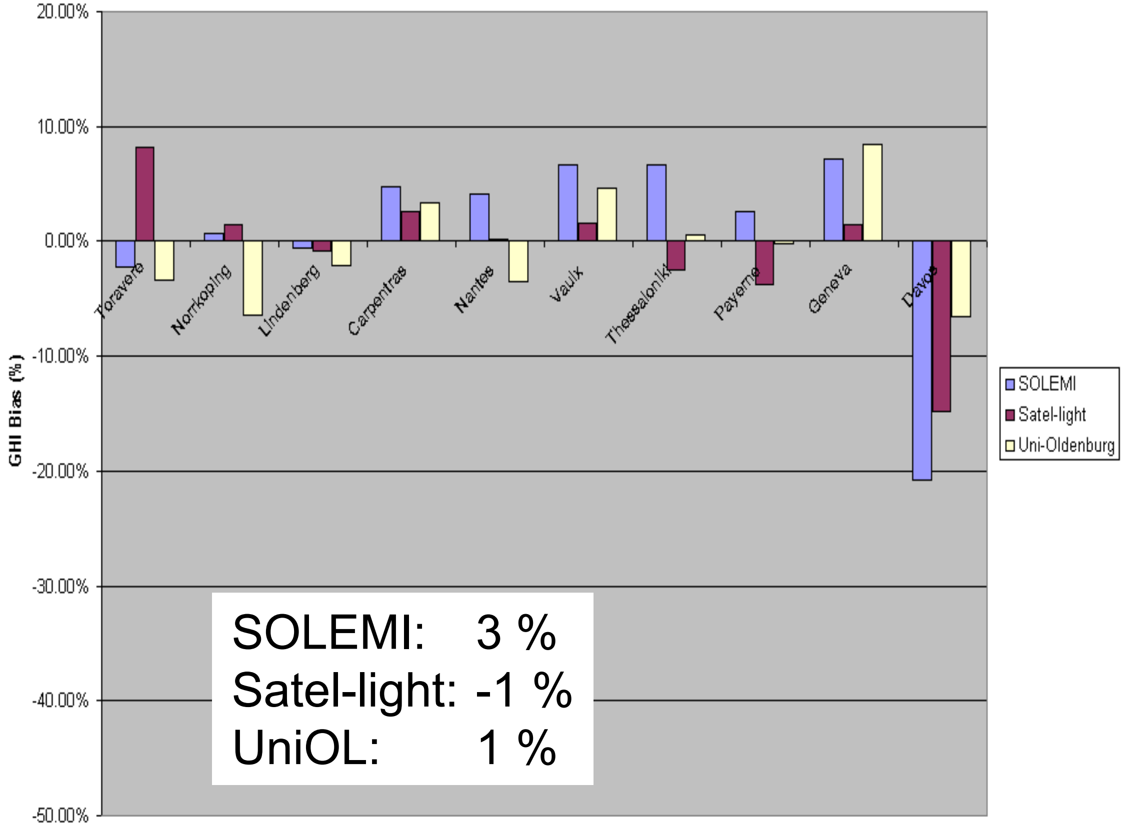

- Large Deviations in Davos
- Overall low bias.

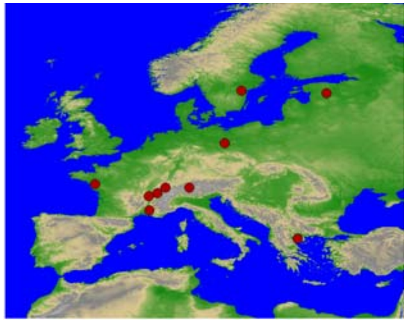

Exercise I – GHI RMSD

SOLEMI: 28 %
Satel-light: 20 %
UniOL: 19 %

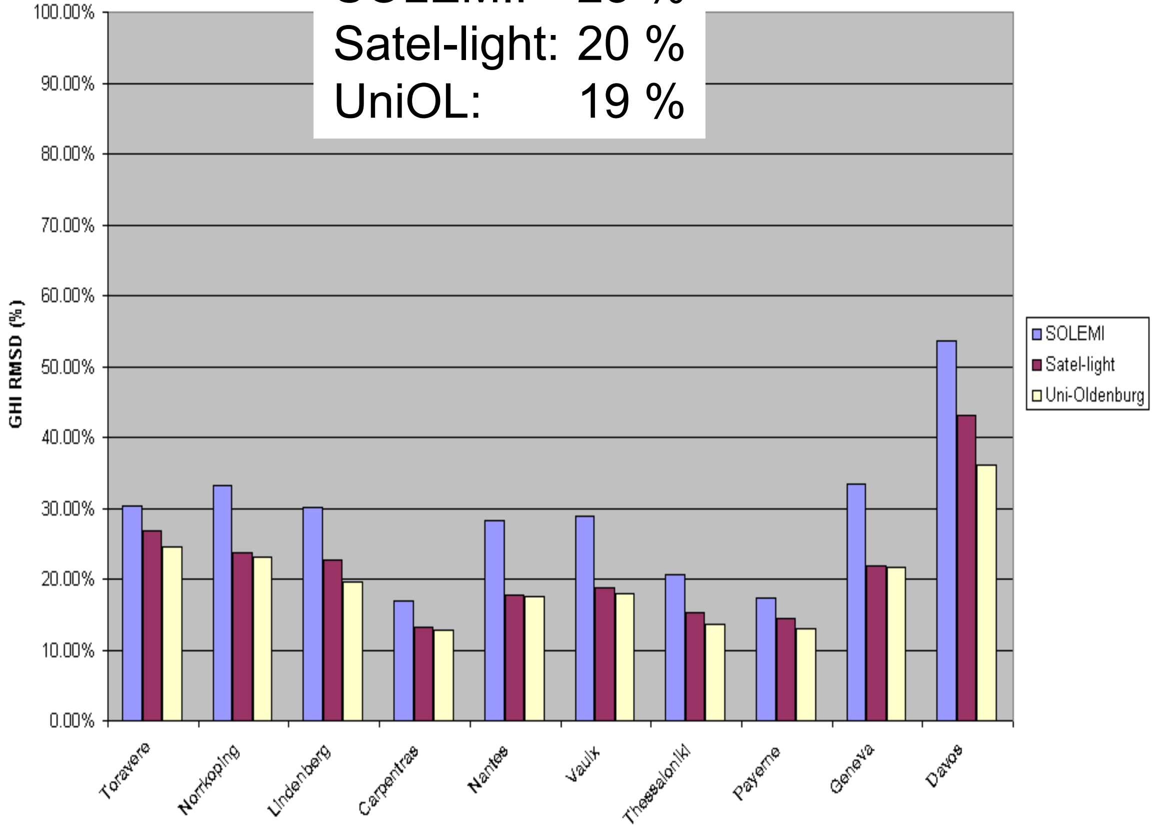

- Large Deviations in Davos

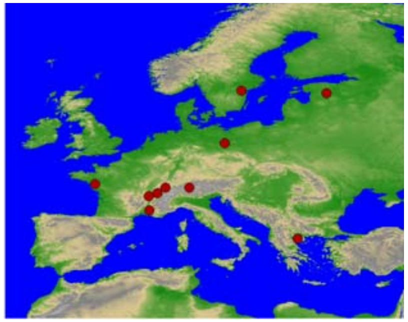

Exercise I – GHI KSI

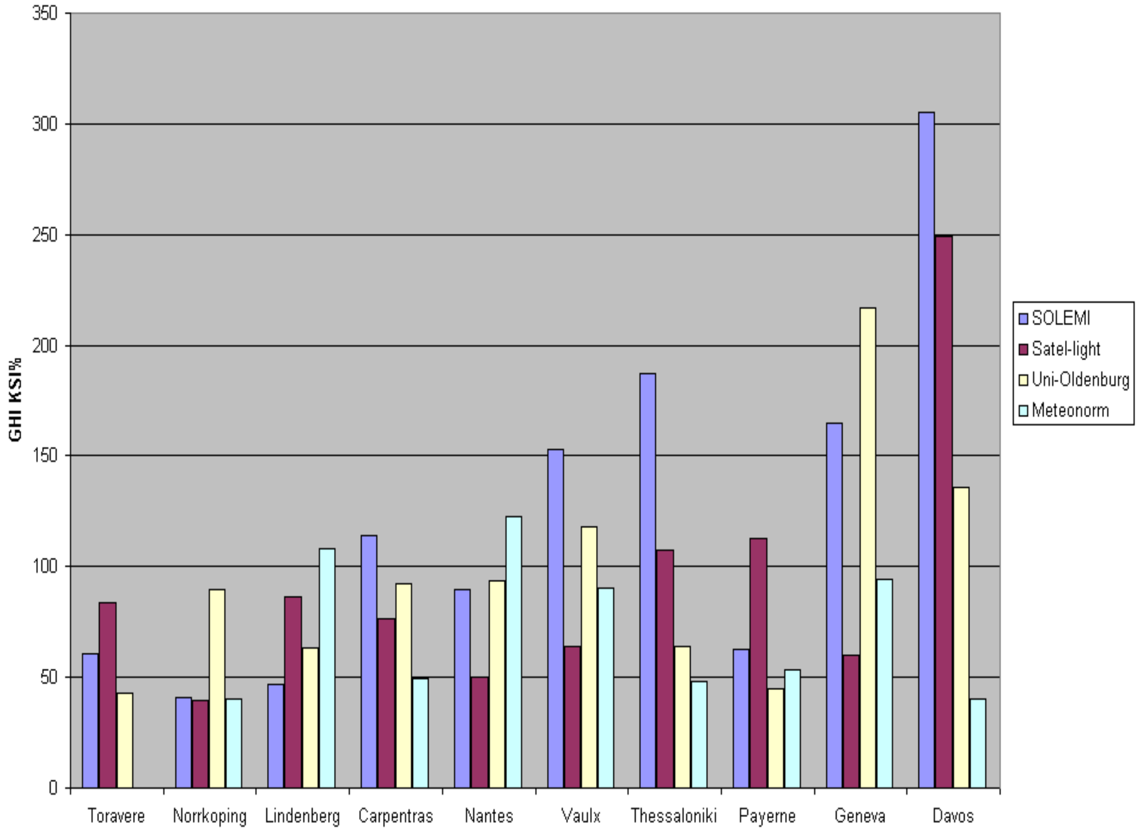

- Large Deviations in Davos

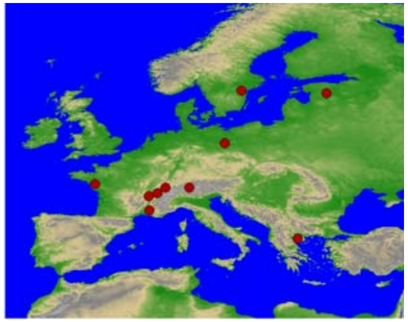

Exercise I – DNI Bias

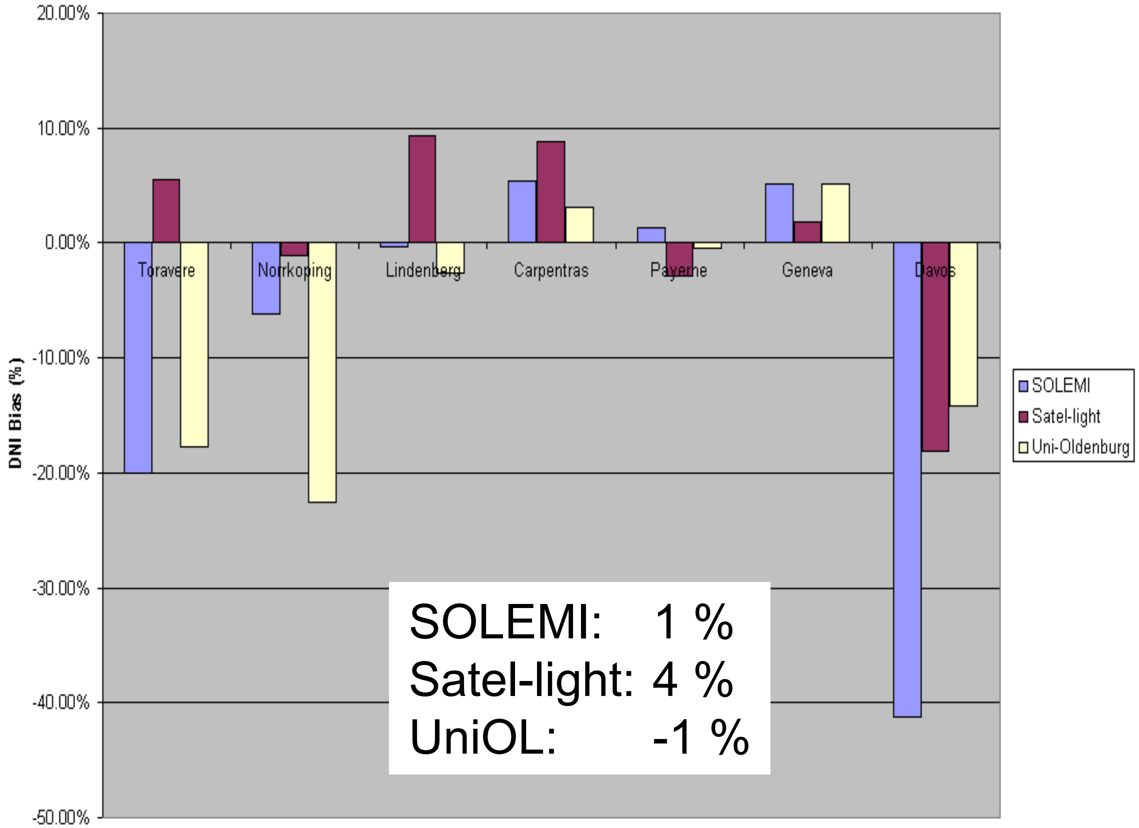

- Large Deviations in Davos, Toravere, Norrkoping, probably Snow
- Overall low bias

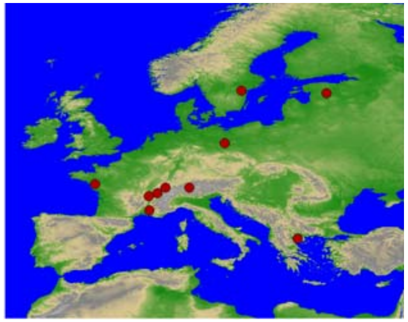

Exercise I – DNI RMSD

SOLEMI: 48 %
Satel-light: 36 %
UniOL: 36 %

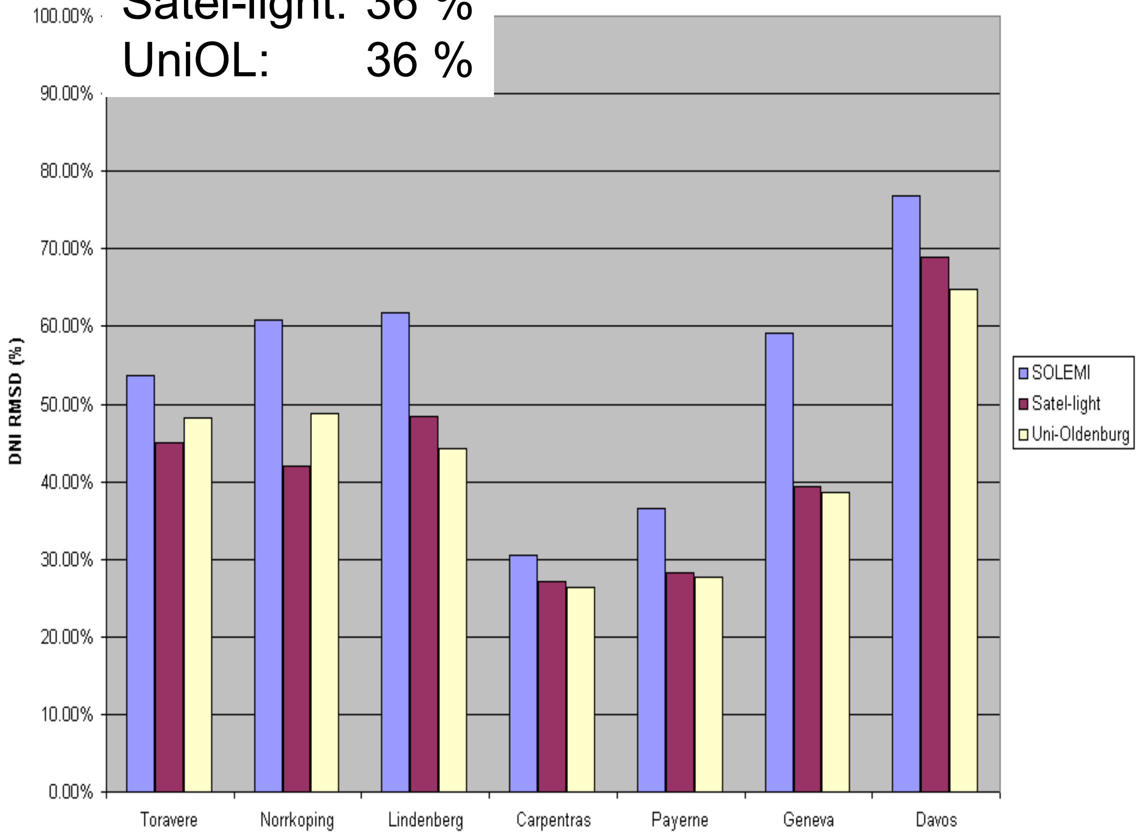

- RMSD is about twice as high as for GHI

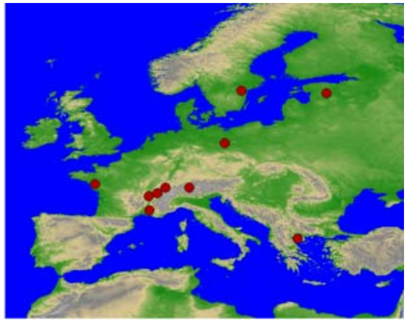

Exercise I – DNI KSI

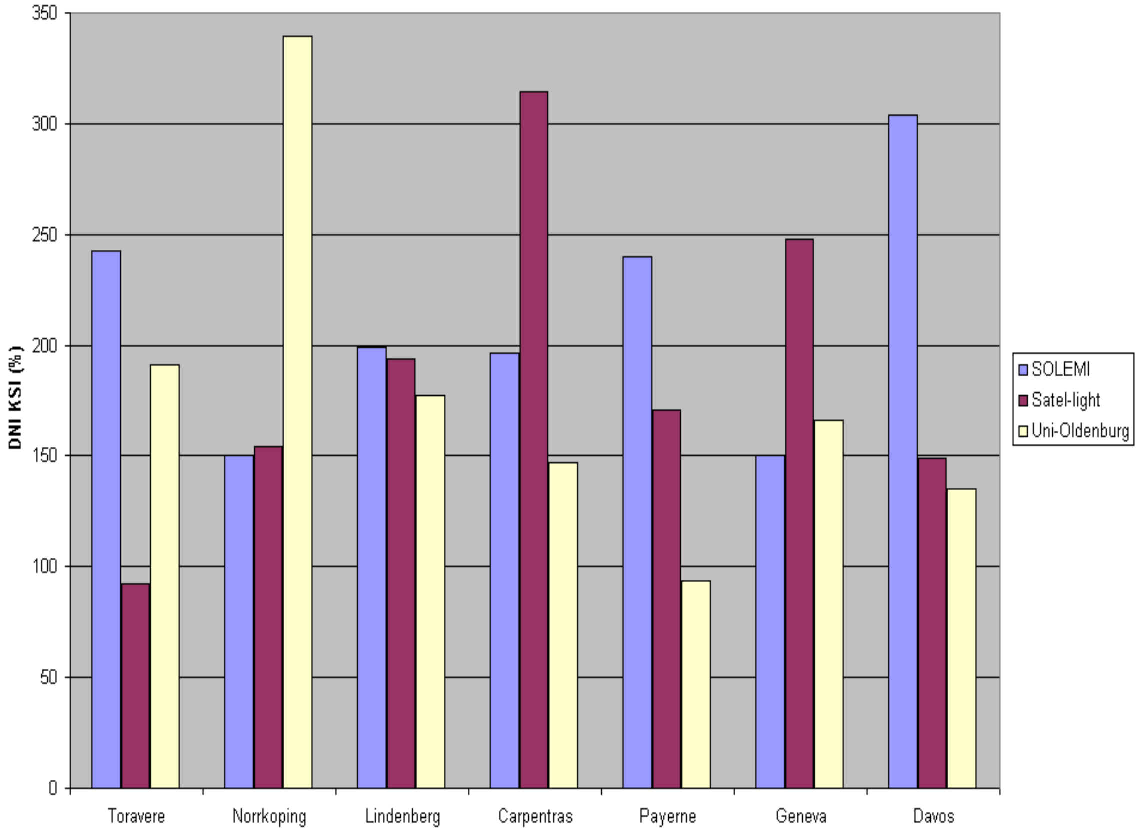

- No clear tendency for specific data set, each one is best and worst in some case.

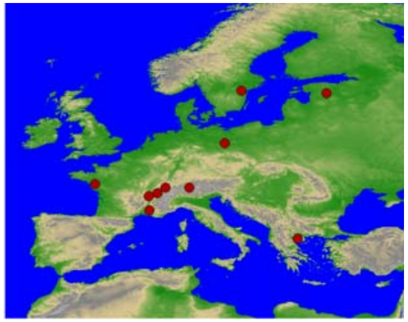

Benchmarking of Maps

- Assessment of the uncertainty of map based products by comparing a number of maps

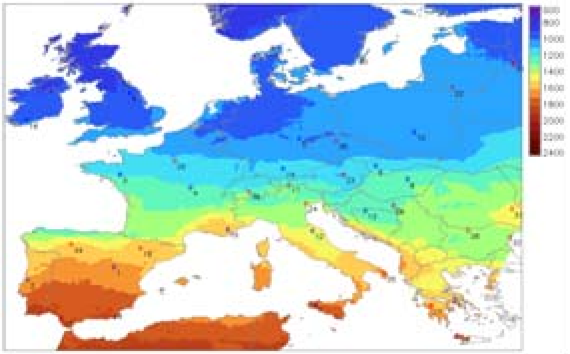

Average solar radiation from different maps

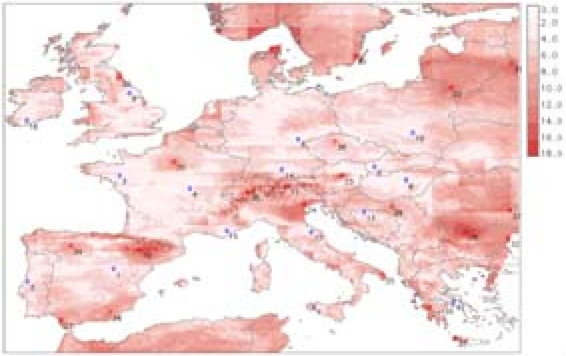

Uncertainty at 95% confidence interval

Data Sources

Resource products: input and extension

product	input	area	period	provider
NASA SSE	ISCCP	World	1983-2005	NASA
Meteonorm		World	1981-2000	Meteotest
Solemi			1991->	DLR
Helioclim			1985->	Ecole de Mines
EnMetSol			1995->	Univ. of Oldenburg
Satel-light		Europe	1996-2001	ENTPE
PVGIS Europe		Europe	1981-1990	JRC
ESRA		Europe	1981-1990	Ecole de Mines

<10 years   10-20years   >20 years

Resource products: Resolution

product	input	temp resolution	spatial resolution
NASA SSE	ISCCP	averag. daily profile	100 km
Meteonorm	 	synthetic hourly/min	1 km (+SRTM)
Solemi		1h	1 km
Helioclim		15min/30min	30 km // 3-7 km
EnMetSol		15min/1h	3-7 km // 1-3 km
Satel-light		30min	5-7 km
PVGIS Europe		averag. daily profile	1 km (+ SRTM)
ESRA		averag. daily profile	10 km

synthetic high resolution values   measured high resolution values

Resource products: parameters

product	parameters
NASA SSE	GHI, DNI, DHI, clouds
Meteonorm	GHI,DNI,DHI, shadowing, illuminace
Solemi	GHI, DNI
Helioclim	GHI, DNI
EnMetSol	GHI, DNI,DHI, spectra
Satel-light	GHI,DNI, DHI, illuminance
PVGIS Europe	GHI,DHI, shadowing
ESRA	GHI, DNI, DHI

NASA-SSE

Earth System Science → Applied Science Outcome

NASA Satellite Measurements, Analysis and

Terra Aqua

ISCCP SRB GMAO CERES

Surface Meteorology and Solar Energy (SSE) Datasets And Web interface

SSE

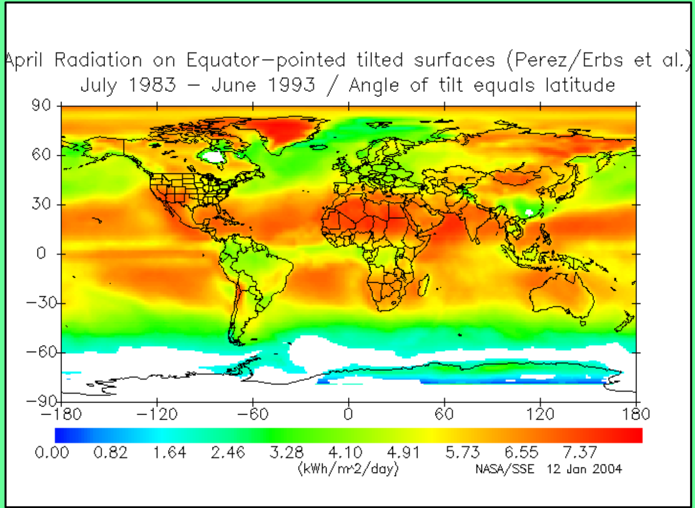

Growing over the last 7 years to nearly 14,000 users, nearly 6.4 million hits and 1.25 million data downloads

SSE Web Site

http://eosweb.larc.nasa.gov/sse/

Over 200 solar energy and meteorology parameters averaged from 10 years of data

Satel-light – www.satel-light.com

- 5 years of half hour data from 1996 to 2000
- Coverage: Europe

Maps

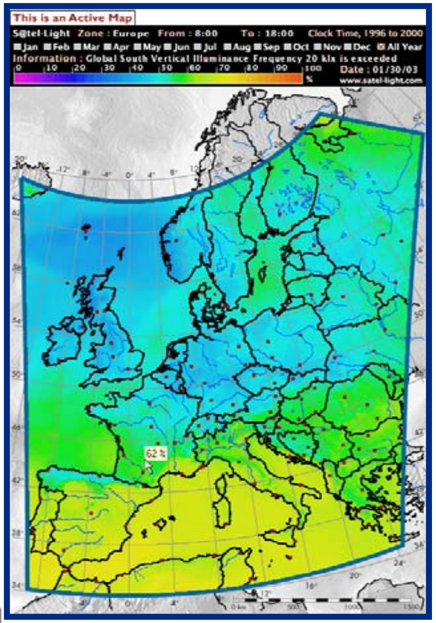

Diagrams

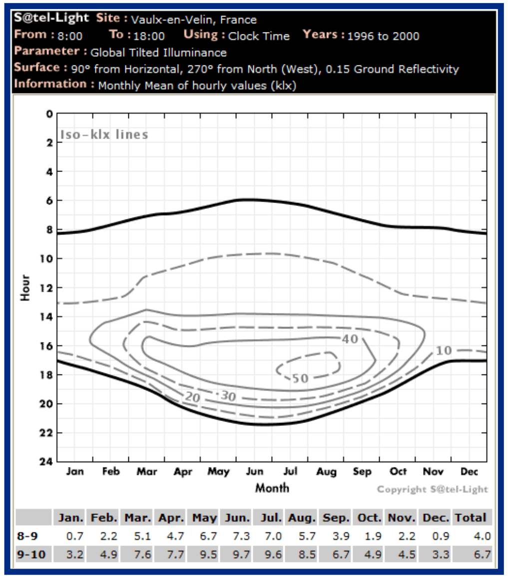

	Jan.	Feb.	Mar.	Apr.	May	Jun.	Jul.	Aug.	Sep.	Oct.	Nov.	Dec.	Total
8-9	0.7	2.2	5.1	4.7	6.7	7.3	7.0	5.7	3.9	1.9	2.2	0.9	4.0
9-10	3.2	4.9	7.6	7.7	9.5	9.7	9.6	8.5	6.7	4.9	4.5	3.3	6.7

Data files

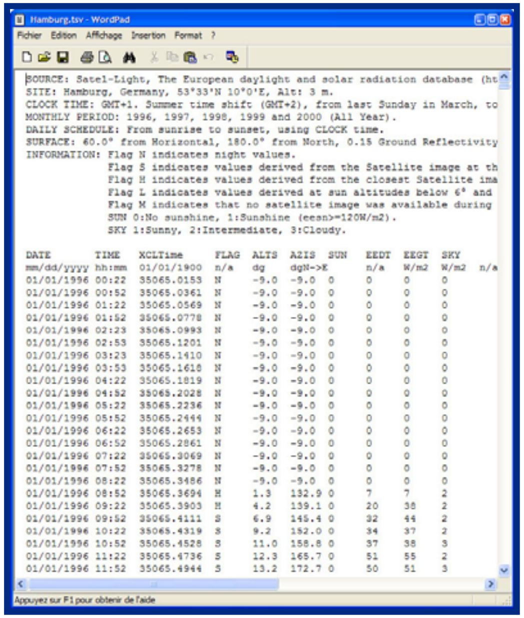

SOURCE: Satel-Light, The European daylight and solar radiation database (ht
SITE: Hamburg, Germany, 53°33'N 10°0'E, Alt: 3 m.
CLOCK TIME: GMT+1. Summer time shift (GMT+2), from last Sunday in March, to
MONTHLY PERIOD: 1996, 1997, 1998, 1999 and 2000 (All Year).
DAILY SCHEDULE: From sunrise to sunset, using CLOCK time.
SURFACE: 60.0° from Horizontal, 180.0° from North, 0.15 Ground Reflectivity
INFORMATION: Flag N indicates night values.
Flag S indicates values derived from the Satellite image at th
Flag H indicates values derived from the closest Satellite ima
Flag L indicates values derived at sun altitudes below 6° and
Flag M indicates that no satellite image was available during
SUN 0:No sunshine, 1:Sunshine (eesn>=120W/m2).
SKY 1:Sunny, 2:Intermediate, 3:Cloudy.

DATE	TIME	XCLTime	FLAG	ALTS	AZIS	SUN	EEDT	EEGT	SKY	
mm/dd/yyyy	hh:mm	01/01/1900	n/a	dg	dgN->E		n/a	W/m2	W/m2	n/a
01/01/1996	00:22	35065.0153	N	-9.0	-9.0	0	0	0	0	
01/01/1996	00:52	35065.0361	N	-9.0	-9.0	0	0	0	0	
01/01/1996	01:22	35065.0569	N	-9.0	-9.0	0	0	0	0	
01/01/1996	01:52	35065.0778	N	-9.0	-9.0	0	0	0	0	
01/01/1996	02:23	35065.0993	N	-9.0	-9.0	0	0	0	0	
01/01/1996	02:53	35065.1201	N	-9.0	-9.0	0	0	0	0	
01/01/1996	03:23	35065.1410	N	-9.0	-9.0	0	0	0	0	
01/01/1996	03:53	35065.1618	N	-9.0	-9.0	0	0	0	0	
01/01/1996	04:22	35065.1819	N	-9.0	-9.0	0	0	0	0	
01/01/1996	04:52	35065.2028	N	-9.0	-9.0	0	0	0	0	
01/01/1996	05:22	35065.2236	N	-9.0	-9.0	0	0	0	0	
01/01/1996	05:52	35065.2444	N	-9.0	-9.0	0	0	0	0	
01/01/1996	06:22	35065.2653	N	-9.0	-9.0	0	0	0	0	
01/01/1996	06:52	35065.2861	N	-9.0	-9.0	0	0	0	0	
01/01/1996	07:22	35065.3069	N	-9.0	-9.0	0	0	0	0	
01/01/1996	07:52	35065.3278	N	-9.0	-9.0	0	0	0	0	
01/01/1996	08:22	35065.3486	N	-9.0	-9.0	0	0	0	0	
01/01/1996	08:52	35065.3694	H	1.3	132.9	0	7	7	2	
01/01/1996	09:22	35065.3903	H	4.2	139.1	0	20	38	2	
01/01/1996	09:52	35065.4111	S	6.9	145.4	0	32	44	2	
01/01/1996	10:22	35065.4319	S	9.2	152.0	0	34	37	2	
01/01/1996	10:52	35065.4528	S	11.0	158.8	0	37	38	3	
01/01/1996	11:22	35065.4736	S	12.3	165.7	0	51	55	2	
01/01/1996	11:52	35065.4944	S	13.2	172.7	0	50	51	3	

Meteonorm

- Based on ground data
- Satellite assisted interpolation between stations
- stoacstic models to derive higher resolution data
- global to tilted models

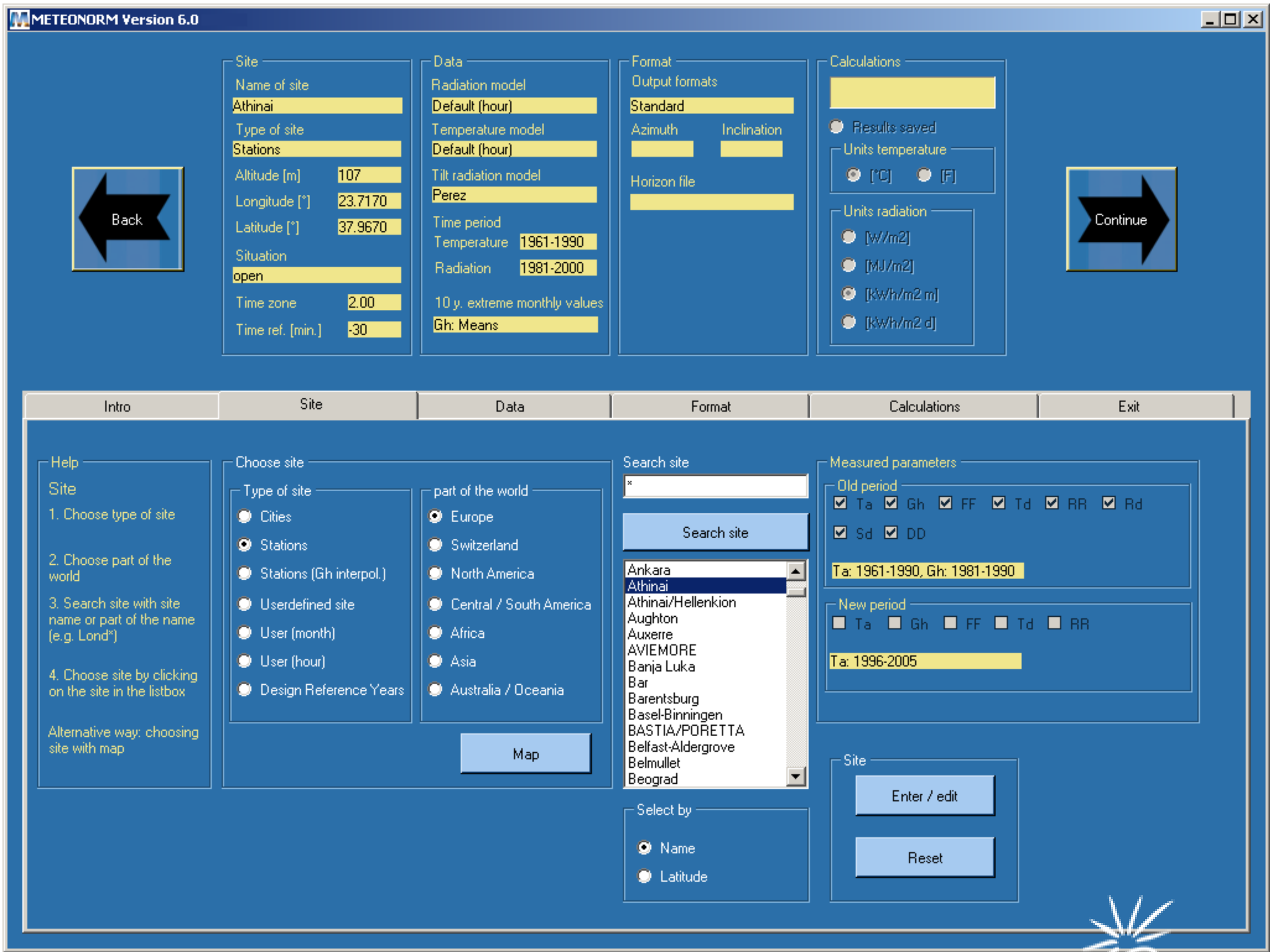

Meteonorm

Climate data

- 8050 stations
- 8 parameters:
  - Global radiation (horizontal, inclined)
  - Air temperature
  - Dewpoint temperature
  - Wind speed and direction
  - Sunshine duration
  - Precipitation
  - Days with precipitation

Chain of Algorithms

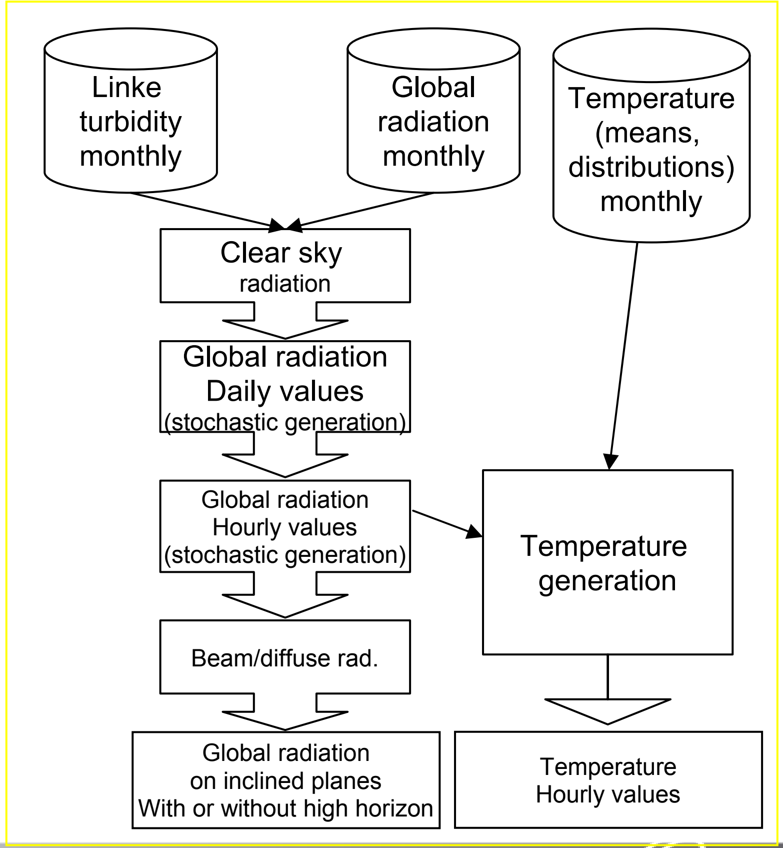

PVGIS - http://re.jrc.ec.europa.eu/pvgis/

- **DATA**
  - *solar radiation (Europe, Africa & SW Asia)*
  - *ambient temperature (Europe)*
  - *+ terrain, land cover…*

- **ASSESSMENT TOOLS**
  - *solar radiation for fixed and sun-tracking surfaces*
  - *output from grid-connected PV*
  - *performance of standalone PV (only Africa)*

- **MAPS**
  - *interactive*
  - *static*

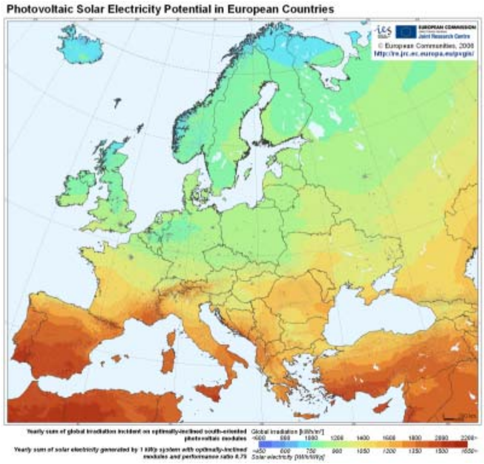

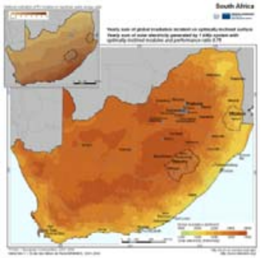

PVGIS

Calculation of grid-connected PV performance

- Calculation takes into account angle-of-incidence effects
- For crystalline silicon and CIS/CIGS, the effects of temperature and irradiance on the conversion efficiency are modeled.
- Generic (user-selected) value for BOS losses.
- Calculates output for:
  - Specified inclination and orientation
  - Optimum inclination for given orientation
  - Optimum inclination and orientation
  - 1- and 2-axis flat-plate tracking

Helioclim

- same area for H1, H2, H3
- uncertainties of irradiance values assessed and provided
- dissemination through the SoDa Service
  - *www.soda-is.com*
- access to data in one click
- access on-pay, except 1985-1989 (daily) and 2005
- coupled to other services, e.g. irradiance on inclined surface

Satellite data: SOLEMI – Solar Energy Mining

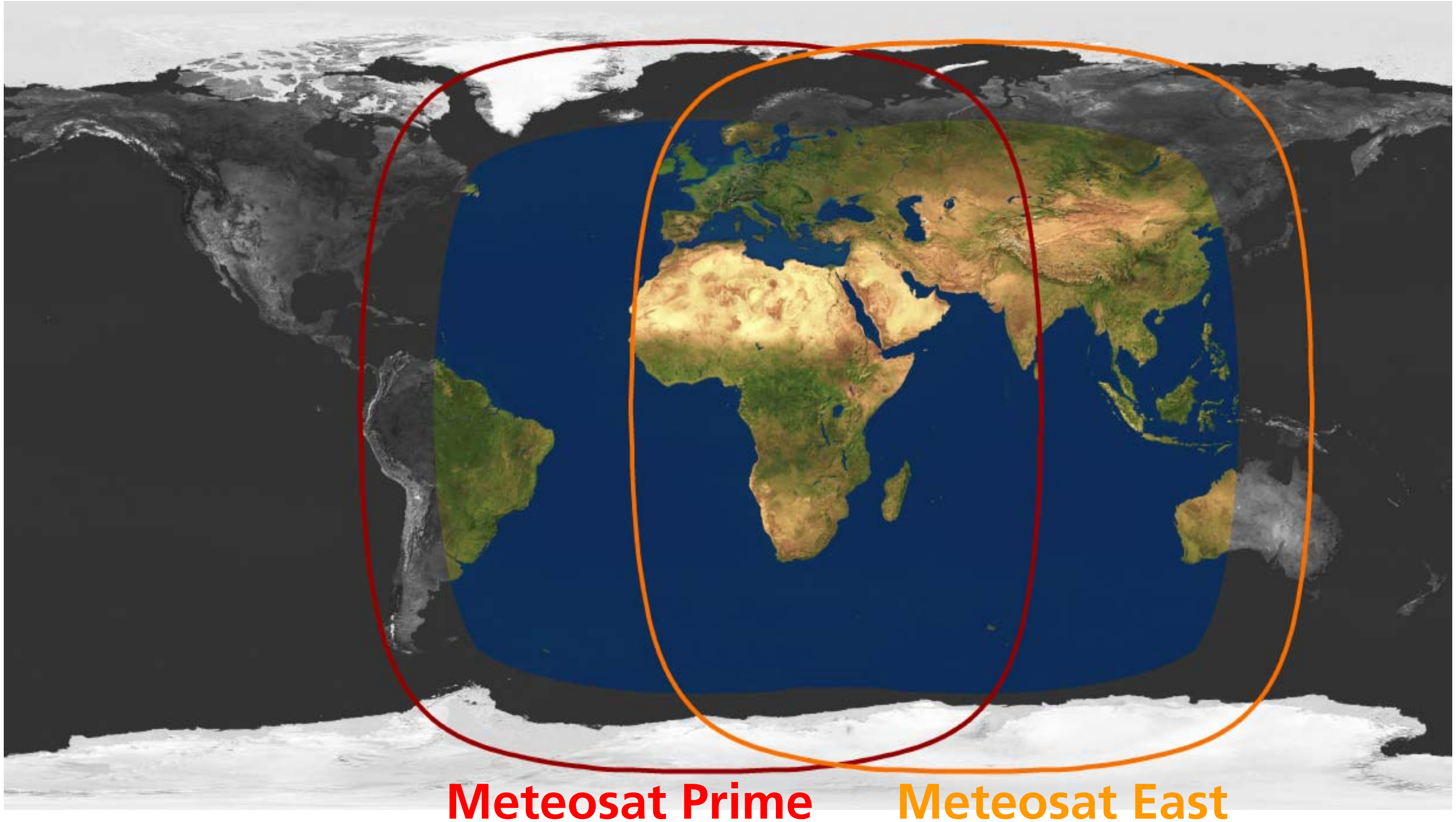

- SOLEMI is a service for high resolution and high quality data
- Coverage: Meteosat Prime up to 22 years, Meteosat East 10 years (in 2008)

SWERA – Solar and Wind Energy Resource Assessment

- Initial GEF funded project to asses solar and wind resources in 13 developing countries
- Now turned into a programme of UNEP, most recent assessment in the United Arab Emirates
- Archive consists a number of different country specific and regional data sets
- Access at: http://swera.unep.net

SWERA – Renewable Energy Explorer

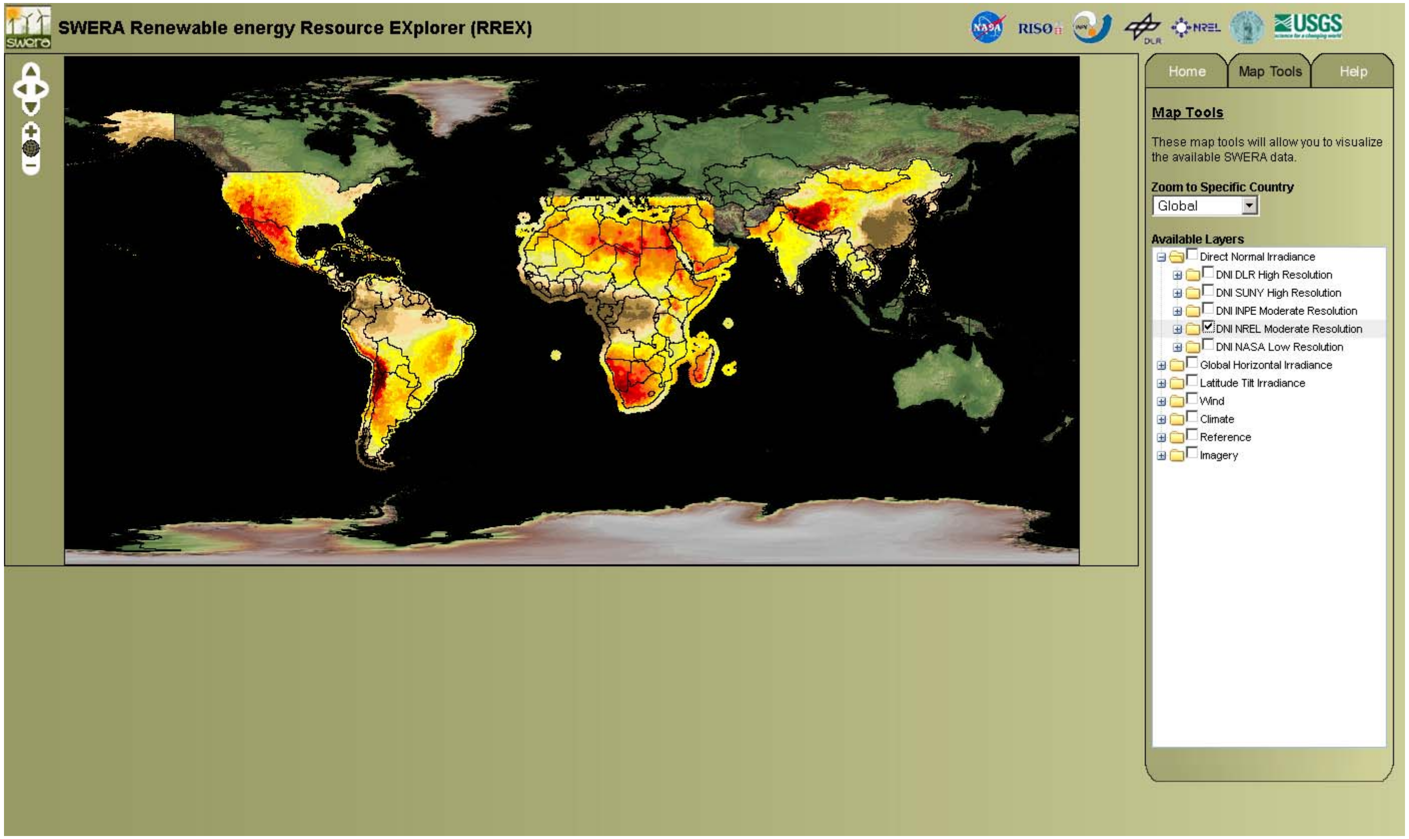

SWERA Renewable Energy Explorer

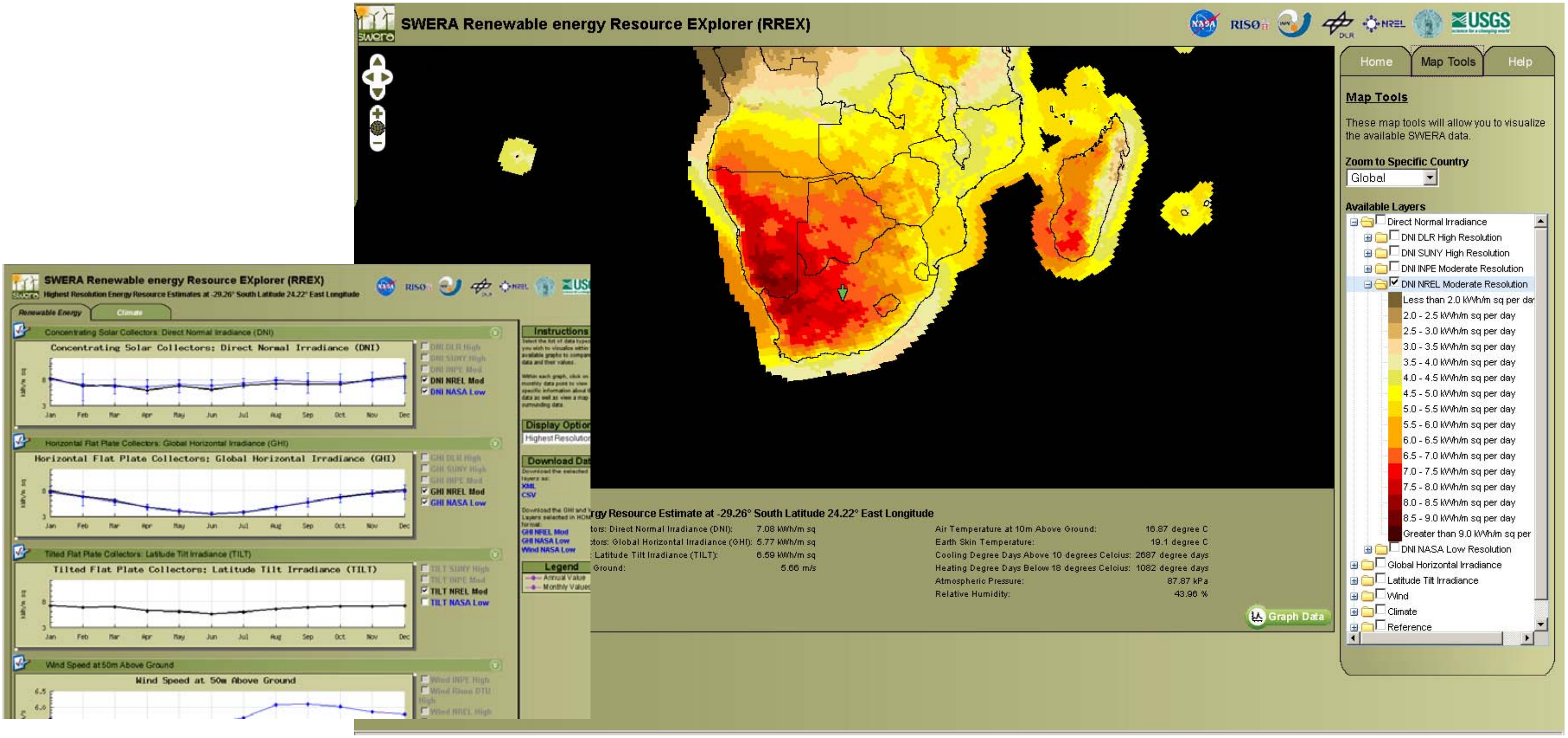

Typical Meteorological years

- A typical meteorological year (TMY) data set provides designers and other users with a reasonably sized annual data set that holds hourly meteorological values that typify conditions at a specific location over a longer period of time, such as 30 years.
- The TMY data set is composed of 12 typical meteorological months (January through December) that are concatenated essentially without modification to form a single year with a serially complete data record for primary measurements. These monthly data sets contain actual time-series meteorological measurements and modeled solar values, although some hourly records may contain filled or interpolated data for periods when original observations are missing from the data archive.

Typical Meteorological Years II

- The Sandia method is an empirical approach that selects individual months from different years of the period of record. For example, in the case of the NSRDB that contains 30 years of data, all 30 Januarys are examined, and the one judged most typical is selected to be included in the TMY.
- The Sandia method selects a typical month based on nine daily indices consisting of the maximum, minimum, and mean dry bulb and dew point temperatures; the maximum and mean wind velocity; and the total global horizontal solar radiation. Final selection of a month includes consideration of the monthly mean and median and the persistence of weather patterns. The process may be considered a series of steps.

Results of the satellite-based solar assessment

Digital maps: e.g. annual sum of direct normal irradiation in 2002 in the Mediterranean Region

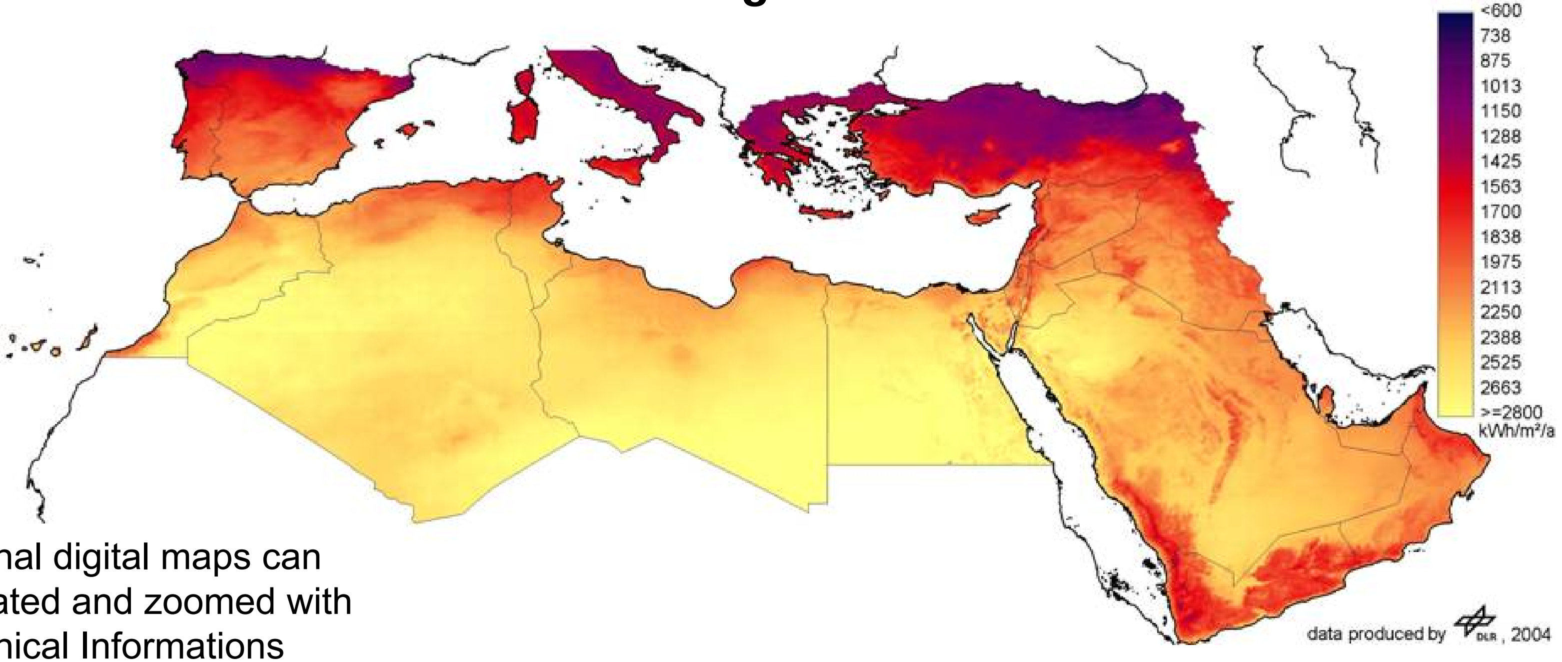

The original digital maps can be navigated and zoomed with Geographical Informations Systems like ArcView or Idrisi.

Temporal resolution of input data: 1 hour
Spatial resolution of digital map: 1 km x 1 km per Pixel
Long term analysis: up to 20 years of data

Results of the satellite-based solar assessment

Time series: for single sites, e.g. hourly, monthly or annual

Hourly DNI [Wh/m²] for one site in Spain

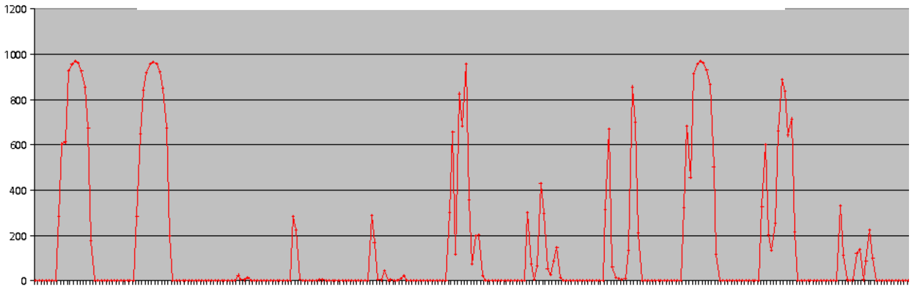

Monthly sums of DNI [kWh/m²] for one site in Spain

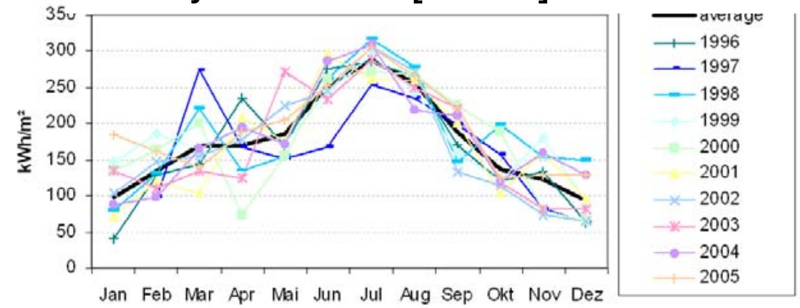

Annual sums of DNI [kWh/m²] for one site in Spain

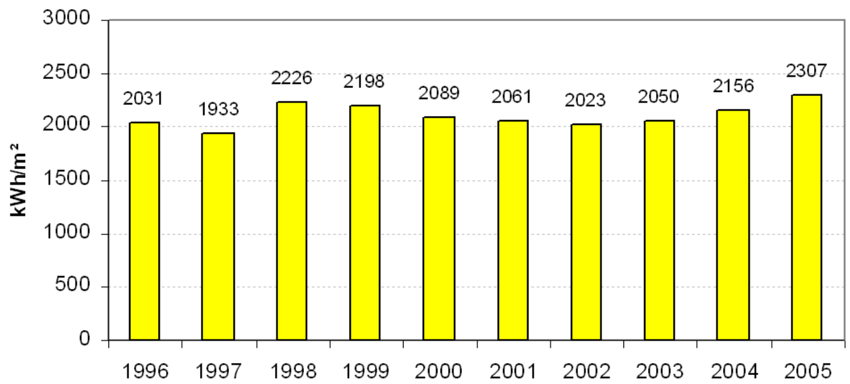

Hourly monthly mean of DNI in Wh/m², Solar Village 2000

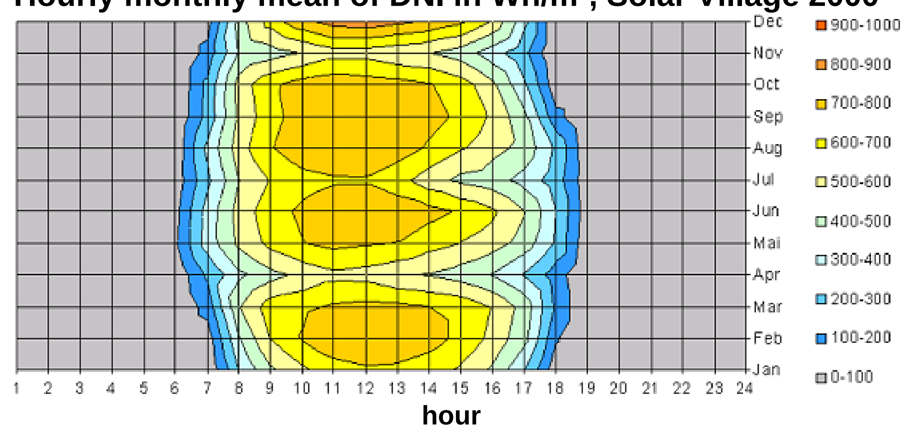

Application Samples

Take from MESoR Users Guide

Assessment of resources and sites for CSP in Mediterranean countries

Context

In 2005, the European Commission wanted to support demonstration activities in concentrating solar and wind power in the eastern and southern Mediterranean countries. It put forward a task in its call for proposal within the 6th Framework programme, with an "Action plan for high priority renewable energy initiatives in Southern and Eastern Mediterranean area".

This resulted in the REMAP project led by the Observatoire Méditerranéen de l'Energie (OME), with the German Aerospace Center (Germany), Acciona (Spain), ADEME (France), ESD (Great Britain), EIE (Turkey), Labein (Spain), NERC (Jordan), CREDEG (Algeria), STEG (Tunisia) and 3E (Belgium).

Study

The resource assessment work within the project consisted in a compilation of the resource data available and in the selection of a number of possible demonstration sites in the targeted countries: Algeria, Tunisia, Turkey and Jordan.

Data

The project was able to collect different data sets describing the solar resource. For further analysis, the direct normal irradiance maps from the NASA SSE 6.0 and a SOLEMI map of 2002 were selected. The NASA data set had the advantage of covering 22 years so that it could describe long term averages. But it had only a coarse spatial resolution of 1°x1°. Therefore, we added a map from the SOLEMI database showing the variations of the annual sum of DNI in 2002 (figure 1). This map has a high spatial resolution of 0.5'x0.5' and the 2002 annual sums compared well to the long term averages derived from the NASA data set.

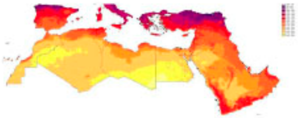

Figure 3: Annual sum of direct normal irradiance in 2002 in kWh/m², in the Mediterranean region.

To ease site selection, we derived exclusion maps for concentrating solar power (CSP) plants. These maps show suitable and unsuitable areas for CSP project developments. Figure 2 shows an example for Tunisia.

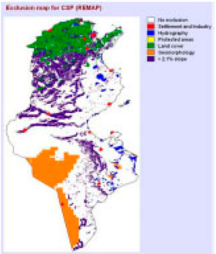

Figure 4: Exclusion map for CSP in Tunisia

The exclusion criteria that we used were the following: terrain slope (<2.1%), settlements (with buffer zone), protected areas (natural reserve, airports, etc.), land cover and properties (e.g. water bodies, woods, agriculture, shifting sand dunes).

Then, we developed a site ranking system for CSP. Points were given based on available solar resource (0 to 20), distance to the electricity grid (0 to 5) and substations (0 to 10), settlements (0 to 5) and roads (0 to 5). The areas reaching the highest score have a high resource, good access to infrastructure and they are close to demand (settlements). Figure 3 shows the results for Tunisia.

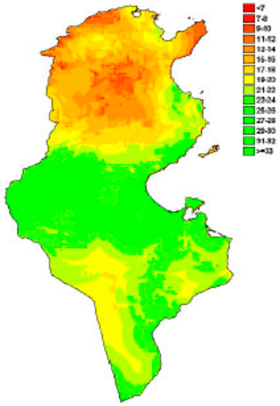

Figure 5: Results from the site ranking for CSP in Tunisia.

All the maps have been included into an Atlas which can be loaded into Google Earth. They are available for download at www.remap-ec.eu.

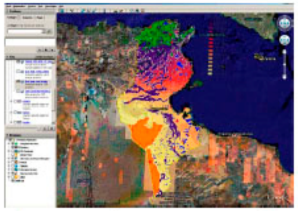

Figure 6: A solar resource map and an exclusion map as Google Earth overlays for Tunisia.

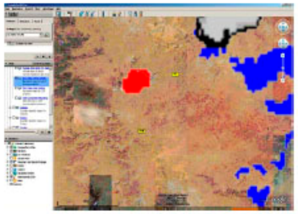

Figure 7: Zoom into an interesting site in eastern Tunisia.

Stakeholder workshops

The maps were used in workshops in each of the targeted countries assembling a number of stakeholders from the public and private sectors. In these workshops, the results from the resource analysis were presented and Google Earth used to zoom into the maps and find possible demonstration sites directly at the workshop.

Contact

carsten.hoyer-klick@dlr.de
Dr. Carsten Hoyer-Click
Deutsches Zentrum für Luft und Raumfahrt e.V.
Institut für Technische Thermodynamik
Pfaffenwaldring 38
D-70569 Stuttgart - Germany

Feasibility study for an integrated solar combined cycle power plant

Context

Integrated Solar Combined Cycle Systems (ISCCS) are a combination of gas fired combined cycle power plants (CC) and parabolic trough solar fields. The heat collected in the solar field is used to boost the electrical output of the CC without increasing the CO_2 emissions. The benefit for the solar part is the usage of the existing steam cycle which reduces the investment costs compared to solar only plants.

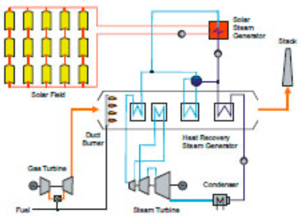

Figure 1: Schematic of an ISCCS.

Feasibility studies are commonly used during the early stage of ISCCS projects to check their economical viability. Concentrating solar power plants and ISCCS plants in particular, are very sensitive to the direct normal irradiance (DNI) and to the ambient temperature and humidity. Therefore, meteorological data for the specific site should be used to conduct an annual performance calculation, preferably at an hourly resolution. The result of such a calculation is the prediction of the solar electricity for a typical year which is then used to compute levelized electricity costs, return on investment and other characteristic numbers.

Company

The Solar Research Division of DLR is often asked to participate in such studies due to its long term experience in concentrating solar power systems and to its modelling and simulation expertise in this area.

Comparison of climatic data

For a specific project in Asia, three datasets were available with different temporal resolutions and different levels of completeness regarding the required variables: (1) monthly means of DNI from eosweb.larc.nasa.gov/sse (22 years), (2) hourly values of DNI from www.solemi.de (7 years) and (3) hourly values for all required parameters from METEONORM. Ground measurements were not available.

Since the METEONORM dataset was the only complete one, it was the best suited for the hourly performance calculation of the proposed ISCCS plant. But prior to this, we compared the three datasets in order to insure that the results based on METEONORM would be representative of the site.

As a first check, the mean annual sums of DNI were compared. They match well: NASA-1993 kWh/m², SOLEMI-2080 kWh/m², METEONORM-2090 kWh/m². The largest difference is lower than 4% and thus well within the accepted uncertainty range.

The monthly sums of DNI were also compared (see figure 2). The NASA data shows higher values during the summer months and somewhat lower values during other months. This

EU-MESOR, Case studies, May 26, 2009 — Solar concentration

deviation may be caused by the longer measuring period of the NASA data which can lead to an equalisation.

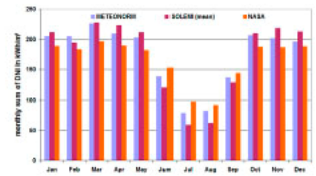

Figure 2: Comparison of the monthly sums of DNI from the 3 datasets.

Finally, we compared the distributions of DNI from SOLEMI and METEONORM. The data from NASA was not used since it does not provide hourly values. Figure 3 shows distributions for the METEONORM year and for three years from the SOLEMI dataset: 2003, 2004 and 2005. The comparison shows that METEONORM has less hours with DNI above 500 W/m² and more hours with DNI below 500 W/m².

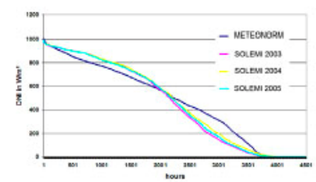

Figure 3: Number of hours during which DNI exceeds a given level.

Impact on power plant performance

We studied the impact of using the METEONORM or the SOLEMI datasets on the electricity output by using both of them for performance calculations and by comparing the results. Figure 4 shows the monthly sums of the electricity produced by the power plant. The annual sum is quite similar: METEONORM-27.93 GWh vs. SOLEMI-27.33 GWh. However, there are larger differences for individual months. Comparing figure 2 and figure 4, it is obvious that a higher DNI sum does not necessarily lead to higher net electricity output (July for instance).

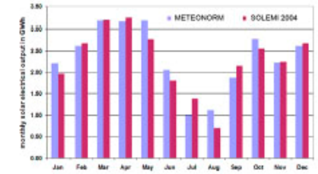

Figure 4: Comparison of monthly solar electrical output.

Conclusion

For feasibility studies or similar economical studies for solar thermal power plants, the availability of high quality data containing DNI as well as ambient temperature and humidity is very important. In order to get reliable performance predictions, the researcher has to use all available data for the specific site and do a cross-check between the different datasets. To be on the safe side, the dataset giving the lowest electricity output should be used, if appropriate, with an additional safety margin of -5 to -10%. Better planning reliability could be achieved by using high quality ground measurements, but their generation would need much more time and investment.

Contact

juergen.dersch@dlr.de
Dr. Jürgen Dersch
Deutsches Zentrum für Luft und Raumfahrt e.V.
Institut für Technische Thermodynamik
Solar Research
D-51170 Köln, Germany

Construction of an artificial average year for CSP Project Development

Context

The development of a 50 MW Concentrating Solar Power plant (CSP) needs high quality solar radiation data. The requirements vary a lot depending on the planning phases. Economic calculations need long term data to compute the expected yield. Engineering calculations require site specific data for all the states of operation. This data should match very well the frequency distribution of the solar radiation at the specific site and should be of high temporal resolution to model transient states of the power plant.

Available data

Currently, the available data does not cover all the requirements stated above. Satellite derived data can cover long time series of solar radiation, as far as 1983, if the first meteorological satellites are used. But the temporal resolution is at best one hour which is often not sufficient for transient modelling. A site specific ground measurement station can deliver high resolution data but the data is only available since the start of the measurement. The measured data can be even different from the long term climatological average due to natural year to year variations.

Figure 1 shows the variability of a long term time series of global horizontal irradiation from 1937 to 2000, in Potsdam, Germany. The annual values are varying by ±15%. A single year of ground measurements may be at the edge of the distribution in the worst case, giving a 15% error to the long term value only due to natural weather variations. This does not include any instrument inaccuracies.

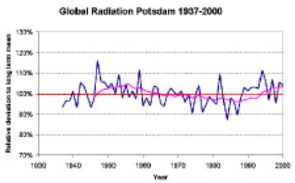

Figure 1: Year to year variability of global radiation in Potsdam, averages 10 year (pink), long term (red).

Artificial average year

The definition of an artificial average year tries to overcome these limitations. It is a combination of long term satellite data with site specific ground measurements. The satellite data should cover at least 10 years. The ground measurements should be of good quality, i.e. there should not be too many days without data: less than 3-4 days per month and no more than 2-3 days in a row.

Long term averages are taken from the satellite data and the ground measurements are modified to match these averages. First the average monthly sums and their standard deviation over at least 10 years are calculated from the satellite data. This shows the natural variability of the values at the specific site.

Figure 2 shows a sample of the monthly sums of satellite data and of ground measurements. The black bars indicate the standard deviation of the monthly sums over the 10 years of satellite derived data.

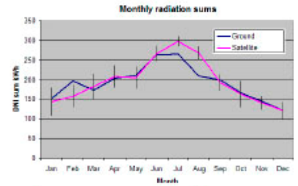

Figure 1: 10 year Monthly averages and standard deviations of satellite data (pink). Monthly averages of ground measurements (blue).

There are two main reasons for the differences between the two curves.

The first one is missing data in the ground measurements. This leads to a reduced total value of the ground data. Missing data are replaced by copying data from the neighbouring days. Therefore, the first step in the construction of an artificial average year is filling up missing values.

The second reason is the year to year variations of the weather. Therefore, the second step in the construction of an artificial year is “changing the weather”, which is done by copying neighbouring days. The neighbour distance is kept below five days to stay within the same sun-earth geometry. If the measured month is below the long term satellite average, cloudy days are replaced by sunny days. If it is above the average, sunny days are replaced by cloudy days.

Figure 3 summarizes the construction of the average artificial year.

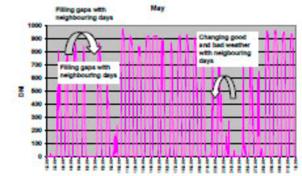

Figure 2: Modifications to the ground data: gaps are filled by neighbouring days, sunny and cloudy days are exchanged to modify the average.

Conclusion

The artificial average year is a dataset where the temporal resolution is the one of ground measurements (less than an hour) and where the monthly sums of solar radiation are the long term averages derived from satellite data. The artificial average year can be used as input to transient system performance models. Since the dataset is entirely derived from ground measurements, it may also include parameters like temperature, wind speed and relative humidity.

Contact

carsten.hoyer-klick@dlr.de
Dr. Carsten Hoyer-Click
Deutsches Zentrum für Luft und Raumfahrt e.V.
Institut für Technische Thermodynamik
Pfaffenwaldring 38
D-70569 Stuttgart
Germany

SPYCE – Satellites help to control the energy yield of solar power systems

Context

The power output of a photovoltaic system is "almost" proportional to the solar irradiance falling onto the modules. Thus to check the proper performance of a PV system, the irradiance should be known. This is a difficult task because measurement instruments, such as reference solar cells or pyranometers, are costly and have to be installed, maintained and calibrated carefully.

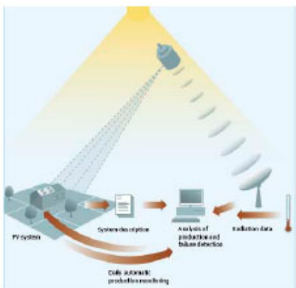

Figure 1: The SPYCE principle

SPYCE principle

The SPYCE service is a web service which offers solar radiation data (derived from satellite images) and algorithms remotely monitoring the PV systems. First, the geographical and technical specifications of the PV system are sent to the SPYCE server. From the SODA server, every night, SPYCE automatically fetches the irradiance data from the previous day for the location of the PV system.

From this data, the SPYCE server calculates the expected energy yield of the PV system. The real yield of the PV system is measured on the site; the data are stored in the data logger and transferred automatically to the SPYCE server. For each PV system, the server compares the expected and the measured energy yields. In case of deviations, a failure detection routine searches the time series to determine the type of failure and sends the analysis result in the form of an email to the operator of the PV system.

Company

The SPYCE service is offered by the company METEOTEST. Enecolo AG was involved in the development of the service. It acts now as a reseller and a supplier of the technical support. This means that it installs the data logger for the owner of the PV system and sends the basic system geographic and technical data to the SPYCE server In addition, Enecolo AG consults the PV owner in case of an alarm, it may then take over the maintenance and operation of the PV system.

Figure 2: view of a SPYCE account

Irradiance data and uncertainty

SPYCE uses primary irradiance data from the SODA Helioclim-3 database which have 15 min. time resolution. These data have an uncertainty of at least 15%, depending on the weather situation. Because this uncertainty limits the reliability of simulated energy yield of a PV system, SPYCE uses several tricks to improve the accuracy of the control procedure:

- Prediction uncertainty is reduced to approximately 10% if daily sums of global irradiation are analyzed.
- Uncertainty of the estimate of the global irradiation leads to stochastic over and under estimations of the real energy yield. However, on average, the ratio of over and under estimations is equal and a change in this ratio means a change in the performance of the PV system.
- Most often, the PV systems are built in a modular way. A failure can be detected more easily if all subsystems are taken separately. At the level of a subsystem, the failures result in a higher fraction of energy loss. Additionally, the performance of the subsystems can be compared to each other.

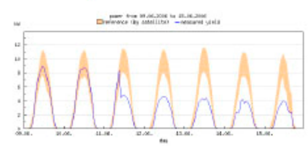

Figure 3: 7 days of monitoring for a PV plant with a failure coming up on the 3rd day. The blue line shows the real energy output, the orange area the expected yield including the uncertainty.

Conclusion

Irradiation data from satellite images are suitable for monitoring small PV systems (up to 10 kW). Outage in one string of such a system leads to an energy loss which is higher than the uncertainty of the expected simulated yield. In case of bigger PV systems, which cannot be divided into small subsystems, other measures than solar radiation need to be used to analyse the data, e.g. comparison with the energy produced by other PV systems.

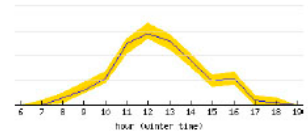

Figure 4: Expected energy yield (yellow area) and the real energy yield (blue line) of a PV system. The expected yield was calculated by comparison with the energy production of other PV systems.

The SPYCE PV control system shows that satellite-derived radiation can be cross-compared with yield data from PV systems to provide cost effective operational service.

Contact

sandra.stettler@enecolo.ch
Sandra Stettler
Enecolo AG
Mönchaltorf, Switzerland
www.enecolo.ch

A method to compute the annual use of artificial light in buildings

Context

Artificial lighting amounts to 30% of the total electricity consumption in office buildings. Its use is directly related to the availability of daylight indoor and increasing daylight reduces the lighting electricity consumption.

The amount of daylight available in a room depends on: the climate of the site, the orientation of the façade, the size of the windows, the type of glazing and shades, and their control by the users...

The current design practice is to evaluate the amount of daylight available in the room under overcast sky conditions. The justification is that there will always be enough daylight under sunny conditions. But this practice ignores the reduction of daylight due to the use of shades to prevent against glare or overheat.

The evaluation of indoor daylight availability should take into account all the sky conditions typical of the site and associate to them strategies for using shades. CSTB, the Centre Scientifique et Technique du Bâtiment in France, has developed a method and a software which does so to produce the annual use of artificial light in a building.

Company

CSTB is a state-owned industrial and commercial corporation which helps the French public authorities to define technical regulations and insure the quality of buildings. With more than 400 engineers and research scientists, it is one of Europe's leading research and evaluation centres dedicated to buildings.

Simulation method

The daylight which enters the building is coming from the sun (if visible) and from the sky vault. Computing the impact of the sun inside the room is not that difficult because it is considered as a point source. The impact of the sky vault inside the room is much more difficult to compute because it depends on the distribution of light over the sky vault and each part of the sky vault has a different influence inside the room.

The distribution of light on the sky varies all the time with the position of the sun and with the sky condition. Since there are about 4400 hours of daylight in a year, the evaluation of daylight for an entire year, with an hourly time step, requires about 4400 computations of the influence of a unique combination of sun and sky inside the room.

In order to reduce simulation time, CSTB has selected a method which isolates the optical computation (the influence of a zone of the sky inside the room) from the climatic computation (the amount of light coming from the zone).

The method (figure 1) divides the sky vault into zones and computes how much light each zone provides inside the room. This gives the relative

contribution of each zone at any given point inside the room.

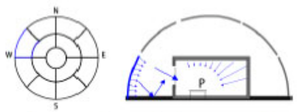

Figure 1: The method computes the contribution of each zone to daylight.

Then, every half hour or more frequently, it uses climatic data to compute the amount of light coming from each zone of the sky vault and sum up the influence of each zone at all points in the room.

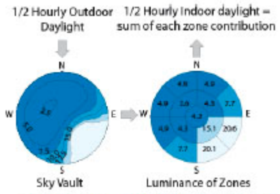

Figure 2: Every half hour, climatic data is used to compute indoor illuminances.

Simulation software

Over the years, CSTB has developed a sophisticated light simulation program called PHANIE, based on a hierarchical radiosity method. PHANIE has been adapted to compute the annual availability of daylight using the method previously described. The number of zones describing the sky vault is selected by the user; CSTB recommends a number of 1000. This way, the zones can also be used to describe the influence of the sun.

Once the influence of each zone has been computed, PHANIE uses the climatic data from the SATEL-LIGHT web server (www.satel-light.com) to compute the distribution of light over the sky vault every half hour. It combines this information with the influence of each zone to obtain the illuminance due to daylight inside the room.

If the daylight illuminance is below the level recommended to perform the activity in the room, a strategy for controlling artificial light is applied: either switch on the artificial light at full power or modulate its power to provide only the amount needed to reach the recommended illuminance. Every half hour, we know how much electric power has been used for lighting the room.

Conclusion

Thanks to CSTB developments and to the daylight information available on the SATEL-LIGHT server, it is now possible to compute the energy savings offered by artificial light control systems. Table 1 below shows that a dimmable system will save 36% electricity compared to a simple on/off control.

No daylight	3986 kwh
Daylight + On/Off control	2993 kwh
Daylight + Dimmable control	1901 kwh

Table 1: Annual electricity consumption used to maintain 500 lux in a room, Nantes, France.

Contact

michel.perraudeau@cstb.fr
Département Acoustique et Éclairage
Centre Scientifique et Technique du Bâtiment
11 rue Henri Picherit
F-44323 Nantes
France
www.cstb.fr

Impact of a highway viaduct on the availability of sunshine and daylight

Context

In 2000, the private company ALIS was charged by the French government to undertake the construction of the highway A28 going from Rouen to Alençon. Environmental studies began in 2002. Parts of the highway needed large viaducts. This was the case of the section going south of the Brionne city over the Risle valley (figure 1). In this valley, the viaduct was going east-west; people were particularly concerned by the shadow that the viaduct would project. ALIS asked the Ingelux engineering office to study the impact of the viaduct on the availability of sunshine and daylight on the areas located close to the viaduct.

Figure 1: Location of the viaduct

Company

The Ingelux engineering office works on projects related to natural and artificial lighting in urban areas and inside buildings. Ingelux started in 2001, it has a team of 3 engineers and 1 architect.

Study

The question was to know how much the viaduct would reduce the access to sunshine and to daylight in the areas close to the viaduct and noticeably on the north of it.

Data

Ingelux used the topographic data of the valley that came from Alis (Autocad dwg format) which they coupled with a geometric model of the viaduct. From this information, they prepared a model describing the terrain and the viaduct (figure 2).

Figure 2: Terrain and viaduct model

They also needed climatic information for the exact area, they selected Valleville. They obtained this information from the SATEL-LIGHT server (www.satel-light.com). The SATEL-LIGHT database was obtained from METEOSAT satellite images. It provides half-hour information on solar radiation and daylight with a 5 km spatial resolution, for 5 years. They obtained from SATEL-LIGHT, statistics on sky conditions (figure 3) as well as a file containing half hour information on sunshine.

Figure 3: Sky frequencies in Valleville (source www.satel-light.com)

Impact on sunshine availability

Ingelux interpolated the half hour data on the availability of sunshine to compute every 6 minutes the impact of the viaduct. They obtained a number of sunshine hours with and without the viaduct. By computing the difference, they could show the impact of the viaduct. They studied the influence over the whole year and from December to March, a period where sunshine is most wanted. Figure 4 shows the number of hours from December 21 to March 21 during which the viaduct has an impact on sunshine.

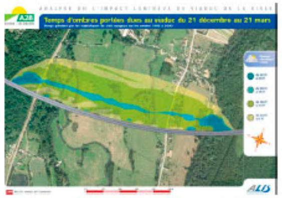

Figure 4: Number of hours during which the viaduct impacts sunshine

Impact on daylight availability

Ingelux used the model to compute daylight factors on the terrain with and without the bridge. The daylight factor is the ratio between the diffuse illuminance at a point taking into account the terrain, the viaduct and the diffuse illuminance available at the same point without the masks of the terrain and the viaduct. Figure 5 shows the Viaduct impact on access to daylight.

Figure 5: Percentage of access to diffuse daylight around the viaduct

Conclusion

Because climatic information was available for the exact location, it could be taken into account in assessing the impact of the viaduct on sunshine and daylight availability. ALIS was able to use the information produced by Ingelux when they met inhabitants. It helped in reducing their concerns.

Contact

ingelux@espace-carco.com
Ingélux Consultants
1 rue Francis Carco
F69120 Vaulx-en-Velin
France
www.ingelux.com

Access to Data

Unifying Access

- Lessons learned from SoDa:
  - General portal is beneficial for solar energy users
  - SoDa used proprietary software and communication standards
  - High maintenance efforts in operating the portal
- New approach in MESoR:
  - Open source software portal with large development community Internet standard communication protocols
  - Google Maps API for ease of use
  - The portal is a broker for data bases located elsewhere, it does not store and offer data itself
  - Connexion with larger intiative (GEO/GEOSS - IEA-Task36 SHC)

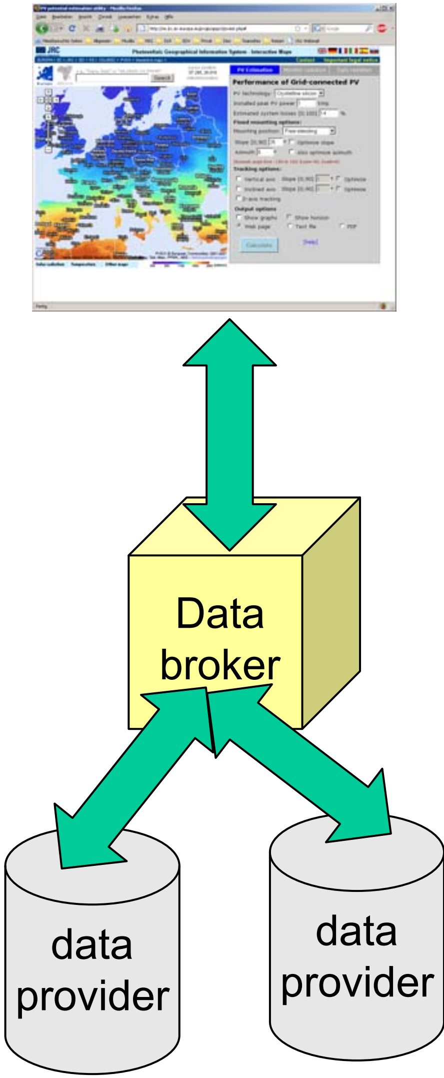

The new MESoR Portal http://project.mesor.net

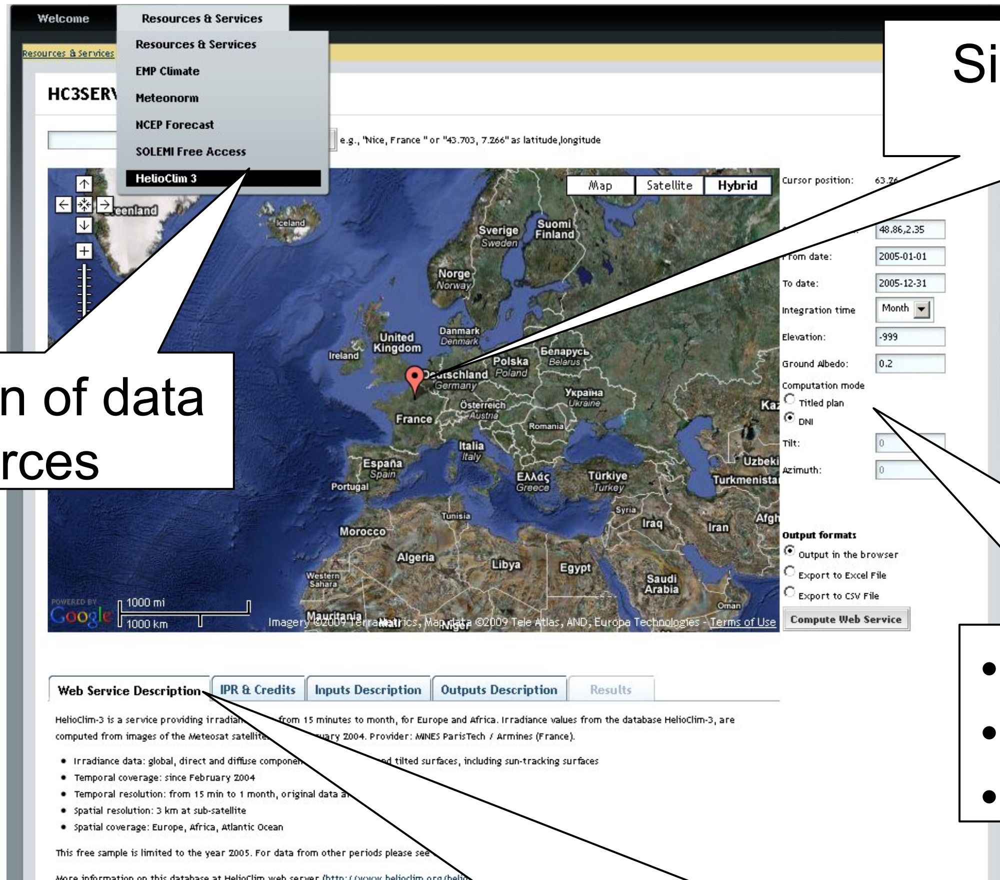

Site selection

Selection of data sources

- Service dedicated forms
- Output to various formats
- Computation launch

- Information about the data source
- Results display

Deutsches Zentrum für Luft- und Raumfahrt e.V. in der Helmholtz-Gemeinschaft

The new MESoR Portal

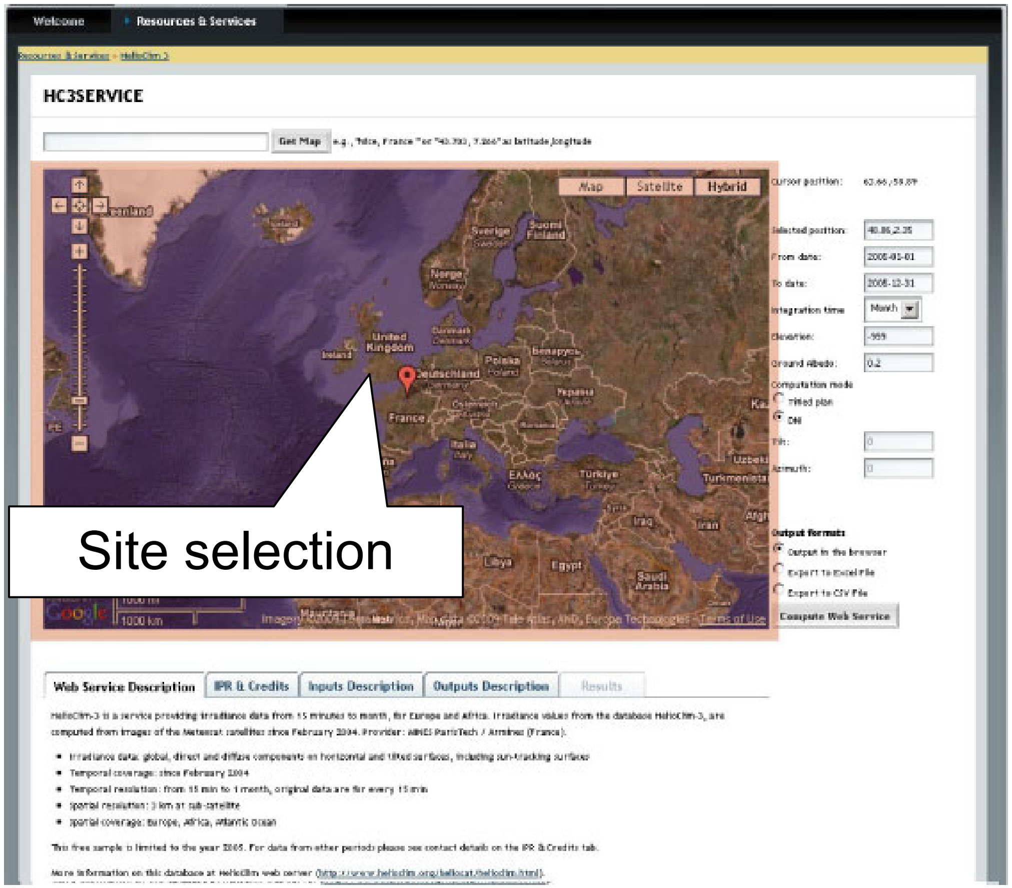

Google Map API

- Ease of use
- No learning curve
- De facto Standard

The new MESoR Portal

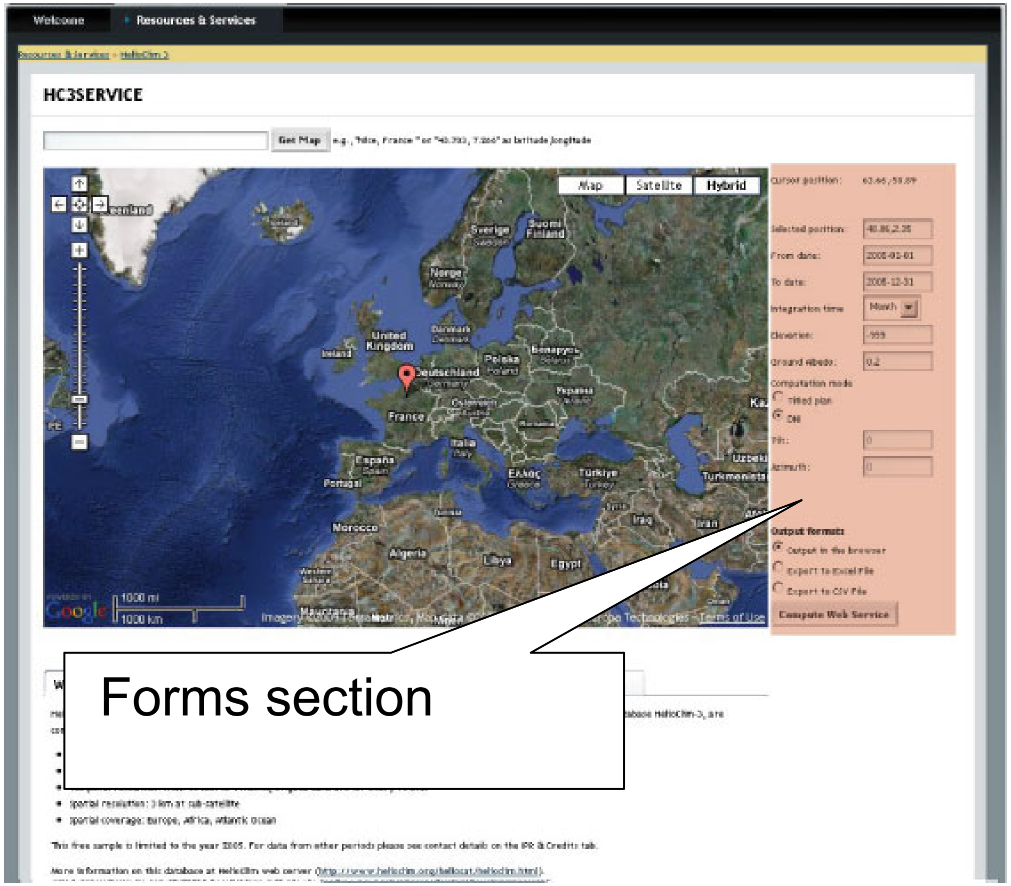

- Forms tailored for each applications
- Handle various output formats
  - Tabular in browsers
  - Excel Spreadsheet
  - PDF
  - CSV

The new MESoR Portal

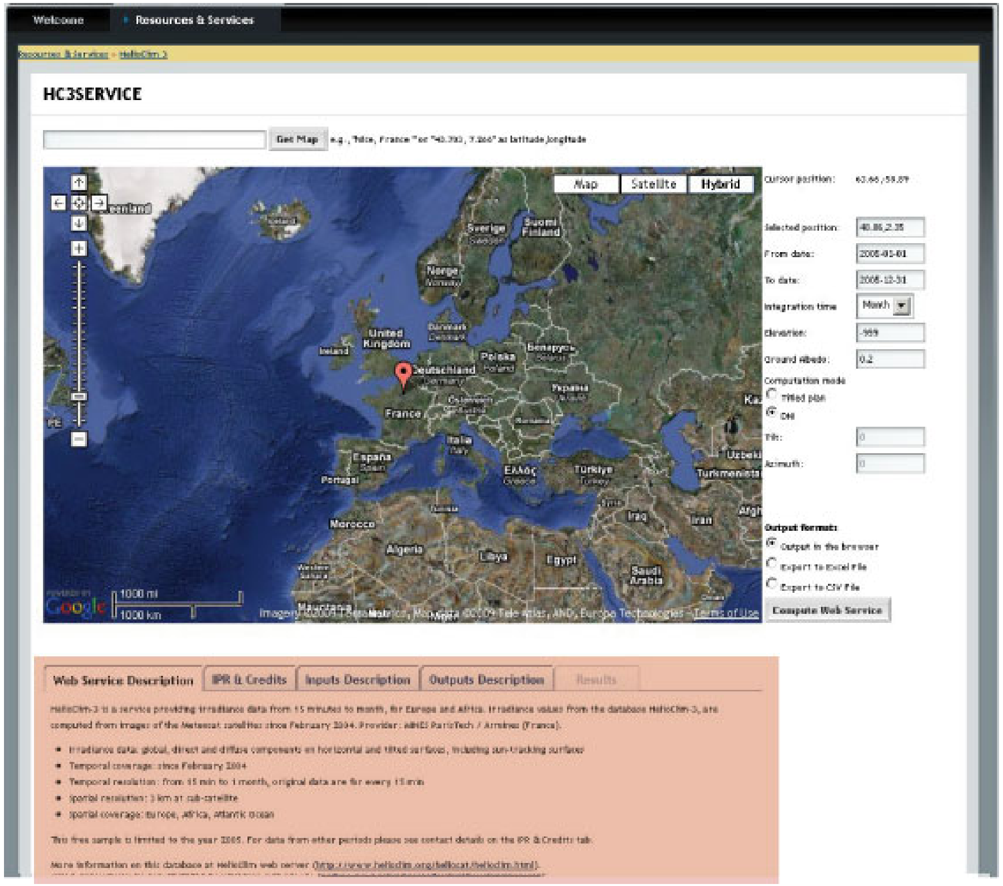

- Tabs handle Service's information
- Build with AJAX (Asynchronous)

- Result tab handle the selected output formats
  - Tabular in browsers
  - Excel Spreadsheet
  - PDF
  - CSV

The new MESoR Portal

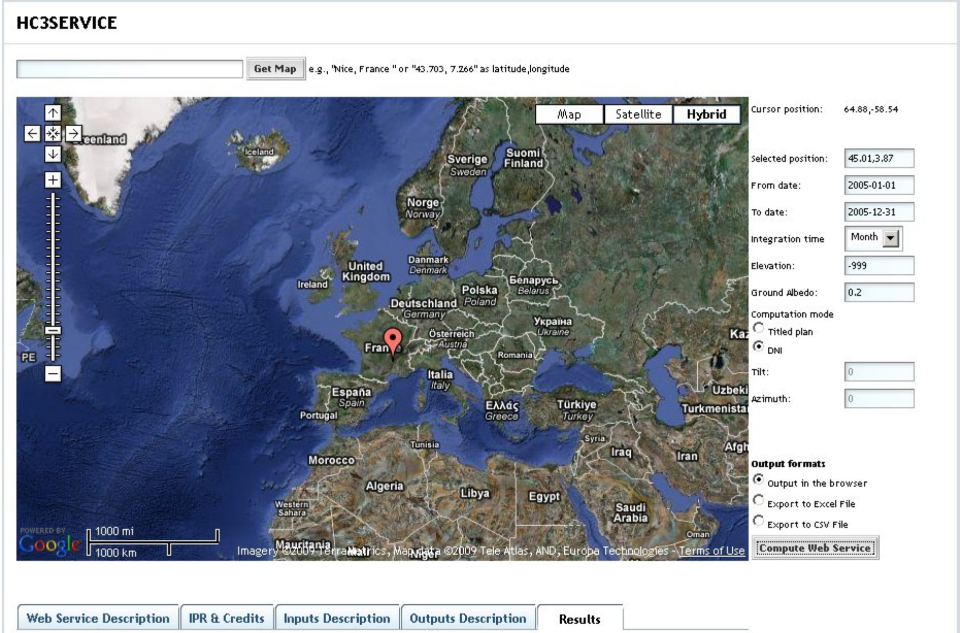

Date	Global	Beam	Diffuse	Reflected
2005-01-31	72275.0	40968.0	28461.0	2846.0
2005-02-28	66371.0	30347.0	33186.0	2839.0
2005-03-31	154737.0	94607.0	55493.0	4712.0
2005-04-30	185370.0	113668.0	67000.0	4703.0
2005-05-31	273147.0	190470.0	77145.0	5606.0
2005-06-30	298701.0	217552.0	75507.0	5641.0
2005-07-31	296268.0	209420.0	80868.0	5904.0
2005-08-31	248555.0	170737.0	72287.0	5532.0
2005-09-30	181138.0	118612.0	57605.0	4921.0
2005-10-31	136033.0	84403.0	47290.0	4340.0
2005-11-30	88750.0	54699.0	30863.0	3188.0
2005-12-31	50317.0	24410.0	23586.0	2396.0

Tabular results output in browser

The new MESoR Portal

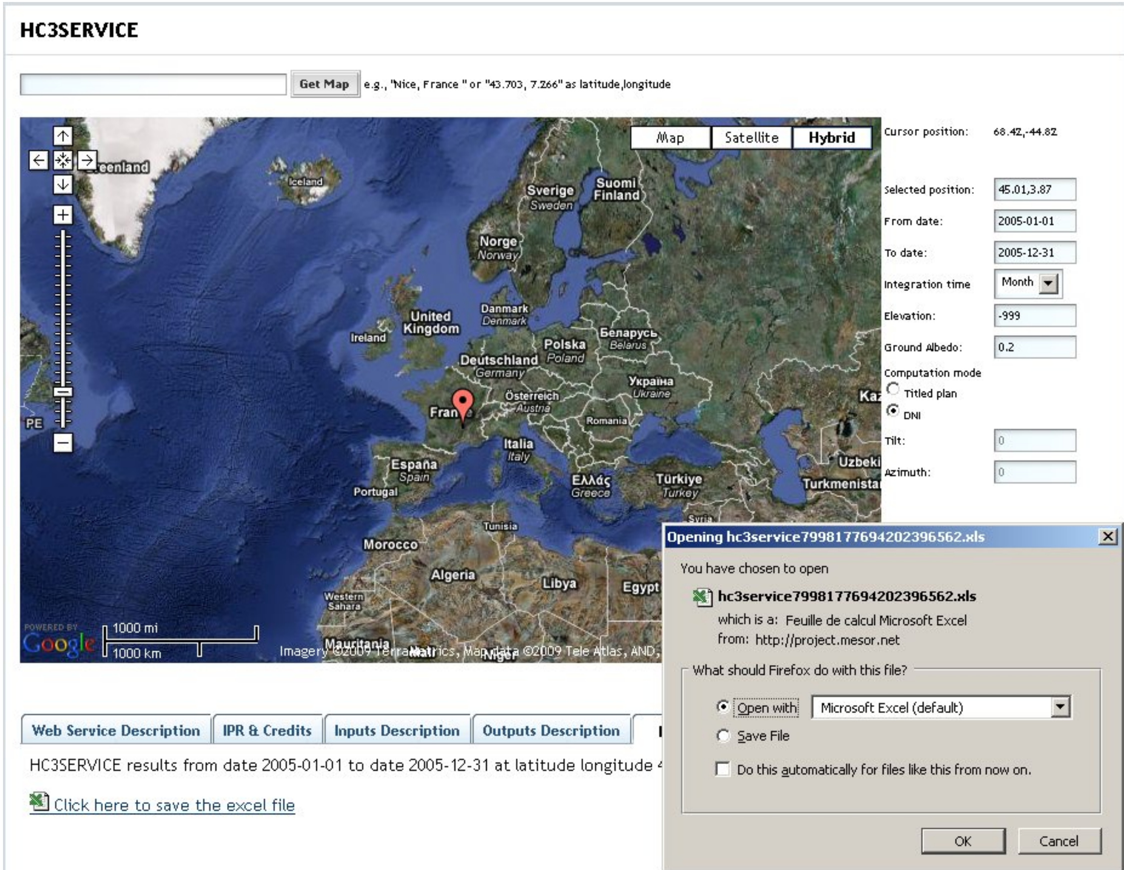

Excel file output sample

The new MESoR Portal

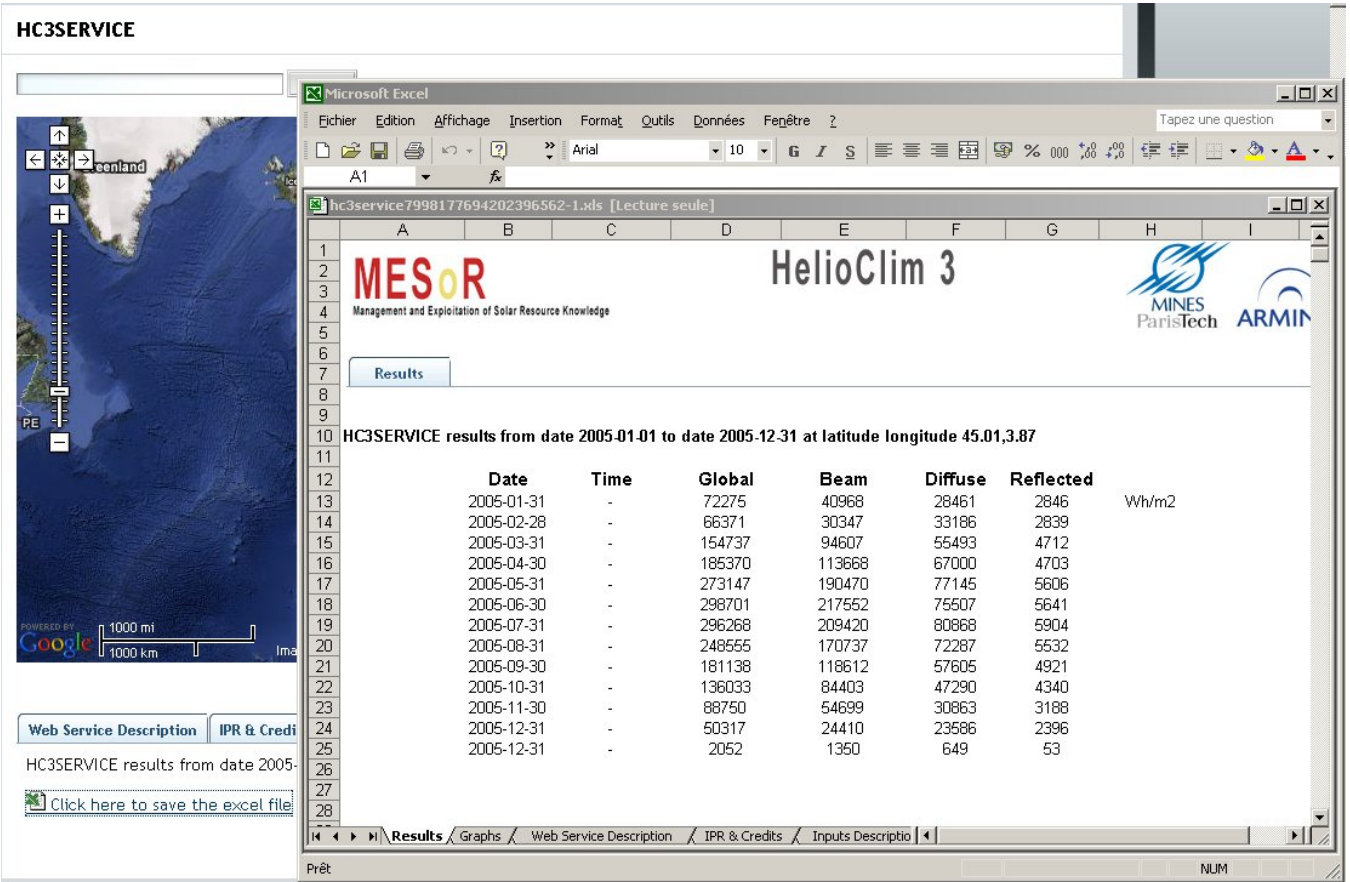

Date	Time	Global	Beam	Diffuse	Reflected	
2005-01-31	-	72275	40968	28461	2846	Wh/m2
2005-02-28	-	66371	30347	33186	2839	
2005-03-31	-	154737	94607	55493	4712	
2005-04-30	-	185370	113668	67000	4703	
2005-05-31	-	273147	190470	77145	5606	
2005-06-30	-	298701	217552	75507	5641	
2005-07-31	-	296268	209420	80868	5904	
2005-08-31	-	248555	170737	72287	5532	
2005-09-30	-	181138	118612	57605	4921	
2005-10-31	-	136033	84403	47290	4340	
2005-11-30	-	88750	54699	30863	3188	
2005-12-31	-	50317	24410	23586	2396	
2005-12-31	-	2052	1350	649	53	

Excel file output result

Selecting the right data source

Required Characteristics

	Minimum spatial resolution [km]	Minimum temporal resolution	Minimum time coverage [years]	Solar radiation components	Database has been validated	Database has been benchmarked according to IEA Task 36	Low Bias	Low root mean square error	Low KSI	Use of multiple independent data source	On site measurement	Current data available / Near real time data
Investment Decision												
Site selection	10	none (map)	10	GHI or DNI	yes	no	yes	n/a	n/a	no	no	no
Pre feasibility	100	annual	5	GHI or DNI	yes	no	yes	no	no	no	no	no
Feasibility	10	hourly	10	DHI or DNI	yes	yes	yes	no	no	no	no	no
Design and construction												
PV Small systems	10	monthly	5	GHI	yes	no	yes	no	no	no	no	no
PV Medium sized systems	50	hourly	5	GHI	yes	yes	yes	no	yes	no	no	no
PV Large systems	10	hourly	10	GHI + DNI	yes	yes	yes	no	yes	yes	yes	yes
Tracking / concentrating PV	10	hourly	10	DNI	yes	yes	yes	no	yes	yes	yes	yes
Solar hot water	100	monthly	5	GHI	yes	no	yes	no	no	no	no	no
Solar cooling	100	monthly	5	GHI	yes	no	yes	no	no	no	no	no
CSP	10	hourly	10	DNI	yes	yes	yes	no	yes	yes	yes	yes
Daylighting		hourly	5	Illuminance	yes	no	yes	no	no	no	no	no
Solar Process Heat	10	hourly	10	GHI	yes	yes	yes	no	yes	yes	yes	yes
Due diligence	10	hourly	10	GHI + DNI	yes	yes	yes	no	yes	yes	yes	yes
Commissioning / System Acceptance	10	hourly	10	GHI + DNI	yes	yes	yes	no	yes	yes	yes	yes
Operation												
Performance monitoring (does the system work corr	10	hourly	n/a		yes		yes	yes	less importan	no	no	yes
Performance improvement (how to improve system imp	10	hourly	n/a		yes		yes	yes	less importan	no	no	yes
Forecasting	10	hourly	n/a		yes		yes	yes	less importan	no	no	yes
Energy policy												
Potential assessment	10	none (map)	5		yes	yes	yes	n/a	n/a	no	no	no
Design of support instruments, e.g. levels of tariffs, in	10	none (map)	10		yes	yes	yes	n/a	n/a	no	no	no
Climate policy												
Climate models	10	hourly	20		yes	yes	yes	no	no	no	no	no
Impact assessment models	10	annual	10		yes	yes	yes	no	no	no	no	no
Climate monitoring		hourly									yes	yes
Science												
Energy system analysis (Systems, components)	10	hourly			yes	yes	yes	no	yes	no	no	no
System simulations	10	hourly			yes	yes	yes		yes	no	no	no
Grid integration studies	10	hourly			yes	yes	yes	yes	yes	no	no	no

Table is still under discussion

GIS Analysis

Generation of an Exclusion Map

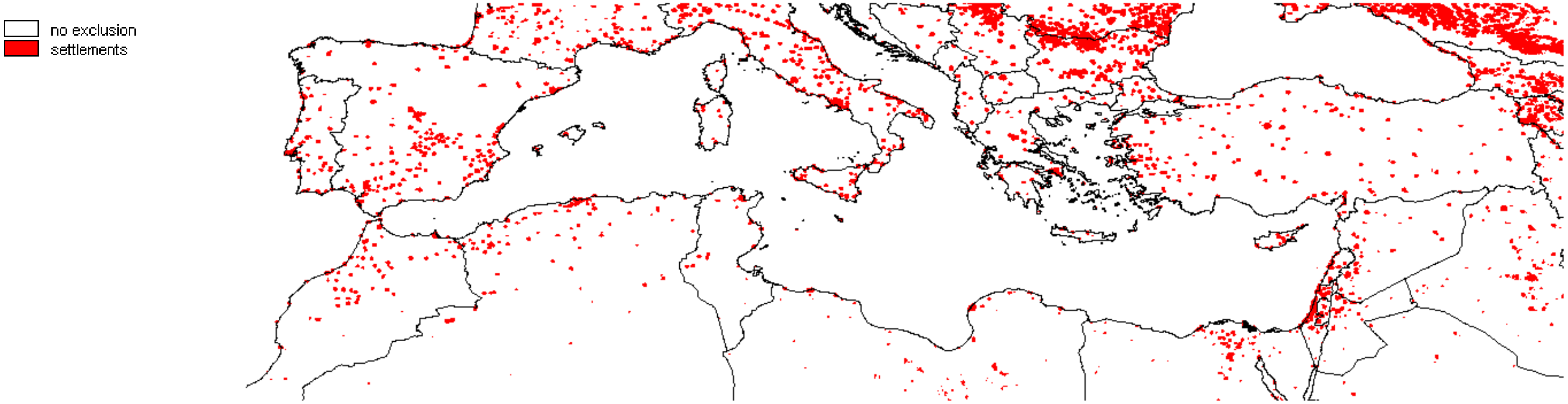

Generation of an Exclusion Map

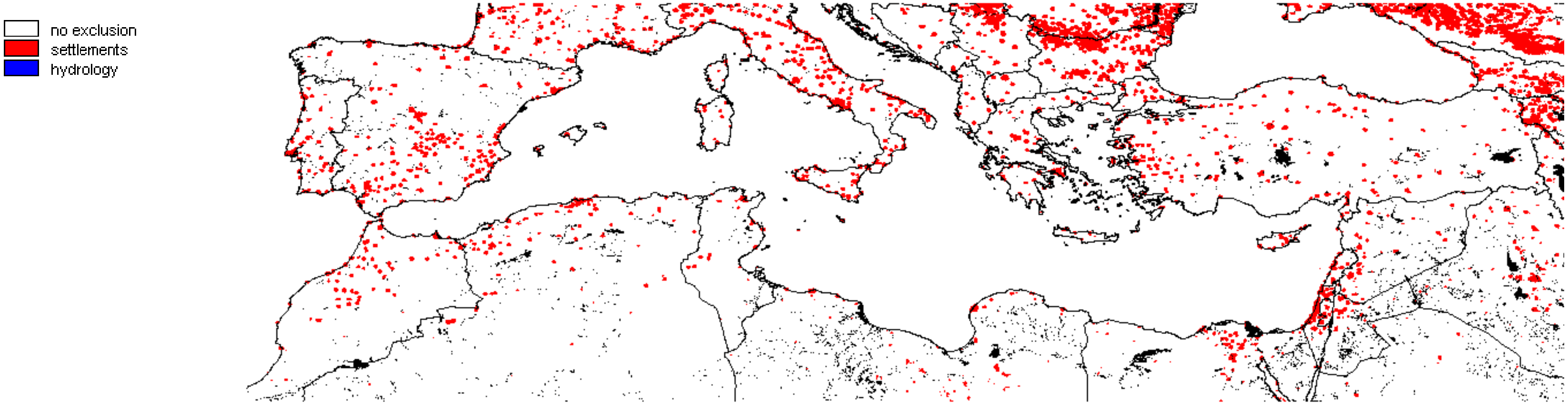

Generation of an Exclusion Map

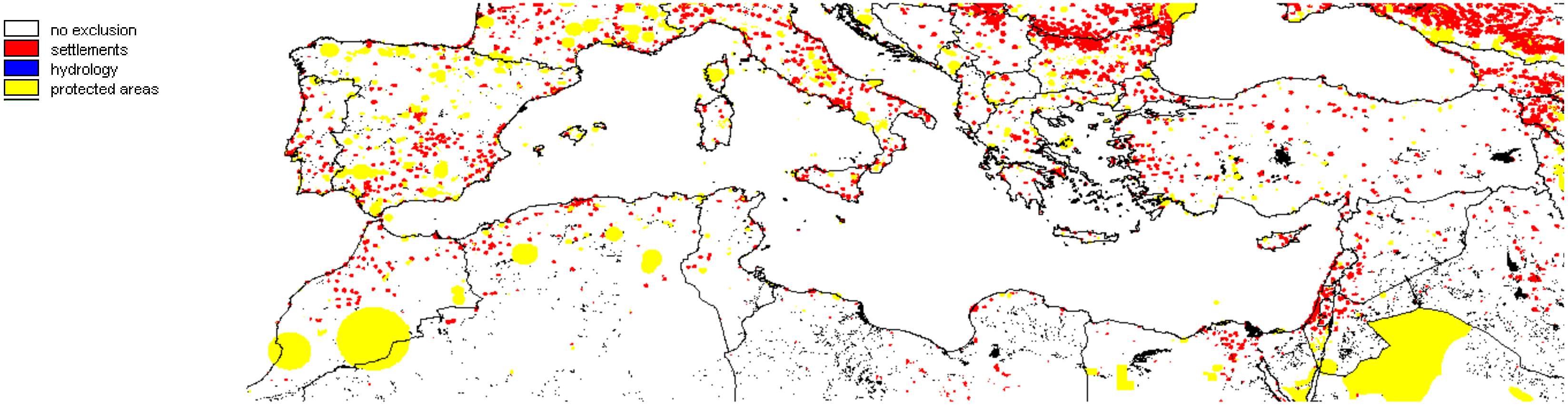

Generation of an Exclusion Map

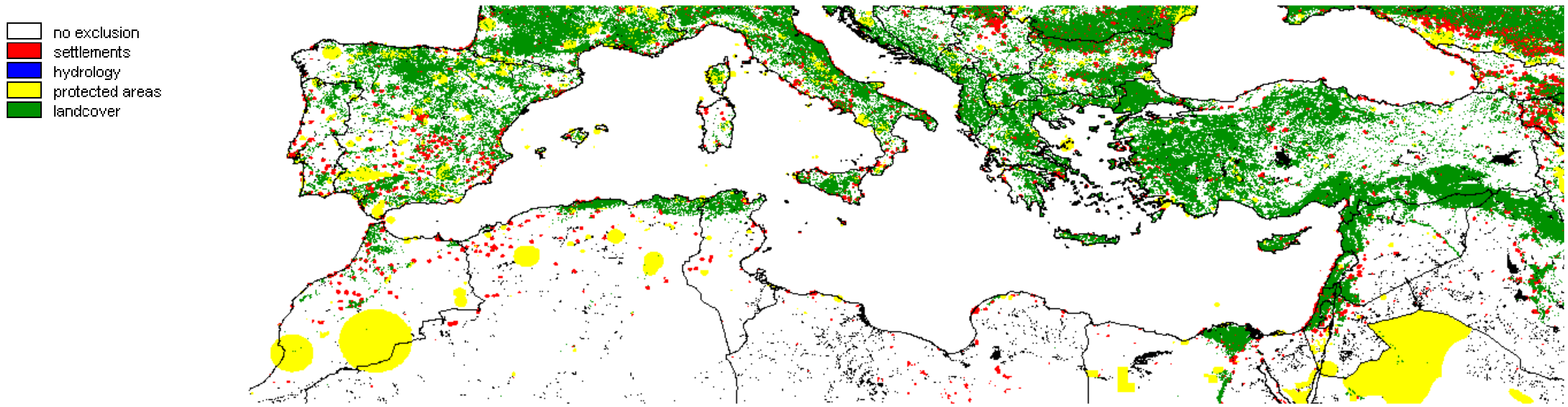

Generation of an Exclusion Map

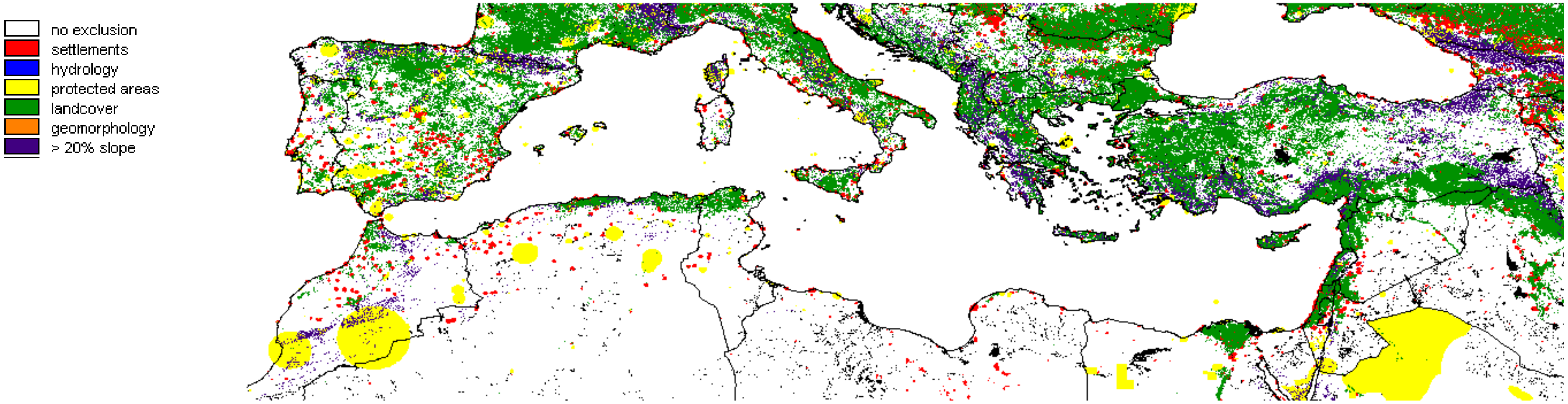

Generation of an Exclusion Map

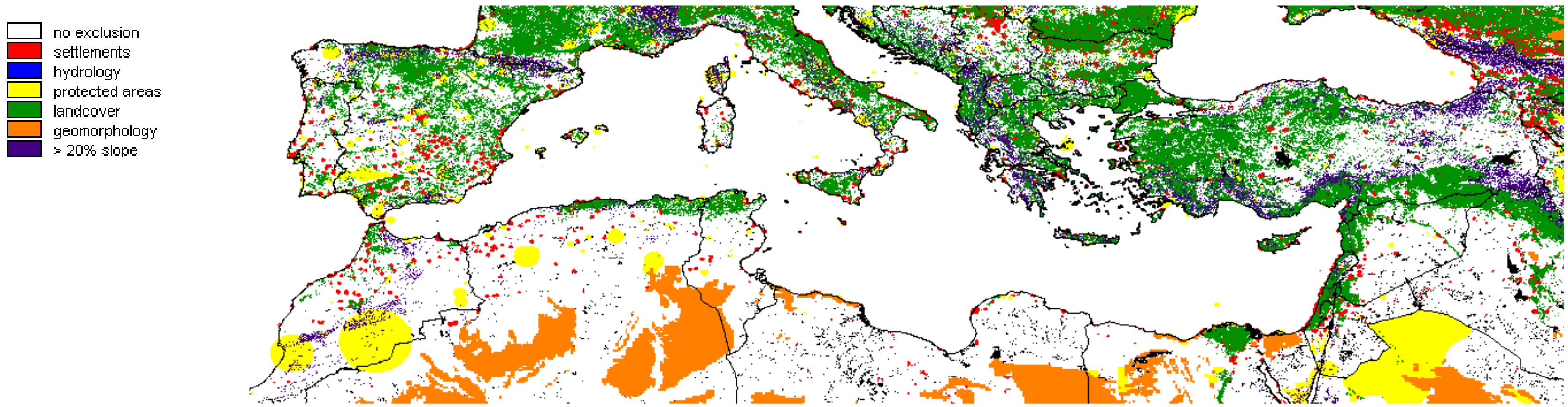

Solar Thermal Electricity Generating Potentials in Morocco

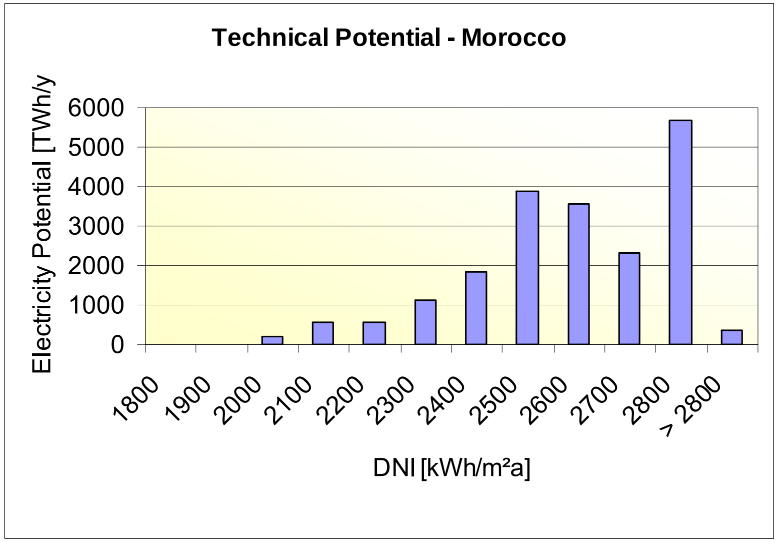

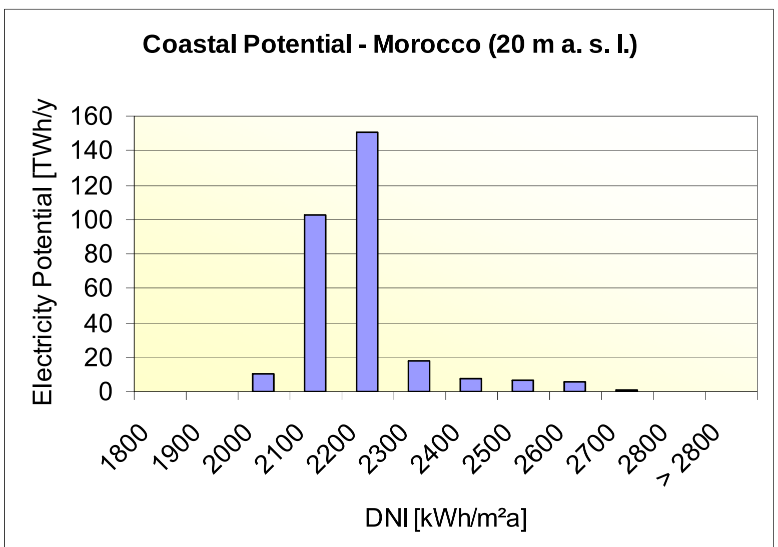

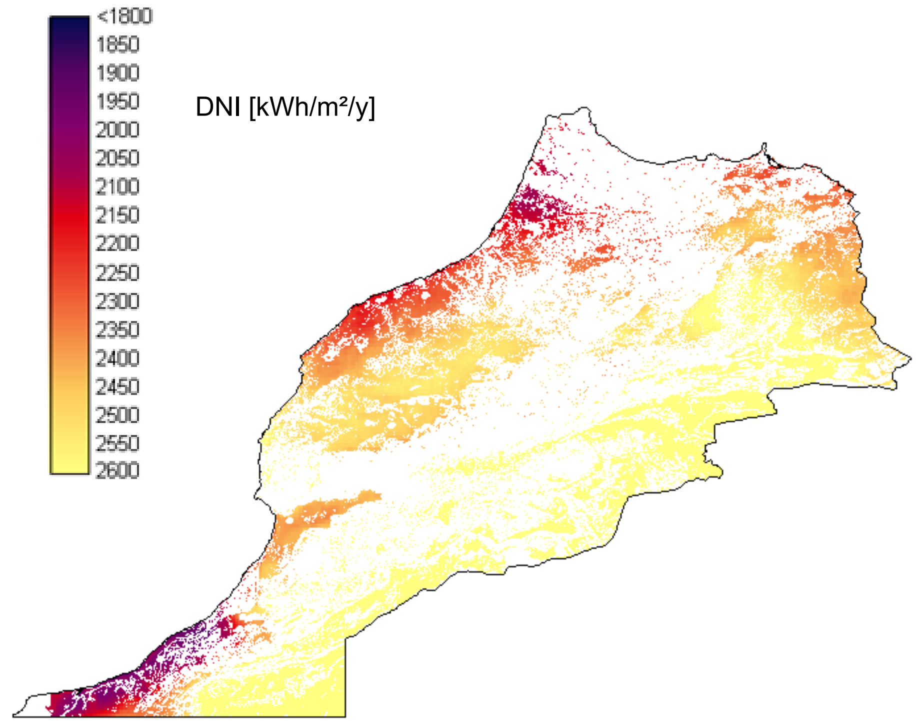

Technical Potential:	**20151 TWh/y (DNI > 1800 kWh/m²/y)**
Economic Potential:	**20146 TWh/y (DNI > 2000 kWh/m²/y)**
Power Demand 2000:	**15 TWh/y**
Power Demand 2050:	**235 TWh/y (Scenario CG/HE)**
Tentative CSP 2050:	**150 TWh/y (Scenario CG/HE)**
Coastal Potential:	**300 TWh/y (< 20 m a. s. l.)**
Water Demand 2050:	**1.2 TWh/y (Power for Desalination)**

New Approach for Site Ranking

- Prerequisite: GIS data for resources and infrastructue
- Idea, giving Points to:
  - Level of available resource
  - Distance to the electricity grid
  - Distance to settlements
  - Distance to infrastructure
- Ranking based on the sum of points.

Determination of weights - DNI

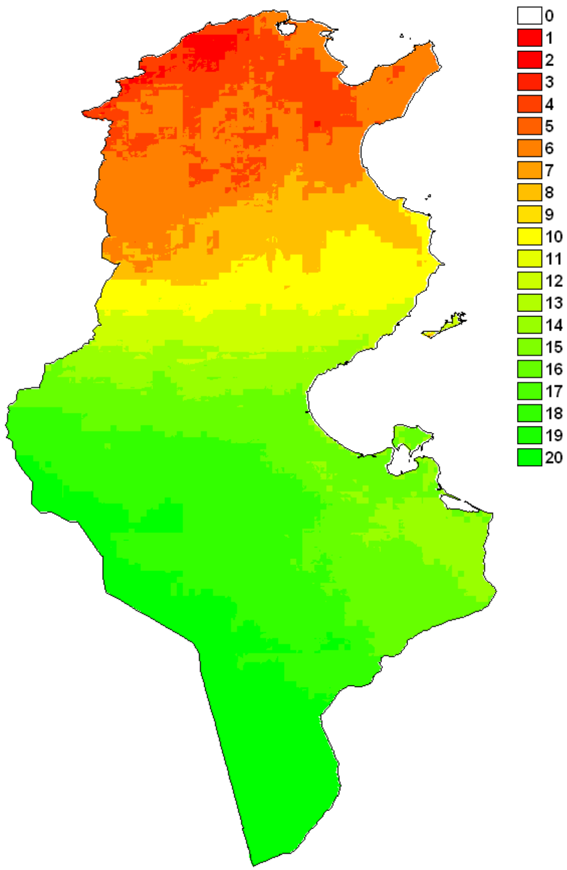

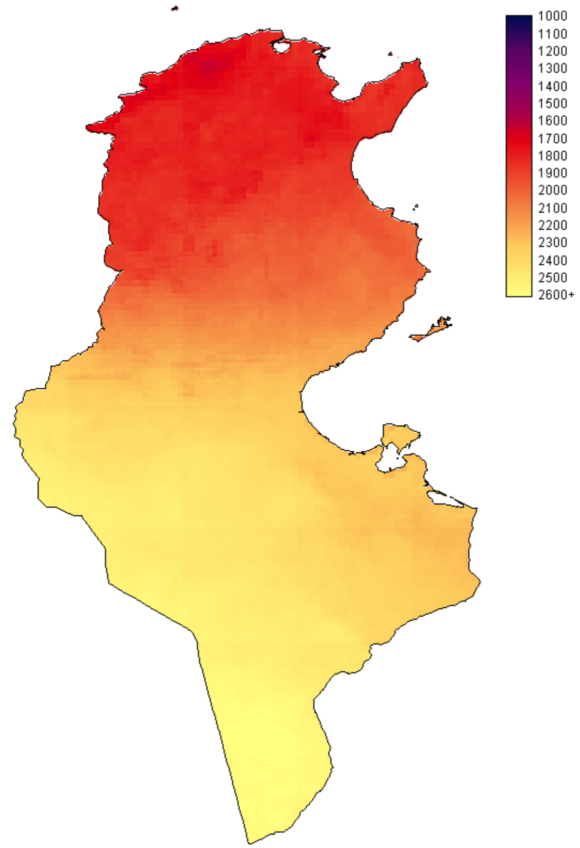

Determination of weights – Population and Infrastructure

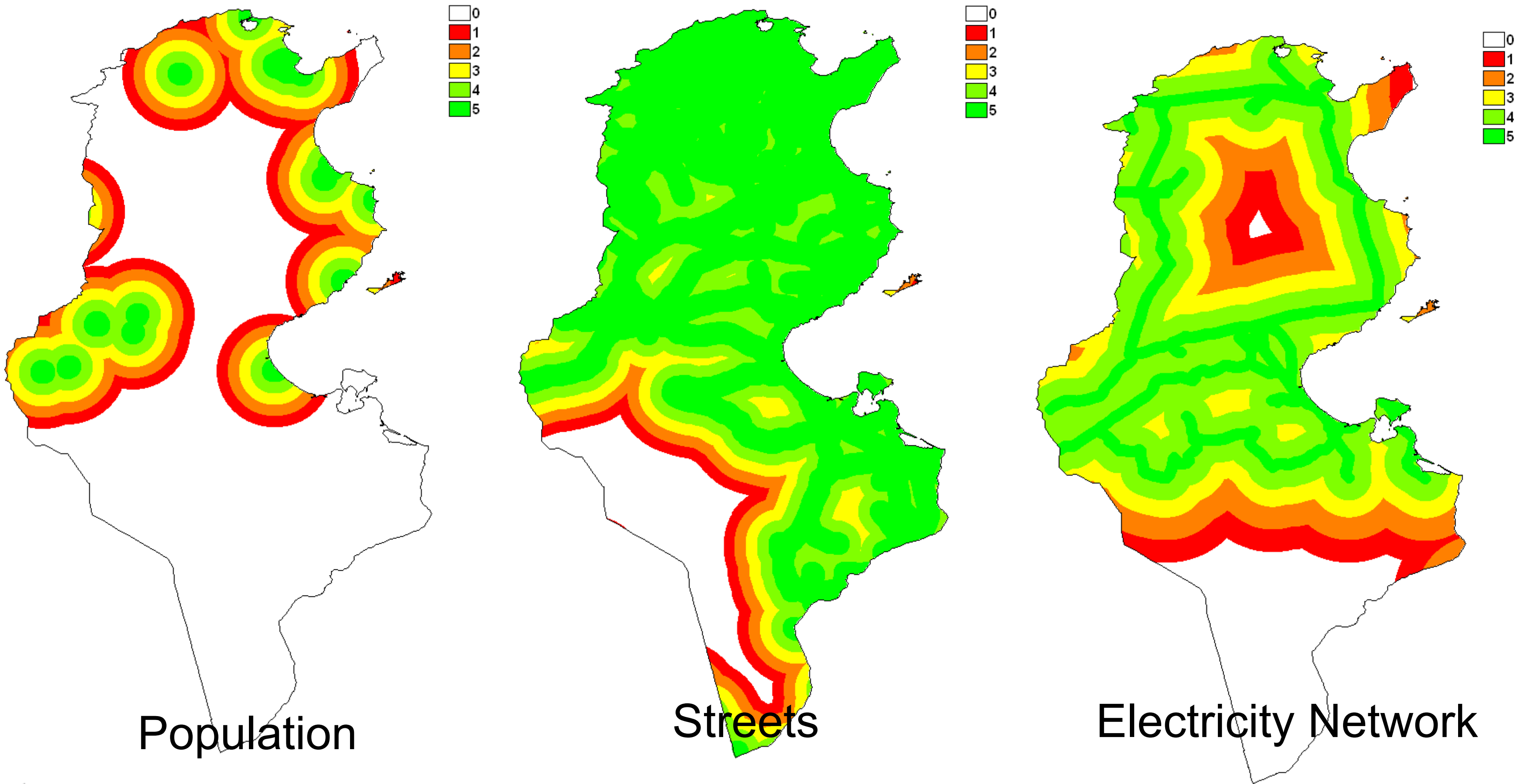

Site Ranking for CSP Tunisia

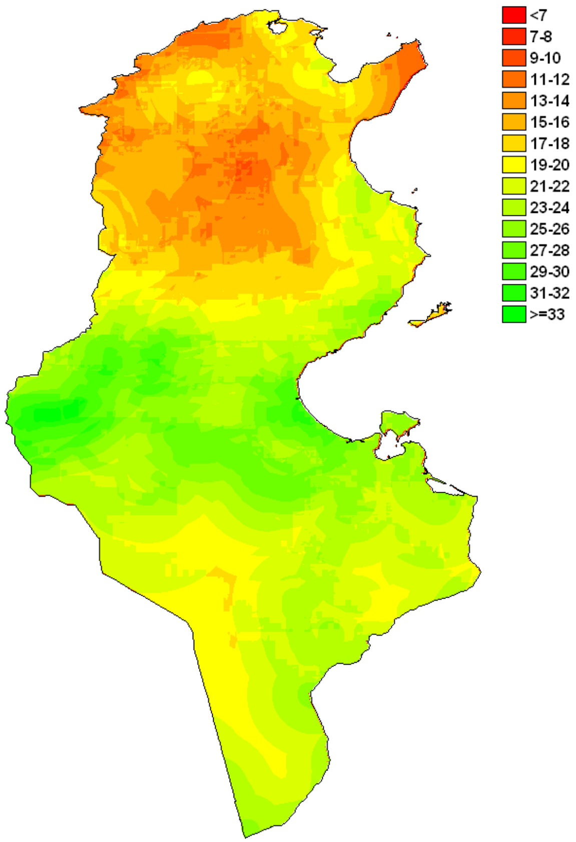

Site Ranking based on:

	Value		Points	
	Min	Max	min	max
Resource DNI	1900	2300	2	20
Transmission	0	75	5	0
Substations	0	75	10	0
Settlements	0	50	5	0
Roads	0	50	5	0

Good Solar Resource Assessments

- Based on long term data
- Site specific, high spatial resolution
- Sufficient temporal resolution for the application
- Modeled data set has been benchmarked, information on quality is available
- For large projects: Based on different sources (e.g. Satellite and ground data).

Conclusions

- High quality resource assessments are part of the basic infrastructure for market development and investments into an energy technology
- Nobody would invest in an oil field if he would not have a pretty good idea on what he expects from it.
- Renewable Energy Sources are highly variable in time and space: Their assessment needs a detailed investigation of high quality long term measurements from ground and space which requires a lot of effort.
- Planning infrastructures (as good maps) may be a public good. Everybody profits of it, but no single one will be willing to pay for it alone.

Acknowledgements

- Many thanks for a large number of slides by Detlev Heinemann, University of Oldenburg, Energymeteorology group
- Thanks to Norbert Geuder (DLR/CSP-Services) for a number of slides
- Thanks to Christoph Schillings (DLR), for input for many slides, especially GIS
- Thanks to Benedikt Pulvermüller, Solar Millennium AG, for some slides
- Tanks to a lot of others I forgot.

- Thanks to UNEP, the German Federal Minstriy for the Environment for the financial support
- Thanks for Stellenbosch University for organizing all of this